

M-AM-Pos35 DYNAMIC Ca²⁺ MEASUREMENTS IN ISOLATED APLYSIA BAG CELLS. John C. Woolum and Felix Strumwasser, Division of Biology, California Institute of Technology, Pasadena, CA, 91125.

We are using the dye arsenazo III to study the changes in internal Ca²⁺, [Ca_i²⁺] in the neurosecretory bag cells of Aplysia. The bag cells undergo a period of spontaneous discharge (and secretion of egg laying hormone in the intact system) when treated with cyclic AMP analogs. A similar spontaneous discharge can be obtained with the potassium channel blocker TEA. We have pressure injected arsenazo III into isolated bag cells grown on culture dishes. The cells are trans-illuminated with white light in an inverted microscope. The light is picked up by a fiber optic probe and separated into its component wavelengths with a grating monochromator similar to one designed by Steve Smith (Yale University). The change in the difference in light transmitted at 700±15 nm and that at 660±15 nm gives a measure of change in [Ca_i²⁺]. We have detected changes in [Ca_i²⁺] during a train of stimulated action potentials (A.P.s). Five A.P.s produce a differential absorbance change of as much as 2.2 x 10⁻⁴. Such measurements show that there is significant Ca²⁺ influx during an A.P. and that there is potentiation of the Ca²⁺ influx if the spacing of the A.P.s is less than about one second. [Ca_i²⁺] usually returns to its previous level within about 10 to 20 sec showing that the cell is able to buffer small Ca²⁺ changes. The change in internal Ca²⁺ during an A.P. can be greatly enhanced with TEA. 50 mM TEA allows a change in differential absorbance of as much as 3.8 x 10⁻⁴ with a single stimulated (much lengthened) A.P. We have also been able to detect Ca²⁺ influx during spontaneous discharges induced by N^o-n-butyl-8-(benzylthio)-cAMP and TEA or by TEA alone. Sizeable changes in [Ca_i²⁺] are evident during membrane depolarizations (both long and short).

M-AM-Pos36 AN EFFECT OF WEAK, ELF SIGNALS ON BRAIN TISSUE, IN VITRO. C.F. Blackman, S.G. Benane, L.S. Kinney, W.T. Joines, and D.E. House. Health Effects Research Laboratory, U.S. Environmental Protection Agency, Research Triangle Park, NC 27711

RF radiation, amplitude modulated at ELF, has been shown to cause changes in the efflux of calcium ions from brain tissue, in vitro. These responses occur in the absence of temperature rise in the samples, and occur only at certain modulation frequencies. We have examined the effects of ELF signals alone on calcium ion efflux in the following manner: the entire forebrain is removed from newly-hatched chickens and incubated for 30 minutes in a buffer containing ⁴⁵Ca⁺⁺. After rinsing to remove any loosely-bound ⁴⁵Ca⁺⁺, the tissues are placed in test tubes containing unlabeled buffer and treated for 20 minutes either to an ELF signal or to a sham exposure. The buffer is then assayed for the presence of ⁴⁵Ca⁺⁺. Compared to the sham exposures, specific frequencies and intensities of ELF signals were able to cause enhanced efflux of ⁴⁵Ca⁺⁺ during the treatment period. We recently reported that 16-Hz signals within two intensity ranges, 5-7.5 and 35-50 Vp-p/m, could cause enhanced efflux while intensities outside these ranges, as well as 1-Hz and 30-Hz signals at 40 V/m, would not affect the efflux. We now demonstrate that 45-Hz and 50-Hz signals at intensities between 45 and 50 V/m can also induce enhanced efflux. The underlying mechanism and the physiological significance of the phenomenon are unknown.

M-AM-Pos37 CALCIUM-DEPENDENT CHLORIDE CURRENT IN THE IMMATURE XENOPUS OOCYTE. Michael E. Barish, Department of Physiology, University of California, Los Angeles, CA 90024.

Membrane currents in immature (stage V and VI) Xenopus oocytes were studied using the two microelectrode voltage clamp technique. Oocytes were clamped to their approximate resting voltage (-70 or -80 mV). During step depolarizations, total membrane current showed a transient outward peak between -20 and +30 mV, with a maximum amplitude near 0 mV. At 0 mV, 21°C and the normal external Ca concentration (1 mM), the peak occurred at about 0.3 seconds, and the steady state was reached after about 3 seconds. Removal of external Cl reversed the outward peak to a transient inward surge without affecting the shape of the steady state V-I relation. Tail currents recorded after the peak showed a component not present in those recorded at the steady state, and which inverted at about -25 to -30 mV. This was the approximate E_{Cl} in the normal external solution (87.5 mM Cl) as determined with Cl-selective microelectrodes. The reversal potential for tail current changed with the external Cl concentration as predicted by the Nernst relation. The transient outward peak seen in records of total membrane current thus appeared to be due to a Cl current. Removal of external Ca (Mg, Sr or Ba substitution), or addition of low concentrations of Ni, blocked the appearance of the peak outward current, and increasing the external Ca concentration increased its amplitude. These treatments did not affect the amplitude of the steady state currents. These experiments suggested that the activation of the Cl current was dependent on Ca entry. This Ca-dependent Cl current could be related to the activation potential of amphibian oocytes, which is Cl-sensitive and which can be elicited by Ca injection. (Supported by N.I.H. grant NS09012 to S. Hagiwara, and fellowship GM08676).

M-AM-Pos38 KINETICS OF CALCIUM CURRENT INACTIVATION SIMULATED WITH A HEURISTIC MODEL. J. Chad, R. Eckert, and D. Ewald, (Intr. by G. Augustine), Department of Biology, UCLA, Los Angeles, CA.

Calcium current, I_{Ca} , was isolated under voltage clamp in axotomized *Aplysia* neurons and dialyzed *Helix* neurons. Intracellular TEA and/or Cs plus extracellular TEA and 4-aminopyridine blocked virtually all outward current at membrane potentials up to 0 mV. I_{Ca} exhibited current-dependent decay with an initial rapid, τ_1 , and a subsequent slow, τ_2 , time constant toward a steady inward current, I_{∞} . Factors that reduce the current amplitude (i.e., partial Cd²⁺ block, previous Ca influx, reduced V_m) preferentially reduced the early peak I_{Ca} , while having less effect in reducing the late phases. These kinetics were accurately fitted with an equation based on a six-state model that includes H-H m² activation plus inactivation that depends on elevation of intracellular free Ca²⁺, Ca_i , resulting from the influx of Ca²⁺ carrying the current:

$$I_{Ca} = \bar{g}_{Ca}(V_m - E_{Ca}) [m_{\infty} - (m_{\infty} - m_0)e^{-t/\tau_m}]^2 \cdot 1/(1+K \cdot S)$$

in which K = efficacy of Ca²⁺ in inactivating Ca channels; $S = \int_0^t (1-P_B) I_{Ca} dt$; and P_B = probability that Ca²⁺ entering will be lost to diffusion or buffering. The inactivation term $1/(1+K \cdot S)$ represents the kinetics of Ca interacting with a receptor site to cause the inactivation of the channel. In this model the two phases of inactivation, τ_1 and τ_2 , result from successive increments in Ca_i producing progressively smaller increments of inactivation, and from the reduction in current due to inactivation decreasing progressively the rate of increase of Ca_i with time. The disproportionate loss of the initial phase of current with diminished current flow results from the slower increase in Ca_i and thus slower, more uniform increase in the Ca-mediated inactivation. Supported by USPHS NS8364 and NSF BNS 80-12346 and the Epilepsy Foundation of America.

M-AM-Pos39 Ca⁺⁺ ACTION POTENTIALS AND Ca⁺⁺ CURRENTS IN TONIC MUSCLE FIBERS OF THE FROG. M. Huerta and E. Stefani. Department of Physiology and Biophysics, Centro de Investigación del IPN, Apartado Postal 14-740, México, D.F. 07000.

Cruralis tonic and twitch fibers from *Rana Pipiens* were exposed to a saline containing (mM): TEA methanesulphonate (MeSO₃), 120; Ca MeSO₃ 10; and 3,4-diaminopyridine 5 (pH 7.3). In this solution g_{Na} and g_{Cl} were eliminated and g_K was greatly reduced. Contraction was blocked by 350 mM-sucrose. Experiments were performed at 18°C. Muscle fibers were current clamped with standard two microelectrode technique using 1 sec pulses. Membrane potential was held at -80 mV. Tonic and twitch fibers were identified by their passive electrical properties. Tonic fibers had a very large effective resistance (V_o/I_o) of $54.8 \pm 7 \text{ M}\Omega$ ($\bar{X} \pm S.E.$ $n=21$) resulting in a very large membrane time constant (τ_m) of $440 \pm 70 \text{ sec}$ $n=8$. In contrast, in twitch fibers $V_o/I_o = 3.5 \pm 0.8 \text{ M}\Omega$ $n=10$ and $\tau_m = 56 \pm 4 \text{ sec}$ $n=6$. Tonic fibers elicited a slow action potential when depolarizing pulses were applied. This response had a threshold of about -40 mV reaching a peak amplitude of -10 mV at 0.5 sec and had a plateau phase of variable duration (1-10 sec) after termination of the pulse. It was blocked by 2 mM Cd⁺⁺ and 5 mM Co⁺⁺. The three microelectrode voltage technique was used to study the underlying currents. The holding potential was -100 mV and 8 sec pulses of variable amplitude were delivered. Slow inward currents were detected at -60 mV reaching a maximum value at 0 mV and having a reversal potential of about 40 mV. In three fibers the main peak current measured at 0 mV was $25 \mu\text{A}/\text{cm}^2$. It had a peak time of 1.2 sec and decayed with a time constant of 3.3 sec. These currents were blocked by 2 mM Cd⁺⁺. Ca currents in tonic fibers are much smaller than in twitch fibers.

M-AM-Pos40 VERATRIDINE STIMULATION OF CALCIUM UPTAKE INTO CHICK EMBRYONIC HEART CELLS IN CULTURE. David C. Pang and Nick Sperelakis. Dept. Physiol., Univ. Va., Charlottesville, Virginia 22908.

Sperelakis and Pappano (1969) showed that veratridine depolarized cultured heart cells to -5 mV and that this effect was prevented by TTX. In Na-free solution, veratridine hyperpolarized and lowered R_m , consistent with an increase in g_K . Catterall and Luzzunski and their associates have confirmed these observations, but attributed their results to the presence of silent fast Na channels, i.e. they assumed that veratridine can only act on the fast Na channels. To test this possibility, we have studied the effect of veratridine on Ca uptake into cultured heart cell monolayers. Veratridine (10^{-5} - 10^{-4} M) stimulated Ca uptake into the heart cells in a dose-dependent manner. The half-maximal dose was 37 μM . The veratridine stimulation was independent of the age of the chick embryos from which the heart cells were taken, and was inhibited by TTX (3 μM). Since young embryonic hearts have few or no functional fast Na channels (Sperelakis, N., *Cardiol. Toxicol.* 1: 39-108, 1981), the present results indicate that the action of veratridine is not dependent solely on fast Na channels. For example, veratridine may increase the resting Na permeability and/or open the slow channels. The increased Ca influx could then be a consequence of $Ca_o:Na_i$ exchange reaction. In addition, veratridine stimulated Ca uptake into cat ileal smooth muscle, which possess only slow channels. It is concluded that veratridine does not act solely on fast Na channels, but also affects other types of ion channels. It is even possible that veratridine opens the voltage-independent, Ca-operated, non-specific Na-K channel ($g_{Na,K(Ca)}$), since this can account for its effects on g_{Na} and g_K . (Supported by HL-18711 and American Heart Association, Virginia affiliate).

M-AM-Pos41 CALCIUM CURRENT AND CALCIUM-DEPENDENT INWARD CURRENT IN THE STARFISH OOCYTE MEMBRANE.

Jeffrey Lansman, Dept. of Physiology and Jerry Lewis Neuromuscular Res. Ctr., UCLA, Los Angeles, CA

Transient inward currents in the immature starfish (*Leptasterias hexactis*) oocyte were studied using two microelectrode voltage clamp. Inward currents appeared with voltage steps more positive than about -50 mV (holding potential, -80 mV). Removal of Ca by substitution with Mg or addition of Co or Cd to artificial seawater (ASW) completely blocked inward current suggesting it was carried mainly by Ca. During maintained depolarizations (approx. 1 sec.) to elicit maximal inward current, the current decayed with a time course which could be described as the sum of two exponentials (τ -fast= 80-200 ms, τ -slow= 600-900 ms). Replacement of Na with choline or substitution of Ba for Ca abolished the slowly decaying component of inward current. Inward current then decayed with a single exponential time constant τ = τ -fast. The fast relaxation was identified as voltage-dependent inactivation of the Ca current. The slowly relaxing component, seen only in ASW containing both Ca (but not Ba) and Na, appeared to be due to an inward current carried by Na but dependent upon Ca entry.

M-AM-Pos42 MODELING OF Ca CURRENT ACTIVATION. David Wilson, A. M. Brown, and Y. Tsuda, Department of Physiology and Biophysics, University of Texas Medical Branch, Galveston, Texas 77550.

Models of Ca current activation are being explored with systems theory concepts and computer modeling techniques that are of general applicability. A combined suction pipette-microelectrode system for voltage clamp and internal perfusion was used to separate Ca currents in isolated *Helix* neurons. The Ca current turns on with a phasic delay and turns off as a sum of at least two exponentials with time constants of approximately 1.3 msec and .15 msec at the holding potential. An m^2 description is inadequate because these τ values do not have the ratio of 1:2 prescribed by an m^2 model. Sequential state-transition models have been considered in which the rate constants and thus the system eigenvalues are assumed to be functions of potential alone. Turn-on and turn-off currents were fit to sum-of-exponentials models using a Marquardt optimization method with the aim of determining the minimum number of states in the system. Three exponentials were clearly defined in the data. We are presently testing the applicability of a 4-state model using an interactive computer modeling procedure in which both turn-on and turn-off current pairs at various test potentials are simultaneously fit with a numerically simulated model. Using a model in which the rate constants and probabilities are constrained to be positive assures the realizability of the modeled response. Mathematical analysis indicate that in the absence of noise the rate constants of the general sequential model are uniquely identifiable from turn-off but not from turn-on measurements. A useful aid in modeling has been sensitivity analysis which allows one to see the effect of each parameter on the modeled output as a function of time.

(Supported by NIH NS-11453)

M-AM-Pos43 TERBIUM FLUORESCENCE STUDIES OF GH3 PITUITARY TUMOR CELLS. Robert G. Canada.

Laboratory of Neurophysiology, National Institute of Neurological and Communicative Disorders and Stroke, Bethesda, Maryland 20205. (Present Address: Department of Physiology and Biophysics, Howard University, College of Medicine, Washington, D.C. 20059).

Thyrotropin-releasing hormone or depolarizing concentrations of K⁺ have been shown to stimulate the release of prolactin and growth hormone from neoplastic GH3 pituitary cells, in the presence of extracellular calcium (Ca²⁺). GH3 cells like normal anterior pituitary cells are capable of generating Ca²⁺ action potentials in culture. In this study, the fluorescent properties of terbium (Tb³⁺) were used to detect and monitor the Ca²⁺ binding sites on GH3 cells. The Tb³⁺ fluorescence emission was enhanced with the binding of GH3 cells, accompanied by a red shift in its excitation maximum to resemble the excitation peak of the native cell fluorescence. The fluorescence enhancement of Tb³⁺ increased with increasing concentrations of GH3 cells. Scatchard plots of a fluorometric titration procedure revealed at least two classes of binding sites. The low and high affinity sites have apparent dissociation constants equal to 0.56 mM and 11 μ M, respectively. The high affinity Tb³⁺ binding was displaced by Ca²⁺, but the more abundant low affinity site was not sensitive to Ca²⁺. The data suggests that GH3 cells have a specific Ca²⁺ binding receptor on their plasma membrane.

M-AM-Pos44 RECONSTITUTION OF A VOLTAGE-DEPENDENT ANION-PREFERRING PORIN FROM NEISSERIA GONOCOCCUS. E.C. Lynch, M. Blake, E. Gotschlich, and A. Mauro, The Rockefeller University, N.Y., N.Y. 10021.

The ability of the pathogen Neisseria gonorrhoeae and its purified proteins to introduce ion channels into planar lipid bilayers and vesicles has been examined. Channel-forming activity has been resolved into single unit conductances that proceed to macroscopic increases in membrane permeability upon the incorporation of many channels. Channel formation in the lipid bilayers exposed to whole bacteria can occur spontaneously. The rate of insertion is augmented by the addition of detergents and the application of a transmembrane potential. Channel-forming activity appears to reside in the major outer membrane protein (protein I) of the gonococcus. Channels derived from both whole cells and purified protein I show voltage-dependent lifetimes and anion-preferring permeability with a unit conductance of approximately 230 picosiemens (pS) in .1M NaCl. Initial studies indicate that the porins from two gonococcal strains show differences in both rate of spontaneous transfer into and other channel characteristics within the model membrane system. (Supported in part by NIH Training Grant T32GM7288 and the Winston Fellowship Foundation.)

M-AM-Pos45 ANOMALOUS BEHAVIOR OF GLYCINE-ACTIVATED Cl^- CHANNELS IN LAMPREY BRAINSTEM NEURONS.

A. R. Martin and M. R. Gold. Dept. of Physiology, Univ. Colorado Sch. of Med., DENVER CO 80262.

The technique of spectral density analysis was used to determine the conductance and mean open time of glycine-activated channels in voltage-clamped Müller cells in the brainstem of the lamprey. In normal bathing solution the channels, which are permeable exclusively to Cl^- , had a mean conductance of the order of 75 pS and a mean open time of about 33 msec at 6° C. Neither mean open time nor conductance was markedly dependent on holding potential. When cells were loaded with Cl^- , either by using KCl-filled micropipettes or by raising extracellular K^+ , channel conductance decreased rapidly, falling toward an asymptotic value of about 10 pS. This effect occurred over an internal concentration range of 6 mM to 35 mM, as determined from the reversal potential for the glycine effect. Channel mean open times were unaltered. Channel conductance also decreased with decreasing intracellular Cl^- concentration below 5 mM, so that the maximum conductance occurred at 5 - 6 mM intracellular Cl^- . Reducing extracellular Cl^- concentration from 126 to 31 mM reduced channel conductance at all levels of intracellular Cl^- from 2 mM to 12 mM but the variation of conductance with internal concentration was unaffected: the maximum conductance of about 50 pS occurred at an intracellular concentration of about 5 mM and conductance decreased from this maximum with either increases or decreases in intracellular concentration. The reduction in conductance with increasing intracellular concentration is inconsistent with a constant-field channel model, with a single-site model and with a two-site, three barrier model, and suggests that there may be an internal binding site for Cl^- which affects channel conductance.

M-AM-Pos46 VOLTAGE DEPENDENT CHLORIDE-SELECTIVE CHANNELS OF LARGE CONDUCTANCE IN CULTURED RAT SKELETAL MUSCLE. A. L. Blatz and K. L. Magleby, Dept. of Physiology and Biophysics, University of Miami School of Medicine, Miami, FL 33101.

The extracellular patch clamp technique was used to measure single channel currents in both inside-out and outside-out patches of cultured rat skeletal muscle plasma membrane. In less than 10 % of the membrane patches we observed an anion-selective channel with an unusually large single channel conductance of 440 ± 13 pS with 143 mM KCl bathing both membrane surfaces. The very large conductance of these channels and their characteristic kinetics allowed them to be differentiated from the Ca-activated K channel and other channels of smaller conductance. Increasing $[\text{KCl}]_i$ from 143 mM to 400 and 600 mM shifted the reversal potential of these currents from 0 to 18 and 32 mV, respectively. Reversal potential shifts of 26 and 36 mV would have been expected if the channels were exclusively permeable to chloride. This result suggests that chloride ions are the major charge carriers through this channel. Channels were open immediately after voltage steps to positive or negative potentials and then closed within several hundred milliseconds to an inactivated state. Recovery from inactivation occurred in about 100 ms at 0 mV. The channel typically opened and closed spontaneously at 0 mV ($[\text{KCl}]_o:143\text{mM}$, $[\text{KCl}]_i:400\text{mM}$). Current noise was significantly greater when channels were open, particularly at negative potentials. Replacing KCl with NaCl, tetraethylammonium chloride, or NH_4Cl , or adding 1 mM 4-aminopyridine to the internal solution had little effect on channel properties. Supported by: NIH grants NS 07044, NS 10277, NS 12207, and the Muscular Dystrophy Association.

M-AM-Pos47 CONTRIBUTIONS OF SLIPPAGE AND TUNNELING TO ANION NET TRANSPORT ACROSS THE HUMAN RED BLOOD CELL MEMBRANE. O. Fröhlich. Dept. Physiol., Emory Univ. Sch. Med., Atlanta, GA 30322

DNDS-inhibitable chloride net efflux from gramicidin-treated red cells can be divided into two components: one component that decreases hyperbolically with increasing Cl_o , and a Cl_o -independent component. Previously we have tentatively assigned the Cl_o -inhibitable component to slippage and the Cl_o -independent component to tunneling. Slippage refers to net transport mediated by the return conformational change of the unloaded transport site subsequent to translocation of the loaded transporter, and tunneling refers to the movement of the anion through the transport protein without a conformation change of the protein. Bromide and nitrate net efflux also exhibited anion-inhibitable and -independent components. Both components were larger than for chloride net efflux: 230 and 300, respectively, compared to 50 $\text{mmoles (kg Hgb} \cdot \text{min)}^{-1}$ for anion-inhibitable efflux, and 20 and 50, respectively, compared to 10 $\text{mmoles (kg Hgb} \cdot \text{min)}^{-1}$ for the independent component. Since slippage in this system is limited by the return reaction of the empty transporter, it is independent of the nature of the transported anion. The data, therefore, suggest that even at low extracellular anion concentrations net efflux is mainly accomplished by tunneling and not by slippage as previously assumed. This is also supported by experiments in which chloride net efflux was measured as function of Cl_i . At $Cl_o=0$ net efflux was proportional to Cl_i between $Cl_i=25 - 200$ mM and became saturating above 300 mM. If net efflux under these conditions had been mostly by slippage one should have observed a nearly Cl_i -independent rate of chloride net efflux. It therefore appears that the proposed tunneling mechanism can account for a major portion of the anion net transport and that the slippage process is only a minor component. (Supported by NIH grant HL-28674)

M-AM-Pos48 IN VITRO MODULATION OF BOVINE CAUDATE MUSCARINIC RECEPTOR NUMBER BY SUBACUTE CONCENTRATIONS OF PARAOXON. By L.S. Volpe & J.K. Marquis, (Intr. by E. Simons) Dept. of Pharmacology & Exp. Therapy. Boston Univ. School of Medicine, Boston, MA 02118

The toxic action of organophosphate acetylcholinesterase (AChE) inhibitors is due primarily to the formation of a very stable phosphorylated enzyme intermediate. Prolonged exposure to subacute levels of organophosphates produces tolerance in both animals and humans, a phenomenon generally attributed to desensitization of cholinergic receptors. Recent studies, however, found no correlation between levels of brain acetylcholine and tolerance to AChE inhibitors, suggesting that organophosphates may exert a direct effect on the receptors. In vitro binding assays to measure muscarinic receptor number and affinity were carried out with isolated synaptic plasma membranes from bovine caudate nuclei. Diethyl p-nitrophenyl phosphate (Paraoxon; PX) was demonstrated to be a weak noncompetitive receptor inactivator. PX decreased the number of ^3H -quinuclidinyl benzilate (QNB) ($K_d \sim 0.3 \text{ nM}$). PX inhibition of ^3H -QNB binding occurred at much lower concentrations ($\sim 5 \text{ nM}$) than were needed to inhibit AChE by 20% in these membranes ($\sim 60 \text{ nM}$). These data contrast with in vitro measurements of low-affinity ($\sim 0.1 \text{ mM}$) inhibition of peripheral nicotinic cholinergic receptors by organophosphates, but suggest that a decrease in the number of muscarinic cholinergic receptors in the brain may underlie some of the neurological and affective disorders observed after chronic exposure of humans to organophosphate insecticides. It is furthermore proposed that organophosphates may serve as useful probes of the physiological interactions between the two major cholinergic proteins in the postsynaptic membrane of central muscarinic synapses: ACh receptors and AChE. (Supported by U.S. Army Research Office Grant #DAAG 29-82-K-0042 and a grant from the Center for Brain Sciences and Metabolism, Cambridge, MA).

M-AM-Pos49 DIPOLAR ENERGY TRANSFER BETWEEN FLUORESCENTLY-LABELED α -TOXINS BOUND TO MEMBRANE-ASSOCIATED ACETYLCHOLINE RECEPTORS DISAPPEARS UPON SOLUBILIZATION. David A. Johnson, Judith G. Voet*, and Palmer Taylor*. Division of Pharmacology, UC San Diego, La Jolla, CA 92093

We examined the efficiency of steady state dipolar energy transfer between two fluorescently labeled α -toxins, N ϵ -fluorescein isothiocyanate lys-23 cobra α -toxin (FITC-TX) and a monolabeled tetramethylrhodamine isothiocyanate cobra α -toxin (TRITC-TX), bound to the acetylcholine receptor from the Torpedo californica electric organ. The spectral overlap integral between the bound FITC-TX emission spectra and the TRITC-TX absorption spectra was $2.1 \times 10^{13} \text{ cm}^6/\text{mol}$. The donor quantum yield of the FITC-TX bound to solubilized or membrane-associated AChRs were 0.26 and 0.33, respectively. Based on the axial depolarization factors of the labeled α -toxins the maximum and minimum orientation factors ($\langle K^2 \rangle$) were estimated to be 2.5 and 0.2 respectively. An approach based on the random site occupation of labeled α -toxins was established to achieve 50% of AChRs with one FITC-TX and one TRITC-TX bound. The remaining AChRs had both their sites occupied by either TRITC-TX or FITC-TX. With this paradigm dipolar energy transfer efficiency of 40% was observed between labeled α -toxins when bound only to membrane-associated AChR. No transfer was observed in solubilized AChR. Assuming a detectability of 5% energy transfer efficiency and a minimum estimate for K^2 , the intramolecular distance between conjugated fluorophors on the AChR monomer should be greater than 60 Å. If the membrane-associated AChRs are in an ordered array and transfer only occurs between one donor and one acceptor, the distance between the bound conjugated fluorophors on separate receptor oligomers is between 41 and 62 Å.

M-AM-Pos50 SUCCESSIVE OPENINGS OF THE SAME ACETYLCHOLINE RECEPTOR CHANNEL ARE CORRELATED IN OPEN-TIME. (Meyer B. Jackson, Biology Dept., UCLA, Harold Lecar, and Brendan S. Wong, Laboratory of Biophysics, NINCDS, NIH). At last years Biophysical Society meeting open-state lifetime distributions derived from patch clamp data of chemically activated channels were analyzed in terms of two exponentials (Biophys. J. 37:310a, 1982). The observation of two components in the kinetics of channel closure is consistent with a number of different models of channel gating having two distinct open states. Here we present a method of analysis which permits one to use single-channel data to discriminate between two classes of models. This analysis was carried out with records of acetylcholine receptor channel currents from cultured rat muscle.

The method exploits the conclusion inferred from analyzing closed-time distributions that a channel can reopen immediately after closing while it is still in an activated state. Successions of openings separated by short closed times produced under conditions such that openings are rare have a very high probability of being successive openings of the same channel. Individual openings were classified with better than 90% confidence as 'fast' or 'slow' by analyzing the open-time distributions. Successions of openings are almost always homogeneous - i.e. they are composed either of only 'fast' or only 'slow' events. Successions that included both 'fast' and 'slow' events are very rare. A chi-square analysis showed that the open-times of successive events are not independent. A class of models with a single activated closed state undergoing transitions to two distinct open states is not consistent with this observation, since such models would produce events uncorrelated in open-time. Models with two activated closed states which produce either 'fast' or 'slow' openings will reopen into the same state, thus producing successions with correlated open-times.

M-AM-Pos51 BLOCK AND POSSIBLE AGONIST ACTION OF PERMEANT ORGANIC IONS AT CHOLINERGIC CHANNELS.

J.A. Sánchez, J.A. Dani, D. Siemen, and B. Hille, Dept. Physiology & Biophysics, Univ. Washington Medical School, Seattle, WA 98195.

Acetylcholine-induced current fluctuations were measured at frog endplates bathed in mixtures of tris, dimethylamine (DMA), dimethyldimethanolamine (DDA), or arginine (arg) with sodium. The calculated single-channel conductances (γ) were reduced by low concentrations of these ions, qualitatively as predicted by Adams et al., 1981 (JGP 78:593). Half maximal reduction required ca. 22 mM arg, 14 mM DMA, 13 mM tris, or 5 mM DDA at -73 mV. Hyperpolarization to -135 mV reduced by at least 2 the concentration of arg, tris, or DDA (but not DMA) needed for half reduction of γ . At high concentrations of arg, tris or DDA, the power spectra of fluctuations were non-Lorentzian, but at 5 to 16 mM, they were Lorentzian. We then switched to observing single ACh-channel currents directly with a patch clamp technique on rat myotubes. We found clear reductions of γ with 6 to 75 mM tris, arg, or DMA. Single-channel I-V curves remained linear in DMA mixtures but were curved in arg mixtures. 16 mM arg on the external side reduced inward currents more than outward currents, as if external arg binds to a site 60% of the way across the membrane electric field from the outside. However 40 mM arg on the internal side had almost no effect on inward or outward currents, as if no arg binding site faces the inside. Even in nominally ACh-free solutions of a variety of compositions we saw openings with the appropriate γ and reversal potential. Perhaps the added cations have some agonist activity or possibly the channels have a weak spontaneous activity. Supported by NIH grants NS-08174, FR-00374, and Deutsche Forschungsgemeinschaft.

M-AM-Pos52 INHIBITION OF RAT BRAIN MUSCARINIC ACETYLCHOLINE RECEPTORS AFTER *in vivo* TREATMENT WITH METHYLMERCURY AND MERCURIC CHLORIDE El. A.M. Abdallah, A.S. Abdelfattah, and A.E. Shamoo, University of Maryland School of Medicine, Membrane Biochemistry Research Laboratory, Dept. of Biol. Chem. 660 W. Redwood St., Baltimore, MD 21201

When methylmercury (MeHg) or mercuric chloride ($HgCl_2$) are administered to male rats by gastric gavage (8mg/kg), they are found to inhibit the binding of [3H] quinuclidinyl benzilate ([3H] QNB) to brain muscarinic acetylcholine receptors. After a single dose treatment, the inhibition of [3H] QNB binding is time-dependent, reaching a maximum of 40-45% inhibition after 15 days, then declining to control levels after 30 days. MeHg was more potent than $HgCl_2$ in inhibiting the [3H] QNB binding. When mercury compounds are administered once a day for five days, [3H] QNB binding is maximally inhibited (45-50%) after 10-20 days from the last dose. The effect of these compounds did not seem to have a differential effect on muscarinic receptor agonist or antagonist binding. In addition, both MeHg and $HgCl_2$ inhibited free sulfhydryl (SH) groups. After a single dose, their effect on SH groups preceded their effect on receptor binding. There is a very good temporal and quantitative correlation between the effects of the mercurial compounds on both these parameters after the repeated dosage schedule. The present results emphasize the importance of SH groups in muscarinic receptor binding. (Supported by the National Institute of Environmental Health Sciences (ES-1248) the Department of Energy (DE-AS0580EV10329).

M-AM-Pos53 THE SECONDARY STRUCTURE OF RECONSTITUTED ACETYLCHOLINE RECEPTOR AS DETERMINED BY RAMAN SPECTROSCOPY. Eddie L. Chang and Paul Yager, Code 6512, Optical Probes Branch, Optical Sciences Division, Naval Research Laboratory, Washington, DC 20375 U.S.A.; Robert W. Williams, Biochemistry Department, Uniformed Services University of the Health Sciences, 4301 Jones Bridge Road, Bethesda, MD 20014 U.S.A.; Adam W. Dalziel, Department of Chemistry, 225 Prospect Street, Yale University, New Haven, CT 06511 U.S.A.

Analysis of the secondary structure of the reconstituted acetylcholine receptor was performed by Raman spectroscopy. The receptor was isolated from electric organ of *Torpedo californica*, purified by affinity chromatography and reconstituted into vesicles of dielaidyl phosphatidylcholine. Because a pure lipid component was used for the reconstitution, the C=C stretching band could be subtracted from the spectra, allowing quantitative analysis of the amide I band of the receptor protein. The percentages of structural types are 25% ordered α -helix, 14% disordered α -helix (helix ends), 34% antiparallel β -sheet, 0% parallel β -sheet, 16% β -turn, and 10% undefined structure. These measurements allow estimates of the maximum number of long α -helical segments that could be present in the receptor. The effects of temperature and binding of agonists on both protein and lipid will also be presented.

M-AM-Pos54 SINGLE ACh-ACTIVATED CHANNELS RECORDED FROM CULTURED CILIARY GANGLION NEURONS WITH PERFUSED PATCH CLAMP ELECTRODES. D.J. Nelson and J.M. Tang. Dept. Physiology, Rush Medical College, Chicago, Illinois 60612.

ACh-activated single channel currents have been examined with internally perfused patch-clamp electrodes in chick ciliary ganglion neurons in dissociated cell culture. Cells were maintained in 25 mM K⁺ MEM. Cells were grown on lysed fibroblast substratum which aided attachment and subsequent neurite outgrowth. Currents were recorded from intact cells and excised membrane patches utilizing the gigohm seal patch clamp technique. Pipettes were used which allowed the addition of the agonist ACh to the electrode tip at a desired interval. Drug solutions applied internally, diffused to the tip within 3 min. Currents activated by ACh appear to be K⁺ selective with conductances scaling in proportion to the K⁺ concentration present within the pipette and bath. As some spontaneous K⁺ channel activity occurred in the absence of ACh in the pipette, the addition of ACh to the tip of the pipette in an on-line fashion was essential in determining conductances activated specifically via ACh binding. Currents recorded from on-cell patches where the pipette contained 160 mM KCl reversed at a pipette potential of approximately -60 mV. The I-V relationship obtained from excised patches in symmetrical 25 mM KCl was linear with a single channel conductance of 100 pS over the voltage range 0 to 100 mV. Single channel lifetimes in excised patches in 25 mM K⁺ were exponentially distributed at any given applied potential with a mean channel lifetime of 2.34 and 0.80 ms at +90 and +20 mV respectively. (Supported by NIH Grant NS18587)

M-AM-Pos55 KINETICS OF ACETYLCHOLINE RECEPTORS ARE SLOWED IN RECEPTOR AGGREGATES INDUCED BY IN SITU ELECTROPHORESIS. S.H. Young and M.-m. Poo. Dept. of Physiology and Biophysics, Univ. of California, Irvine, CA 92717.

During maturation of the neuromuscular synapse, the density of acetylcholine receptors (AChRs) increases at the postsynaptic junctional membrane and decreases at the extrajunctional region. In rat and frog muscle, this change in receptor distribution is accompanied by a shortening of mean open time of the ionic channel associated with the AChR. Two possibilities exist: the kinetics of pre-existing AChR channels may be altered as a result of the clustering of receptors at the junctional membrane, or new AChR channels with faster kinetics are incorporated into the junctional membrane in place of the pre-existing channels. We examined the effect of AChR aggregation on the AChR channel kinetics by artificially inducing AChR aggregates on the surface of spherical *Xenopus* muscle cells in culture using the technique of in situ electrophoresis. Surprisingly, the mean open times increased. Electric fields of 2.5 V/cm were applied to 12-hr old cells for 12-14 hrs. When visualized with fluorescent α -bungarotoxin, 76% of the cells showed dense AChR aggregates within a solid angle of 30° from the cathodal pole. When pre-treated with Con A (10 ug/ml), only 6% of the cells showed such aggregates. The mean open time of the channels was measured with the gigohm-seal technique. Recordings were made on the cell surface within a 30° solid angle of the cathodal and anodal poles. In 6 out of 9 experiments, the ACh channels on the cathodal poles had mean open times which were significantly slower than those from the anodal poles and control cells (cathode: anode: control = 1.88:1.00:0.98). In 5 cells pre-treated with Con A, the mean open times measured at two poles were similar (cathode: anode = 1.04:1.00), consistent with the finding of no aggregation in Con A treated cells. This work is supported by a grant from NSF and a Muscular Dystrophy Association Fellowship.

M-AM-Pos56 CYCLIC AMP-INDUCED POTENTIATION OF MUSCARINIC HYPERPOLARIZATION IN NEUROBLASTOMA CELLS. Akinobu Tsunoo and Toshio Narahashi (Intr. by Stephen M. Vogel). Dept. Pharmacol., Northwestern Univ. Med. Sch., 303 E. Chicago Ave., Chicago, IL 60611.

A variety of neurotransmitters and hormones cause changes in the intraneuronal cyclic nucleotide level. Synaptic potential could also be modulated by a change in the cyclic nucleotide level. We have examined how the acetylcholine (ACh)-induced muscarinic hyperpolarization of N1E-115 neuroblastoma cells is affected by agents known to change the intracellular cyclic AMP level. Membrane potential was measured by an intracellular microelectrode, and ACh was applied by iontophoresis. Other drugs were applied by bath perfusion. ACh produced a transient nicotinic depolarization. Dibutyryl cyclic AMP (1-2 mM) did not markedly affect the nicotinic response, but in 13 out of 17 cells tested, it increased the amplitude of muscarinic hyperpolarization to 161 ± 11% (mean ± S.E.M.) of the control without changing the resting membrane potential. In the other 4 cells, the muscarinic hyperpolarization remained unchanged. Intracellular pressure injection of cyclic AMP also potentiated the muscarinic hyperpolarization. In contrast, dibutyryl cyclic GMP (1-2 mM) did not affect the muscarinic hyperpolarization (109 ± 9%, n=4). RO 20-1724, a phosphodiesterase inhibitor, increased the amplitude of muscarinic hyperpolarization to 228 ± 20% (n=3). 2-chloroadenosine (0.2 mM) and prostaglandin E₁ (4 μM), which are known to increase cyclic AMP, potentiated the muscarinic hyperpolarization to 196 ± 35% (n=4), respectively, without changing the resting membrane potential. It is suggested that cyclic AMP plays a role as a messenger in potentiating the muscarinic hyperpolarization in neuroblastoma cells. Supported by NIH grant ES 02330.

M-AM-Pos57 INTERACTIONS OF TETRAETHYLAMMONIUM IONS WITH SINGLE ACETYLCHOLINE CHANNELS IN CULTURED RAT MUSCLE. Brendan S. Wong and Harold Lecar, Laboratory of Biophysics, NINCDS, NIH, Bethesda, MD 20205, and Michael Adler*, Neurotoxicology Branch, USAMRICD, APG, MD 21010

Tetraethylammonium (TEA) has been reported to modify the kinetics and conductance of the end-plate current (EPC) at frog neuromuscular synapses by inducing a non-linearity in the EPC I-V relationship and a shortening in the EPC decay with a concomitant reduction in its voltage dependence. To elucidate the mechanisms of action of TEA on nicotinic, cholinergic channels, we have examined the effects of TEA (1-200 μ M) on single suberyldicholine (Sub)-induced current fluctuations on both cell-attached and excised patches. Under control conditions, the channel opening frequencies generally increased exponentially with hyperpolarization. However, the opening frequencies were markedly reduced in the presence of TEA. In the presence of 1 μ M Sub and 1 μ M TEA, the frequency of activation was reduced to ~40% of control. For potentials between -50 to -100mV, the opening frequencies decreased in the presence of TEA but showed a tendency to increase with hyperpolarization. While for potentials more negative than -140mV and for TEA concentrations >10 μ M, the opening frequencies decreased with hyperpolarization. In both the presence & absence of TEA, open- and closed-time histograms were found to be better fit by a double than by a single exponential. The mean open-time was reduced in the presence of TEA but did not show a consistent voltage or concentration dependence. Channel openings also tend to occur in bursts in the presence of TEA. At the concentrations examined, TEA did not appreciably alter the single-channel conductance, I-V or reversal potential. The voltage- and concentration-dependent change in channel opening frequency in the presence of TEA appears to underlie the macroscopically observed non-linear I-V relationship.

M-AM-Pos58 THERMODYNAMIC PARAMETERS OF ENDPLATE CHANNEL BLOCKADE. James McLarnon and David M. J. Quastel. Department of Pharmacology, Faculty of Medicine, The University of British Columbia, Vancouver, B.C., CANADA, V6T 1W5.

A thermodynamic analysis has been applied to the reaction kinetics for drug blockade of post-synaptic channels at the mouse neuromuscular junction. The temperature dependence of both the channel plugging and channel unplugging rate constants (determined from a sequential model) was measured over a temperature range from 10°C-25°C for procaine, scopolamine, octanol and heptanol. From this data the thermodynamic parameters of energy of activation, enthalpy, and entropy, associated with the drug effects, were determined. The results indicated that in the formation of the transition state complex the channel blocking step had large positive entropy changes for the two alcohols and smaller positive entropy changes for the two local anaesthetics, and in addition, positive enthalpy changes for all the agents. Similar changes in entropy and enthalpy have been measured in other systems and associated with the formation of hydrophobic bonds. Further evidence for hydrophobic bonding was indicated by the similarity in activation energies for heptanol and octanol channel block despite a two-fold difference in the magnitudes of their onward rate constants. Significant differences were noted between the enthalpies of activation for channel blockade for the alcohols compared with the values for the two charged local anaesthetics. No significant variation in the activation energies for channel unplugging was observed between any of the agents studied. A similar thermodynamic analysis applied to the blocking of ion-selective channels could give some insight into the mechanisms governing reaction kinetics in such systems. (Supported by funds from the British Columbia Health Care Research Foundation).

M-AM-Pos59 FUNCTIONAL PROPERTIES OF NON-JUNCTIONAL ACETYLCHOLINE RECEPTORS ON INNERVATED MUSCLE. P. Brehm, F. Moody-Corbett and R. Kullberg*, Dept. of Physiology, Tufts U. School of Medicine, Boston, MA 02111 and *Dept. of Biology, U. of Alaska, Anchorage, AK 99504. (Intr. by H. Mautner)

Patch clamp recording from acetylcholine-activated channels was performed on *in vivo* myotomal muscle from mature *Xenopus* tadpoles. Intact tails from stage 47 to 50 tadpoles were treated with collagenase, and experiments were performed in high K⁺ solution (20 mM) in order to block contraction. Amplitude-histograms of channels recorded with 0.25 μ M ACh in the pipette often showed two well-separated peaks. At applied hyperpolarizing potentials (40 to 200 mV) the larger amplitude class corresponded to a conductance (γ) of 77 ± 19 pS. A generally less predominant smaller amplitude class corresponded to 57 ± 13 pS. The mean channel open time (τ) of the smaller class averaged 2.1 ms at +40 mV and 3 ms at +120 mV (potential of patch pipette) while the larger amplitude class averaged 0.6 ms and 1.9 ms at these respective potentials (20°C) indicating kinetic differences between amplitude classes. Recordings with either no ACh or with 10^{-6} M α -bungarotoxin revealed channel activity in 35% of patches tested. In the absence of ACh γ was 48 pS and the extrapolated reversal potential was approximately -16 mV, similar to the values for the ACh-activated channels. The kinetics of this channel type differ from either class of ACh-activated channels in that the estimated τ was very short (<0.8 ms) at all measured potentials. The results of this study indicate that at least two functionally different ACh receptor channels are present in the nonjunctional membrane of mature innervated myotomal muscle. The similarities between these channels and the channels recorded in the absence of ACh suggests that ACh receptor channels in *Xenopus* myotomal muscle may open in the absence of ACh. Supported by NIH, MDA & MDAC.

M-AM-Pos60 LIPID PERTURBATIONS MAY ACCOUNT FOR THE ABILITY OF GENERAL ANESTHETICS TO INCREASE THE BINDING OF ACETYLCHOLINE TO ITS RECEPTOR. L.L. Firestone, H.A. Franch, L.M. Braswell and K.W. Miller, Departments of Pharmacology and Anaesthesia, Harvard Medical School, Massachusetts General Hospital, Boston, MA 02114.

Volatile and alkanol general anesthetics increase the equilibrium binding of [³H] acetylcholine (ACh) to receptor-rich membranes from *Torpedo* electroplaques. This effect is attributable to an increase in ACh binding affinity. It may result from a perturbation of the lipids surrounding the receptor. To test this, the anesthetic concentration causing a half-maximal increase in ACh binding (EC₅₀) was determined for eight volatile and six alkanol anesthetics. To a first approximation, their EC₅₀s were about twice their anesthetic concentration (ED₅₀), which suggested their action is related to their lipid solubility. Indeed there is a fair correlation between EC₅₀ and lipid bilayer partition coefficient for the nine agents for which bilayer data is available. However, the most potent anesthetic agents (decanol, octanol and thiomethoxyflurane) were four to seven fold less effective than predicted by either the lipid hypothesis or their ED₅₀s. This would invalidate the lipid hypothesis unless *Torpedo* membranes differ from simple lipid bilayers in their ability to be perturbed by anesthetics. Therefore, *Torpedo* membranes were labeled with 5-doxyl-palmitate and the ability of the deviant agents, octanol and thiomethoxyflurane, to change lipid order were compared to the typical less potent agents, butanol and fluroxene. The mean change in order parameter at the EC₅₀ of these four agents is about 0.02 with a standard deviation of about forty percent of the mean. Thus, these data are consistent with a lipid perturbation hypothesis. (Supported by GM-15904 and GM-07592.)

M-AM-Pos61 NET UPTAKE OF DOPAMINE INTO BOVINE CHROMAFFIN GHOSTS. CHANGES IN V_{max} AND K_M AS A FUNCTION OF THE INTRA AND EXTRAVESICULAR pH. R.G. Johnson, S.J. Hayflick, A. Pallant, S.E. Carty, and A. Scarpa. Univ. of Penna. Dept. Biochem/Biophys., Phila., PA 19104.

Insight into the overall mechanism of catecholamine transport in chromaffin granules, with special emphasis on the molecular species of the catecholamines transported, was obtained using a highly purified preparation of chromaffin ghosts virtually devoid of amines. Net uptake of dopamine in these ghosts was kinetically measured by amperometrically detecting the concentration of extravesicular free dopamine with a glassy carbon electrode (Hayflick et al., *Anal. Biochem.* 126:58, 1982). When ghosts were formed in highly buffered sucrose and the intravesicular pH held constant at pH 5.8, varying the pH of the extravesicular space produced a marked change in apparent K_M . It was 18 μ M at pH 8.2 and progressively increased to 65 μ M at pH 6.6. These data are quantitatively consistent with the notion that the uncharged dopamine is the species which is translocated by the reserpine-sensitive carrier. By contrast, when the extravesicular pH was kept constant at pH 7.0 and the internal pH was changed by the addition of varying concentrations of NH_4^+ , the apparent K_M rose exponentially from 40 to 202 μ M as the intravesicular pH was increased from 5.8 to 6.6. The apparent V_{max} was found to decrease with increasing intravesicular pH, but was constant (51 nmol/min/mg protein) when the extravesicular pH varied over the range of 6.6-7.7. These data are consistent with the operation of a catecholamine carrier transporting undissociated catecholamines across the chromaffin granule membrane and with the requirement of carrier and/or catecholamine protonation on the chromaffin granule inside. (Supported by HL-18708 and HL-24010 from the National Institutes of Health).

M-AM-Pos62 COMPETITIVE BINDING OF β -ENDORPHIN AND DYNORPHIN TO CEREBROSIDE SULFATE IN SOLUTION.

Chuen-Shang C. Wu, Nancy M. Lee,* Horace H. Loh,* and Jen Tsi Yang. Cardiovascular Research Institute and *Langley Porter Psychiatric Institute, University of California, San Francisco, CA 94143.

β -Endorphin and dynorphin are opioid peptides found in living tissues. A dynorphin fragment (1-13) is a weak analgesic, but it can inhibit morphine- or β -endorphin-induced analgesia. We hypothesize that dynorphin may displace bound β -endorphin from the opiate receptor in vivo. Thus, the binding of dynorphin (1-13) and β -endorphin to cerebroside sulfate was studied with circular dichroism as a probe. Cerebroside sulfate, a membrane lipid, is thought to be part of the receptor complex. On the basis that bound β -endorphin, but not bound dynorphin, shows a helical conformation, we found that dynorphin (1-13) stoichiometrically displaced bound β -endorphin from the peptide-lipid complex. Similar results were obtained for the competitive binding of the two peptides to sodium decylsulfate, an amphiphile which simulates cerebroside sulfate and can be quantitated by potentiometric titration. The binding of dynorphin (1-13) to the surfactant was highly cooperative and became saturated at about 1 mM free surfactant, but the binding of β -endorphin was less cooperative and reached its saturation at about 2 mM free surfactant. Therefore, we conclude that the binding affinities of dynorphin (1-13) to cerebroside sulfate and sodium decylsulfate are stronger than those of β -endorphin. These findings support our working hypothesis that dynorphin may displace β -endorphin or morphine at the receptor site.

Supported by USPHS Grant GM-10880, DA-1696, and DA-2643.

M-AM-Pos63 ARCHITECTURAL FEATURES OF ELECTROPHYSIOLOGICAL SUBDIVISIONS OF THE MECHANORECEPTIVE THALAMUS OF RACCOONS. S.I. Wiener, J.I. Johnson, E.-M. Ostapoff, Depts. of Biophysics, Anatomy and Psychology and Neuroscience Program, Michigan State University, East Lansing, MI 48824.

Raccoons have relatively large portions of their nervous systems devoted to receiving projections from mechanoreceptive fields in their forelimbs (e.g., Welker, W.I., *et al.*, *Amer. Zool.*, 4:75-94). In raccoons, immobilized with ketamine and anesthetized with Dial-urethane, we used tungsten microelectrodes to record electrical activity (unit clusters) evoked by mechanical stimulation. A fine grid (0.1-2.0 mm spacings) of microelectrode penetrations was made. The tissues were then frozen sectioned and alternate section series were reacted for Nissl substance, myelin, cytochrome oxidase or acetyl cholinesterase.

Electrolytic lesions placed as tissue markers reveal that: 1) the mechanoreceptor projection zone of the adult raccoon thalamus has higher cytochrome oxidase and lower acetyl cholinesterase staining than other thalamic regions, 2) the kinesthetic projection zone of the ventrobasal thalamus is separated from the rest of ventrobasal thalamus by bundles and laminae of myelinated fibers, 3) fiber bundles divide projections from noncontiguous body parts within both kinesthetic and cutaneous body projection zones. These subdivisions are particularly well marked in histological sections stained for cytochrome oxidase activity. (Supported by NSF Grant BNS 81-080731).

M-AM-Pos64 TIGHT JUNCTIONS AND INTRAMEMBRANE PARTICLES OF CULTURED OLIGODENDROCYTES. PT Massa*, S. Szuchet** & E Mugnaini*, Dept. Biobehavioral Sc, U of Conn, Storrs, CT; Dept. Neurology* U of Chgo, Chgo, IL

Oligodendrocytes are isolated from ovine white matter by our modified procedure. The cells plated on polylysine coated dishes, attach and develop an extensive network of processes. They appear highly differentiated as evidenced by their ability to express characteristic markers; e.g.; they fluoresce intensely when stained with an anti-galactocerebroside serum. One day after isolation and at two and three weeks thereafter, the cells were fixed and processed for thin section and freeze-fracture EM. Thin sections of one day suspension cultures show a nearly homogeneous population of rounded cells of varying electron density resembling oligodendrocytes. One to three weeks after plating, the cell bodies are more homogeneously electron dense, they contain numerous microtubules, large number of electron dense vesicles, well developed Golgi regions and intermediate filaments. The cells emanate numerous processes, cylindrical and flattened, which adhere to one another, to the cell body and to the dish. Freeze-fracture of one day suspension culture shows plasma membrane with patches of intramembrane particles but no cell junctions. After one to three weeks in culture the particles become more numerous and evenly distributed. They cleave somewhat preferentially with the P phase and like those of oligodendrocytes *in vivo* are categorized as globular and elongated. In addition, tight junctional arrays appear and become increasingly numerous with time in culture. These junctions consist of strands and/or rows of particles that are parallel to one another or anastomosed. Thus, the plasma membrane of cultured oligodendrocytes develop features characteristic of mature oligodendrocytes *in situ* in the absence of the normal tissue framework which include neuronal and astrocytic elements. Supported by grants US-PHS #09904 and NMS Soc #RG-1223-B3.

M-AM-Pos65 H^+ TRANSPORT ACROSS THE MEMBRANE OF EHRlich ASCITES TUMOR CELLS. Jesse W. Bowen and Charles Levinson. Univ. of TX. Health Science Center, Department of Physiology, San Antonio, TX. 78284

P_i transport in Ehrlich cells is inhibited following prolonged incubation below pH 6.9. However, upon return to pH 7.4 inhibition of transport is relieved. This observation prompted us to investigate the response of intracellular pH to changes in extracellular pH. Preliminary experiments indicated that ^{14}C -DMO (Dimethylloxazolidine-2,4-Dione,5,5-[2- ^{14}C]) rapidly crossed the membrane and thereby provided a convenient method for monitoring changes in intracellular pH. The intracellular pH approximated the extracellular pH when the medium was pH 7.3. MES (0.3 osmolar) was added to reduce the medium pH to 5.5. Intracellular pH fell to 6.3 with a half-time of approximately 5 min. at 37°C. Influx of H^+ was completely inhibited at 4°C but not by depletion of cellular ATP or reduction of extracellular Na^+ (15 mM). Total replacement of Na^+ by K^+ also did not affect H^+ influx while nigericin (10 μM) decreased the half-time to less than 0.5 min. To study H^+ efflux, cells were incubated at pH 5.5 so that intracellular pH was 6.3. HEPES (0.3 osmolar) was added to increase the medium pH to 7.3. Intracellular pH increased to 7.3 with a half-time of about 1.7 min. at 37°C. Efflux of H^+ was completely inhibited at 4°C as well as by the depletion of cellular ATP. It was not inhibited by the reduction of extracellular Na^+ (15 mM) or when Na^+ was completely replaced by K^+ . Ouabain (1 mM), SITS (0.1 mM), and amiloride (1 mM) had virtually no effect on H^+ efflux. The results of these experiments suggest that H^+ movement in both directions across the membrane is mediated. However, only H^+ efflux is linked to energy metabolism. (Supported by Grant CA32927, NCI, USPHS)

M-AM-Pos66 MEMBRANE POTENTIAL CHANGES DURING D-GLUCOSE AND L-ARGININE TRANSPORT ACROSS RAT RENAL BRUSH BORDER MEMBRANES. G.Nassif, T.Jean, P.Poujeol and P.Ripoche. Dept.of Biology,CEN Saclay, 91191 GIF/YVETTE CEDEX, France.

The fluorescent intensity of the 3, 3'-dimethylindodicarbocyanine iodide (diI-C1-(5)) can be specifically related to changes of electrical membrane potential induced by an artificially imposed valinomycin-potassium diffusion gradient across renal brush border vesicles. The quenching of fluorescence was linear between 60 and 150 mV. An equal reduction of this quenching was observed by an additional inwardly directed gradient of 10mM NaCl or LiCl corresponding to a 10 mV potential variation. As expected, 10 mM D-glucose induced an additional depolarization of 21 mV, only in the presence of a NaCl gradient. If D-glucose was replaced by 10mM L-arginine, a depolarization of about 21 mV was observed in the presence of either a NaCl or a LiCl gradient. This last result was not compatible with the Na^+ cotransported hypothesis for the L-arginine uptake. Moreover, if the electrical membrane potential was carried out by preloading vesicles with 50 mM K_2SO_4 instead 100 mM KCl, the diffusion potential was differently affected in our system by an inwardly directed gradient of 50 mM Na_2SO_4 or Li_2SO_4 . Since SO_4^{2-} was electroneutrally cotransported with Na^+ (Lucke H. et al., *Biochem.J.* 1979,182,223-229), the fluorescence quenching was significantly higher in the presence of Na_2SO_4 than in the presence of Li_2SO_4 . This membrane potential change (10 mV) could explain why the L-arginine uptake measured in Li_2SO_4 has been found lower than the uptake measured in Na_2SO_4 medium.

M-AM-Pos68 PARTIAL PURIFICATION AND CHARACTERIZATION OF THE $(Ca^{2+} + Mg^{2+})$ -ATPase FROM SQUID OPTIC NERVE. Condrescu, M., Osses, L., DiPolo, R. (Intr. by Whittembury, G.). Centro de Biofísica y Bioquímica, Instituto Venezolano de Investigaciones Científicas (IVIC), Apartado 1827, Caracas 1010 A, Venezuela.

A membrane fraction enriched in axolemma was obtained from optic nerves of the squid (*Sepiotheutis sepioidea*) by differential centrifugation and density gradient fractionation. The preparation had an $(Ca^{2+} + Mg^{2+})$ -ATPase specific activity of about 3.0 $\mu mol Pi \cdot mg^{-1} \cdot h^{-1}$, which was oligomycin (10 $\mu g/ml$) and Na azide (1 mM) insensitive. Further treatment of the membrane fraction with 1% Nonidet P-40 resulted in a partial purification of the ATPase of almost 15 fold compared to the initial homogenate. The dependence of the ATPase activity on calcium concentration revealed the presence of two saturable components. One had a high affinity for calcium ($K_m = 0.1 \mu M$) and the second had a comparatively low affinity and was observed above 20 μM free calcium. Calmodulin (12.5 $\mu g/ml$) stimulated the $(Ca^{2+} + Mg^{2+})$ -ATPase by approximately 50% and this stimulation was abolished by Trifluoperazine (10 μM). This $(Ca^{2+} + Mg^{2+})$ -ATPase from squid optic nerve displays properties closely resembling those of the uncoupled Ca pump described in internally dialyzed squid axons.

Supported by Grants N° S1-1144 and RH 15-123 from CONICIT, Venezuela.

M-AM-Pos69 EXTERNAL Na COULD INHIBIT THE Na,K-ATPase AND Na PUMP WITH HIGH APPARENT AFFINITY IN THE ABSENCE OF EXTERNAL SITES WITH HIGH AFFINITY FOR Na, L.Beaugé, División de Biofísica, Instituto M. y M. Ferreyra, 5000 Córdoba, Argentina.

Several reactions catalyzed by the Na,K-ATPase and the Na Pump show biphasic behavior as a function of external Na: when $[Na]_o$ increases between zero and 5-10 mM there is inhibition, which is followed by stimulation at $[Na]_o > 10$ mM. This has been explained on the basis of external sites with high affinity for Na where this cation exerts an inhibitory effect; the stimulation at high $[Na]_o$ is attributed to an unspecified "release of inhibition" by Na_o acting at low affinity sites. This communication shows that similar results can be obtained by a different mechanism which is based on the existence of a single type of sites (3 external Na sites, equivalent and non interacting). According to the $[Na]_o$ there are 4 possible enzyme forms: E, ENa, ENa₂ and ENa₃. Assuming that only E and ENa₃ are catalytic the reaction velocity becomes proportional to

$$(1 - (1 / (1 + K / [Na]_o)))^3 + n (1 / (1 + K / [Na]_o))^3$$

where K is the Na-site dissociation constant and "n" is the catalytic activity of ENa₃ relative to E. This equation predicts a biphasic curve of activity vs. $[Na]_o$ with inhibition by Na_o acting with high apparent affinity.

M-AM-Pos70 Na,K-ATPase: COMPREHENSIVE MODEL FOR THE EFFECT OF Na⁺, K⁺ and TRIS⁺ ON THE PHOSPHOENZYMES Nørby, J.G., Klodos, I. and Christiansen, N., Inst. Biophys. Univ. Aarhus, DK-8000 Aarhus C Denmark (Intr. by John F. White, Dept. Physiol., Emory Univ., Atlanta, Ga 30322, USA). Ox brain Na,K-ATPase was phosphorylated by incubation for 60 sec, with 1 mM Mg²⁺, 25 μM AT₃₂P and $[Na^+] = 20-600$ mM at 0 °C. The dephosphorylation kinetics of E₃₂P was studied under 4 conditions: Addition of 1 mM ATP or 2.5 mM ADP, or 2.5 mM ADP + Na⁺ (up to 600 mM), or 1 mM ATP + 20 mM K⁺. The results could be explained by a 3-pool model (necessary since "ADP-sens.EP" + "K⁺-sens.EP" was always > 100%), each pool, A, B or C, containing an equilibrium (Na⁺-dependent) mixture of EP-forms. The rate coefficients of the 3-pool model depend on $[Na^+]$, $[K^+]$ and $[Tris^+]$. Pool A is ADP-sensitive and at high $[Na^+]$, pool B is also since it is converted rapidly to A. Both B and C are dephosphorylated rapidly by K⁺, but the A→B conversion is blocked by K⁺ so that pool A can be an intermediate only of the Na-ATPase but not of the Na,K-ATPase cycle. Tris⁺ slows the A→B conversion as well as the dephosphorylation of B and C, thus increasing the steady-state proportion of A, the "ADP-sens.EP". A detailed analysis of the 3-pool model, based also on results published by others, shows that a comprehensive model furthermore must have these features: EP in pool A has 3 high aff. inside Na⁺-sites, B has 3 and C 2-3 low aff. outside Na⁺-sites. Either the 3 outside or the 3 inside sites must be occupied for translocation to occur and Na⁺-translocation precedes the major conformational change of E₁P to E₂P. The putative high aff. outside Na⁺-site may be on E₂P in C. The model also accounts quantitatively for the complex relation between $[Na^+]$ and Na-ATPase activity. (Supported in part by the Danish Medical Research Council).

M-AM-Pos71 Sidedness of pH dependence of the sodium pump in dialyzed squid giant axons. Gerda E. Breitwieser and John M. Russell. University of Texas Medical Branch, Dept. of Physiology and Biophysics, Galveston, TX 77550.

The pH optimum for ATP hydrolysis via the isolated sodium pump fails to give information about the specific site of proton action. In order to approach this problem, we have examined the effects of internal and external pH changes on the ouabain-sensitive sodium efflux in dialyzed squid giant axons. The control condition was p_{Ho} = 8.0 and p_{Hi} = 7.35. The external solution composition, in mM, was: 425 NaCl, 10 KCl, 3 CaCl₂, 10 MgCl₂, 0.1 Na₂ EDTA and 10 buffer (EPPS at pH 8.0, HEPES at pH 7.5, PIPES at pH 6.8 and MES at pH 6.2). Final osmolarity was 970 mosm. The dialysis fluid contained, in mM: 250 K glutamate, 50 Na glutamate, 100 KCl, 140 glycine, 25 Mg (glutamate), 2 K₂EGTA, 0.5 phenol red, 20 Na₂ATP and 20 buffer: PIPES (pH range 6.4-7.2), HEPES (pH range 7.0-7.8) or EPPS (pH range 7.8-8.6); final solution osmolarities were adjusted to 965 mosm. We found that external pH changes over the range 6.2-8.1 did not affect the ouabain-sensitive Na efflux. However, ouabain-sensitive Na efflux was quite sensitive to changes in internal pH. The internal pH optimum for Na efflux by the Na pump was 7.3-7.4, with half-maximal inhibition at pH 6.5 and pH 8.6 (at 90 mM Nai + 265 mM Ki and 428 mM Nao + 10 mM Ko). These effects were not due to limiting MgATP concentrations, since the levels are calculated to vary only slightly from pH 6 to pH 9 (MgATP = 19.83 mM at pH 6.0 and 19.99 mM at pH 9.0). Thus, the effects of pH on ouabain-sensitive Na efflux appear to be mediated solely at internal sites. (Supported by NIH grant NS 11946.)

M-AM-Pos72 INTERCELLULAR pH, 2 DEOXYGLUCOSE AND SUGAR PHOSPHATE PROFILE CHANGES IN MORPHOLOGICALLY DIFFERENTIATING NEUROBLASTOMA N1E 115 CELLS

P. Glynn,^{1,2} T. R. Brown,¹ K. Ugurbil,³ R. Chappel,² 1. Bell Laboratories, Murray Hill, NJ 07974
2. Department of Biological Sciences, Hunter College of the City University of New York, NY, NY
3. Gray Freshwater Biological Institute, Navarre, MN 55392

We have determined the ability of differentiated and undifferentiated N1E 115 cells to adhere to four different types of microcarriers and have used cytodex III microcarriers to establish a circulating closed culture system in a single turn ³¹P solenoid probe built for use with a Bruker 360 wide bore NMR spectrometer. We were able to resolve the alpha peak of ATP with a signal to noise ratio of 4:1 in 1.5 minutes. The cells were established on the culture system for three days, induced to differentiate morphologically by switching from 10% FBS supplemented medium to 1.5% DMSO, 1% FBS supplemented medium, and monitored for an additional five days for intercellular pH, high energy sugar phosphates and ATP. In a second experiment the rate of appearance of 2 deoxyglucose was also monitored by supplementing the medium with 5mM 2DG for thirty minute pulses. Similar experiments were run and extracts made for pre and post differentiated cells. Experiments are in progress to determine the rate of 2DG uptake at various times during the cell growth and differentiation.

M-AM-Pos73 ELECTRICAL AND CONTRACTILE ACTIVITY OF SINGLE ADULT MAMMALIAN CARDIAC CELLS
M. Horackova, Dalhousie University, Halifax, Nova Scotia, Canada

The electrical and contractile activities of enzymatically dissociated cardiac myocytes (from dog and rabbit) are recorded simultaneously. The Ca-tolerant isolated cardiac cells are stimulated and the action potentials are recorded by conventional microelectrodes. The contractile activity of these electrically driven single cells is at the same time recorded by T.V. camera (attached to an inverted microscope) and the amplified images of these contracting cells are recorded by video cassette recorder. Later, these contractions are analysed on a T.V. monitor by using the stop-frame capability of the video recorder and the Zeiss Interactive Image Analysis System (IBAS). With this system we can manually measure the shortening of the muscle fibre - represented by changes in cell's length at the frequency of T.V. recording (30/sec), i.e. the contractile ("isotonic") activity is measured at 33-msec intervals. These contractions are then plotted and analysed by computer in terms of their amplitude, dT/dt and rate of relaxation. Our data demonstrate that this technique is sufficiently sensitive to record changes in contractile force (in the rate and the amplitude of shortening) caused by modifications of frequency of stimulation or ionic composition of the bathing solution. Furthermore, our data suggest that the properties of these preparations of single cardiac cells resemble closely those of the respective intact tissues, and thus, these isolated myocytes could serve as a valuable tool in studies of excitation-contraction coupling in the heart.

(Supported by MRC of Canada, MT-4128, and the Nova Scotia Heart Foundation)

M-AM-Pos74 IONIC & PHARMACOLOGICAL DEPENDENCE OF POST-DRIVE CURRENT IN CANINE PURKINJE FIBERS.
Falk & I.S.Cohen, Dept. of Physiology & Biophysics, SUNY at Stony Brook, N.Y. 11794

Post-drive current was induced as previously described (Cohen, Falk, & Kline, 1981.Biophys.J.33:281-288; Falk & Cohen, 1981.Biophys.J.33:36a). We have reported that current through both the TTX-sensitive fast inward channel and the D600-sensitive slow inward channel during drive can generate post-drive current (Falk & Cohen, 1982.Biophys.J.37: 244a). Post-drive current generated in either of these 2 ways is eliminated by 10^{-5} M dihydro-ouabain. We also examined the effect of $[K^+]$ on the post-drive current. The K_m , mean τ in 4 mM $[K^+]_B$, and k_{max} are 1.2 mM, 83.2 ± 7.0 sec (\pm S.E.M.), and $.017$ sec $^{-1}$, respectively (n=9). These results include experiments in which depolarizing pulses during the drive opened only fast inward channels and also include experiments in which loading occurred through both fast & slow inward channels. The $[K^+]$ and DHO effects suggest that the post-drive current is largely Na/K pump current. Epinephrine speeds the decay time constant. The mean normalized τ in $5-10 \times 10^{-6}$ M epinephrine is $.80 \pm .07$ (\pm S.E.M., n=6). We also looked at the effects of Ca^{+2} and Na^+ . Reducing $[Ca^{+2}]$ below 4 mM slows τ . The mean τ , normalized to that obtained in 4 mM $[Ca^{+2}]$ for each fiber in 1, 2, 2.7, and 8 mM $[Ca^{+2}]$ is $1.12 \pm .05$ (n=4), $1.15 \pm .11$ (n=7), $1.19 \pm .03$ (n=6), and $1.00 \pm .05$ (n=4), respectively. 50% $[Na^+]$ (choline subst.) may speed the decay time constant. The mean normalized time constant in 50% $[Na^+]$ is $.92 \pm .08$ (n=3). The effects of Na^+ and Ca^{+2} might be due to saturation effects, even at low $[Na^+]_i$, on an internal Na^+ site of the ATPase or to direct/indirect contributions from other currents (e.g. Na/Ca exchange, Ca mediated g_K). Supported by HL 20558 and the AHA.

M-AM-Pos75 EXCITABLE MEMBRANE FUNCTION OF CULTURED PURKINJE NEURONS: INTRACELLULAR AND SINGLE CHANNEL ANALYSIS. D.L. Gruol (Intr. by G. Giotta), A.V. Davis Center for Behavioral Neurobiology, The Salk Institute, La Jolla, CA 92037.

Recent data suggest that intrinsic mechanisms, in addition to neuronal circuitry, play an important role in generating and regulating the electrical activity of vertebrate CNS neurons. To test this hypothesis, a cultured cerebellar model system was developed for studies of excitable membrane function in a well characterized CNS cell type, the Purkinje neuron (PN). Intracellular voltage recordings from cultured PNs revealed both intrinsic (pacemaker-like) and extrinsic (synaptic) components of activity. PNs displayed spontaneous synaptic potentials, evoked by cerebellar interneurons, and action potentials, occurring in either a simple spike firing pattern or burst mode. Both firing patterns were identified as arising from intrinsic, voltage-sensitive mechanisms. The extracellular patch clamp technique was used to resolve the ion channel population mediating the voltage-sensitive electrical activity characteristic of this neuronal type. Single channel recordings from the somal region of the PNs revealed a variety of inward and outward voltage-sensitive ionic channels. All patches studied (n=15) contained multiple channels (the same or different type). Channel activity was infrequent at 0 applied voltage and at hyperpolarized membrane potentials, but depolarization evoked extensive channel activity. The most easily characterized activity resulted from a 40 pS outward channel activated at +20mV depolarization and a 100 pS outward channel activated +60mV depolarization. The membrane distribution (soma vs dendrite), gating kinetics, ion selectivity and pharmacological specificity of these two channels are presently under investigation. (Supported by NIAAA 03504)

M-AM-Pos76 IONIC BASIS FOR DELAYED RECTIFICATION IN CARDIAC PURKINJE FIBERS. W.Green, J.Goto, and T.J.Colatsky, Dept. of Physiology, Cornell Medical College, New York, NY 10021 and Dept. of Medicine, University of Pennsylvania, Philadelphia, PA 19104.

The delayed rectifying outward current believed to govern termination of the cardiac action potential plateau was characterized in short (0.8-1.2 mm) rabbit Purkinje fibers using the two-microelectrode voltage clamp technique. Depolarizations positive to -40 mV lasting 1-10 sec activated outward currents which decayed slowly following repolarization. The outward tails could be fitted as the sum of two exponentials, with $\tau_1 \approx 500-600$ msec and $\tau_2 \approx 5-6$ sec at -50 mV. Reversal potentials (Erev) were determined from fully-activated current-voltage relations obtained using conventional protocols. These measurements were facilitated by the natural absence of a pacemaker current in the rabbit Purkinje fiber. Erev for the faster decaying component of tail current varied directly with external potassium concentration (K_o) as predicted by the Nernst relation: Erev = -87 ± 2 mV at $K_o = 4$ mM (mean \pm SD). The slower component of tail current reversed more positively at -62 ± 2 mV, consistent with a K channel having $P_{Na}/P_K = 0.04$. This channel appeared to become more K-selective as K_o was increased; Erev = -54 mV when $K_o = 16$ mM. The reversal of the slow component was not greatly altered by substituting isethionate for chloride in the bathing solution, or by addition of 2.7 mM $MnCl_2$. The fully-activated current-voltage relation for both components exhibited inward-going rectification and cross-over at higher K_o . These data confirm that the delayed rectifier current in cardiac Purkinje fibers is carried largely by K ions through two kinetically distinct channels, as previously reported by Noble and Tsien.

M-AM-Pos77 SINGLE K^+ CHANNELS OF THE INWARD RECTIFIER IN RAT VENTRICULAR MYOCYTES. I. R. Josephson and A. M. Brown, Department of Physiology and Biophysics, University of Texas Medical Branch, Galveston, Texas 77550.

Single K^+ channel and whole-cell currents have been recorded from adult (freshly dispersed) and neonatal (primary culture) ventricular myocytes using the cell-attached patch clamp method. The bath contained normal Tyrode solution and the patch pipette was filled with 150 mM KCL buffered to pH 7.4. During hyperpolarizing voltage steps (150 msec duration) from a holding potential of -50 mV the whole-cell currents showed an instantaneous component followed by a further transient increase in current which became very rapid at more negative potentials. A time-dependent decrease or inactivation of the peak inward current was observed and could be fit with two exponentials. The rate of inactivation became more marked at more negative potentials. The I-V curve of the steady state inward current (measured at 150 msec) displayed a negative resistance region below -100 mV. Single channel currents were inward and their amplitudes increased linearly as the potential was made more negative. The single channel conductance was found to be approximately proportional to $[K]_o^2$. The frequency of channel closures increased as the potential was made more negative. This "flickering" behavior may be associated with the relaxations seen in the whole-cell current. Power spectra of the single channel currents were fit best with a sum of two Lorentzians; one of which corresponded to the faster exponential rate of inactivation. The role of external Na and Cs ions in blocking the inward rectifier is presently under study.

Supported by NIH HL-25145 to AMB and NIH HL-06556 to IRJ.

M-AM-Pos78 EFFECTS OF 4-AMINOPYRIDINE ON CARDIAC ELECTRICAL ACTIVITY

Robert Bauer, Intr. by George E. Dambach, Wayne State U., Detroit, Michigan

Myocardial cells in the isolated tricuspid valve (TCV) of the rabbit exhibit rhythmic spontaneous activity. The activity is typically 1/2 to 2/3 of the sinoatrial nodal (SAN) rate, is not blocked by tetrodotoxin (TTX), but is blocked by verapamil. Action potentials have a maximum depolarization rate of 13 V/sec and a diastolic depolarization rate of 21 mV/sec. Preliminary studies have shown that external K^+ concentration affects this myocardial cell automaticity. To further clarify the role of K^+ in myocardial cell automaticity 4-aminopyridine (4-AP) was used in studies on TCV, SAN and right atrial (RA) tissues. A cumulative dose method was used with concentrations of 4-AP of 0.3 to 9mM. In these three tissues 4-AP caused a dose dependent prolongation of the action potential (150-250 msec in TCV). An increase in diastolic depolarization rate was observed in both the TCV and the SAN. The increased action potential duration in all tissues included both prolongation of the plateau and decreased repolarization rate (phase 3). In RA, 4-AP caused partial conversion of the action potential from "Na" type (TTX blocked) to "Ca" type (only partial TTX block) and also produced a small after-hyperpolarization. However, automaticity was elicited by 4-AP in RA only under conditions of tissue hypoxia.

The similarity of 4-AP actions on the three tissues indicates that the same K channels operate in these tissues, however, suppression of the K channels alone is not sufficient to elicit automaticity.

M-AM-Pos79 EFFECTS OF EPINEPHRINE, Ni⁺⁺, and Mn⁺⁺ ON EXTRACELLULAR CA⁺⁺ ACTIVITY FLUCTUATIONS IN BEATING FROG VENTRICLE USING CALCIUM ION SELECTIVE MICROELECTRODES.

K. Dresdner & R.P. Kline, Dept. Pharmacology, Mt. Sinai Med. Cntr. CUNY, NY, NY 10029.

Using single barrel calcium ion (Ca⁺⁺) selective microelectrodes (Ca-ISEs), we recorded extracellular calcium ion concentration (Cao) fluctuations in the extracellular spaces (ETS; Cohen & Kline, *Circ. Res.*, 50:1-16, 1982) of beating frog (*Rana pipiens*) ventricular strips (~1-3 mm. dia.) superfused with Ringers (0.05 - 0.2 mM Ca⁺⁺) and field stimulated at 1-60 beats per minute. Ca-ISEs (tip O.D. 1.5-2.0 microns) were constructed from trimethylchlorosilanized aluminosilicate micropipettes using Simon's neutral Ca⁺⁺ carrier resin at the tip and a 0.1 M CaCl₂ backfill. Worst case Ca-ISE error (at 10 micromolar Cao) from fluctuations of interfering ions (in mM) 3-20 K⁺, 101-118 Na⁺, or 0.0-1.0 Mn⁺⁺ or Ni⁺⁺ was 4%. ETS Cao depleted up to 25% during single beats (1 per minute) and decayed over 20-60 seconds. The envelope of Cao depletion induced during transient increases in heart rate (1 to 3-60 per minute) reached an apparent minimum in 2-4 minutes with a time course dependent upon Ca-ISE tip depth, bath Ca⁺⁺ concentration, stimulus rate, and state of activation of membrane Ca⁺⁺ pumps. Epinephrine (1-100 micromolar in 0.05 mM Ca⁺⁺ Ringers) markedly increased the rate of beat to beat Cao depletion while elevating action potential (AP) plateau and prolonging AP duration (0.8 to 3.0 seconds). Propranolol antagonized. Epinephrine increased the rate of depletion of the Cao envelope at moderate heart rates (3-24 per minute). Ni⁺⁺ (0.2 - 1.0 mM in 0.05 mM Ca⁺⁺ Ringers) blocked this effect without shortening AP duration. Mn⁺⁺ (1 mM in 0.2 mM Ca⁺⁺ Ringers) blocked this depletion by approximately 50% while AP duration was decreased by only 15%.

M-AM-Pos80 INSULIN REGULATES THE IONIC CONDUCTANCE OF THE EMBRYONIC HEART CELL MEMBRANE.

R. Fischmeister, R. K. Ayer, and R. L. DeHaan, Dept. of Anatomy, Emory University, Atlanta GA 30322

Insulin caused a ouabain-insensitive hyperpolarization of the resting potential (E_r) in quiescent aggregates of 14-day embryonic heart cells that had been washed in insulin-free buffer for 2-3 hrs (Lantz *et al.*, 1980, *PNAS* 77: 3062) and slowed the beat rate of similar preparations of 7-day cells which beat spontaneously (Shipley & DeHaan, 1981, *Fed. Proc.* 40: 367). We analyzed the mechanisms responsible for these effects with the whole-cell patch-clamp technique applied to single 10-12 μm chicken cardiac myocytes, or to clusters of 5-10 coupled cells. Patch-electrodes (2-6 MΩ) were filled with buffer containing (mM) KCH₃SO₄, 100; KOH, 28; NaCl, 50; MgCl₂, 1; CaCl₂, 0.2; EGTA, 5; Hepes, 10; pCa 8.16; pH 7.2. After a seal-resistance of 5-15 GΩ was achieved, the patch membrane was broken by suction and I(V) relationships were determined using 400 msec command voltage pulses, from a holding potential of -80 mV. Tetrodotoxin (45 nM) was added to block a small fast inward component. In cells resting at E_r ≈ -40 mV perfusion with porcine Na-insulin (17 nM) caused a large hyperpolarization (to E_r ≈ -100 mV) and a rapid increase (40% within 1 min to a maximum of 400% after 20 min) in a time-independent background outward current, with a reversal potential (-117 mV) consistent with the known value of E_K. The insulin-induced current showed a strong rectifying voltage dependence; it increased linearly to a maximum of about 30 μA/cm² at +45 mV, and exhibited a negative slope between +45 and +110 mV. A TTX-insensitive, D600-sensitive, time-dependent inward current was reduced in amplitude or blocked altogether by insulin in some preparations. These effects were partially reversible after 2 hrs washout of the hormone. (Supported by NIH P01-HL27385 and R01-HL16567)

M-AM-Pos81 EFFECT OF PHOSPHATIDYLCHOLINE LIPOSOMES CONTAINING Na⁺ or Ca²⁺ ON THE ELECTRICAL ACTIVITY OF CULTURED HEART CELLS. G. Bkaily, N. Sperelakis, Y. Elishalom and C. Barenholz. University of Virginia School of Medicine, Charlottesville, Virginia 22908.

Phosphatidylcholine (PC) liposomes were used to deliver their entrapped ions into spontaneously contracting cultured heart cells (reaggregates) prepared from 15-day embryonic chick ventricles (superfused at 8 ml/min). With slowly-rising action potentials (APs) (+v̇_{max} < 30 V/s), when Na-liposomes were added (13.2% v/v), there was a progressive decrease in slope of the pacemaker potential and in firing frequency. Recovery upon washout was rapid. When vesicles containing Ca²⁺ (6.6% v/v) were added, there was an immediate decrease in AP duration. Within 10 min, +v̇_{max}, overshoot, MDP, and frequency decreased, and all spontaneous activity stopped within 30 min. Electrical stimulation could not elicit AP responses. Partial recovery of APs occurred after 60 min of washout, but the recovering APs initially were abnormal. Lower liposome concentration (3.3%) had a slower effect. The rapidity of the effects depended on the Ca²⁺ concentration inside the vesicles (0.15 M and 1 M). K⁺-containing liposomes had no effect. This difference between liposomes containing Na⁺, Ca²⁺, and K⁺ suggests that the effects observed were due to the ions and not to the phosphatidylcholine. Injection of Ca²⁺ could cause depolarization by the Ca²⁺-activation of a non-specific Na-K channel (i.e., g_{Na,K}(Ca)); inhibition of automaticity by injection of Na⁺ or Ca²⁺ could be due to diminution of the electrochemical gradient for inward background depolarizing current. Thus, PC liposomes provide a good means for delivering substances inside the cells without altering the electrical properties of the membrane by the lipid vehicle. (This work was supported by grant HL-18711 and by a fellowship of the Canadian Heart Foundation to Dr. Bkaily.)

M-AM-Pos82 IS CALCIUM ENTRY RELATED TO PACEMAKER ACTIVITY IN MAMMALIAN SINUATRIAL NODE? Kevin J. Malloy & Martin Morad, Dept of Physiology, University of Pennsylvania, Phila., Pa. 19104.

We have attempted to determine the relationship between the influx of calcium ions and diastolic pacemaker activity in mammalian sinoatrial (SA) node. Thin (0.3 x 0.2 mm) strips of rabbit SA node are voltage clamped in a single sucrose gap setup which permits measurement of membrane voltage and current. Simultaneous monitoring of twitch tension provides a relative measure of Ca^{2+} levels during the various procedures used to alter Ca^{2+} entry. Reduction of Ca^{2+} from 1.8 mM to 0.9 mM produced a 50% decline in peak tension, a 5-8 mV depolarization of the maximum diastolic potential (MDP), and a two-fold reduction of pacemaker slope and pacemaker current (I_f). Elevation of Ca^{2+} to 3.6 mM doubled twitch tension, increased pacemaker slope by 30% and hyperpolarized the MDP. Application of 1.0 μ M epinephrine enhanced twitch tension 3-4 fold, while increasing pacemaker slope and I_f 2-fold. Replacement of Ca^{2+} with 1.8 mM Sr^{2+} caused a 5-fold decrease in diastolic rate, a 4-fold prolongation of twitch, and a marked outward shift in I_f . AP amplitude and late repolarization were unaffected by Sr^{2+} . No effects were seen when 1.8 mM Sr^{2+} was added to 1.8 mM Ca^{2+} Tyrode's. In the presence of Ca^{2+} antagonist D600 (5 μ M) AP's were simulated by 200 msec clamp steps to plateau voltages. After clamp release and subsequent repolarization, clamp steps were reimposed during pacemaker potential. The magnitude of I_f in D600 was less than 50% of that measured under drug-free conditions. Similar results were obtained whether 5 mM Mn^{2+} or 2 mM Ni^{2+} was added to inhibit Ca^{2+} entry. In all procedures using Ca^{2+} blockers, twitch tension could not be elicited either by current or voltage clamp procedures. The results are consistent with the idea that increases in Ca^{2+} influx as indicated by enhanced twitch are well correlated with increased pacemaker activity.

M-AM-Pos83 SLOW INACTIVATION OF TETRODOTOXIN-SENSITIVE CURRENT IN CARDIAC FIBERS

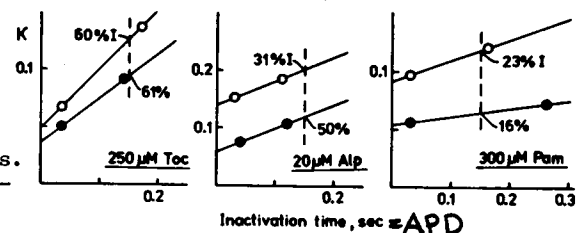
G.A. Gintant, N.B. Dwyer and I.S. Cohen, Dept. of Physiology and Biophysics, SUNY at Stony Brook, Stony Brook, N.Y. 11794

The shortening of the cardiac action potential duration by tetrodotoxin (TTX) is postulated to be due to a reduction of a time-independent background sodium conductance (the TTX-sensitive "window current", Attwell et al., 1979). To further study the possible role of sodium current on the cardiac action potential, we used the two microelectrode voltage clamp technique and canine cardiac Purkinje strands (35°C) to examine the effects of TTX (5-30 μ M) on membrane currents during prolonged (5-20 sec) clamp pulses. The increase in net outward current caused by TTX during step depolarizations to potentials ranging from -60 to -10 mV is time-dependent, being maximal immediately following depolarization, and declining thereafter towards a steady value. To eliminate the possibility that the time-dependent current was due to inadequate voltage control early in the square pulses, we used depolarizing voltage clamp ramps (range 0.1 V/sec to 0.01 V/sec) to ensure voltage control. A TTX-sensitive current was observed with ramps; the peak magnitude of the current was progressively diminished with slower ramps, demonstrating the time-dependence of the current. Ramps from progressively more hyperpolarized holding potentials (-60 to -90 mV) were associated with greater TTX-sensitive current. Similar results were obtained with square and ramp pulse protocols in the presence of CsCl (10 mM) which reduces pacemaker current and background potassium permeability. In nerve, there is a slow component of sodium channel inactivation. Our results suggest the existence of a similar slow component of sodium channel inactivation which may influence the action potential duration in canine cardiac strands.

M-AM-Pos84 INACTIVE VERSUS OPEN CHANNEL BLOCKING OF CARDIAC SODIUM CHANNELS. Kenneth R. Courtney
Research Institute of the Palo Alto Medical Foundation, Palo Alto, Calif. 94301

This report concerns the blocking effects that several antiarrhythmic drugs have on Na channels in guinea pig papillary muscle. Block of these channels is observed by recording beat by beat declines in upstroke velocities of succeeding action potentials (APs) evoked after a period of rest. A finite difference equation can be solved for "K" - a parameter that represents net blocking of upstroke velocity that occurs during each AP. For application to myocardium three measurements are required (B_f = the amount of upstroke block achieved by the end of the AP train, r = the rate of block development during the train, and l = the rate of unblocking after the train) in order to calculate $K = B_f(1 - e^{-r})/e^{-ld}$, where d is the time repolarized between APs. K contains contributions of both open channel and inactive channel blocking. Voltage clamp modulation of APD (time spent inactivated) was used in order to assess the relative importance of inactive versus open channel blocking to the blocking parameter K . Tocainide blocking showed a much greater dependence on APD than did procainamide blocking. Results at right suggest that about 60% of tocainide block, 40% of alprenolol and only 20% of procainamide block occurs via inactive channels. Thus different drugs give differing amounts of inactive versus open Na channel block in myocardium.

Supported by NIH grant HL24156.



M-AM-Pos85 α -ADRENOCCEPTOR-MEDIATED CURRENT CHANGES IN VOLTAGE-CLAMPED CANINE CARDIAC PURKINJE FIBERS. D.C. Gadsby & H.G. Glitsch. The Rockefeller University, New York, N.Y. 10021.

The sympathetic transmitter norepinephrine can activate both α -adrenoceptors and β -adrenoceptors in mammalian cardiac preparations. Selective activation of α -adrenoceptors in Purkinje fibers leads to elevation and prolongation of the action potential plateau. We used two microelectrodes to voltage clamp small Purkinje fibers suspended in a fast-flow chamber to investigate the changes in the steady-state membrane current-voltage relationship that presumably underlie these changes in the action potential. In 4 mM K solution, at plateau potentials, brief applications (e.g. 10-60 sec) of μ M concentrations of the α -adrenoceptor agonist methoxamine caused an inward shift of holding current which reached a peak usually within about 60 sec, but which decayed much more slowly (half time of several min) after washing out the methoxamine. During longer exposures to methoxamine an additional, slower, inward current shift was sometimes seen. The methoxamine-induced inward current shifts are abolished by 1 μ M phentolamine; they are half-maximal in amplitude at about 0.3 μ M methoxamine; they are unaffected by replacing extracellular Cl with isethionate; they are diminished neither by a 10-fold reduction in extracellular Ca concentration (from 2.7 to 0.27 mM), nor by Na/K pump inhibition with 5 μ M acetylstrophanthidin; they are rapidly and reversibly abolished by low concentrations of Ba (0.5-2 mM); they are diminished by moving the holding potential (V_H) towards the expected K equilibrium potential (E_K); the methoxamine-induced current- V_H relationship extrapolates to near E_K in 16 mM K solution, but at lower K concentrations it has a smaller slope and extrapolates to potentials positive to E_K . Possibly, an initial effect of α -adrenoceptor activation in canine Purkinje fibers might be a reduction in resting membrane permeability principally to K ions but, perhaps, also to other (e.g. Na) ions. Grants: HL-14899 & Est. Fellowship of NY Heart Assocn.

M-AM-Pos91 TRANSEPITHELIAL AND CELL MEMBRANES ELECTRICAL RESISTANCES OF RABBIT PROXIMAL CONVOLUTED TUBULE. J.Y. Lapointe, R. Laprade, and J. Cardinal. Dépt de Physique, Université de Montréal and Centre de Recherches, Hôpital Maisonneuve-Rosemont, Montréal, Québec.

Transepithelial, apical, and basolateral membrane electrical resistances (R_T , R_A , R_{BL} , respectively) were measured on rabbit proximal convoluted tubule (PCT) perfused *in vitro*. In order to obtain R_T ($\Omega \cdot \text{cm}$), R_A/R_{BL} , and the longitudinal lumen resistance (R_C , Ω/cm), a current pulse (I_0 : 150–300 nA, 1.5 s duration) was injected in the lumen by one channel of a double barrelled perfusion pipette and the electrotonic voltages were measured at both ends of the tubule (V_O , V_L) and in a cell (V_C) at a measured distance from the injection site. A linear relationship is found between I_0 and V_O from -300 nA to +300 nA and the mean R_T is $1050 \pm 390 \Omega \cdot \text{cm}$ (or $8.2 \Omega \cdot \text{cm}^2$) in control solutions ($n=33$). R_T is weakly correlated to transepithelial potential difference and not systematically related to the transepithelial sodium to chloride permeability ratio ($n = 22$). Substitution of 50 mM NaCl by mannitol in perfusate solution increases R_T by 21% ($n=7$) while the same manoeuvre in the peritubular solution has no significant effect. The ratio R_A/R_{BL} is 2.7 ± 1.5 ($n=12$) in control solutions and increases by 41% within 1 min when glucose and amino acids are substituted by mannitol in the perfusate solution. The concomitant initial changes in transepithelial and basolateral potential difference upon removal of glucose and amino acids allow then to evaluate the individual values of R_A and R_{BL} . $R_{BL} = 7.5 \times 10^3 \Omega \cdot \text{cm}$ ($590 \Omega \cdot \text{cm}^2$) and $R_A = 20 \times 10^3 \Omega \cdot \text{cm}$ ($1580 \Omega \cdot \text{cm}^2$). These values of membrane resistance confirm that the Rabbit PCT is a very leaky epithelium, the cellular pathway being about 30 times more resistive than the paracellular shunt.

M-AM-Pos92 INTRACELLULAR POTENTIAL OF RABBIT PROXIMAL CONVOLUTED TUBULE: EFFECT OF LUMINAL AND PERITUBULAR SOLUTE SUBSTITUTION. R. Laprade, J. Cardinal, and J.Y. Lapointe. Dépt de Physique, Université de Montréal and Centre de Recherches, Hôpital Maisonneuve-Rosemont, Montréal, Québec.

Proximal convoluted tubules of rabbit were perfused *in vitro* and the basolateral membrane potential (ψ_{BL}) was measured. Perfusate and bath solutions were continuously and rapidly exchanged and tubule perfusion rate was high ($> 100 \text{ nl min}^{-1}$). In control solution without proteins, ψ_{BL} was $54 \pm 3 \text{ mV}$, ($n=37$). Luminal substitution of K by Na had no effect. Complete luminal substitution of glucose and amino acids by mannitol produced a transient hyperpolarization of ψ_{BL} (14 mV) with return close to control value within 10 min. Returning to the control solution produced a similar time course transient depolarization of 12 mV. Similarly, 75% luminal substitution of NaCl by mannitol and of Na by choline also produced transient hyperpolarizations (13 and 10 mV, respectively) and depolarizations (16 and 11 mV, respectively). In contrast, 95% luminal substitution of Cl by cyclamate or SO_4 induced a smaller (2–6 mV) but relatively more sustained hyperpolarization. On the other hand, a 95% peritubular substitution of Cl by cyclamate or SO_4 had little effect, while a complete substitution of K by Na, a 75% substitution of NaCl by mannitol and of Na by choline, produced a sustained but reversible depolarization (37, 19, and 10 mV, respectively). The transient nature of the hyperpolarizations following luminal substitution of glucose, amino acids or Na could be interpreted in terms of a decrease of the basolateral ionic pump activity and/or variations of the luminal and apical membrane resistances. On the other hand, the sustained depolarizations seen after peritubular substitution of Na or K would suggest in these cases a decreased ionic pump activity.

M-AM-Pos93 DEVELOPMENT OF Ca^{++} REABSORPTION BY THE ALLANTOIC EPITHELIUM IN CHICK EMBRYOS GROWN IN SHELL-LESS CULTURE. J.S. Graves, E.L. Helms, III and H.F. Martin, III. Department of Physiology, Medical University of South Carolina, Charleston S.C. 29425.

The allantoic sac of the chick embryo functions as a primitive urinary bladder, storing and modifying the excretory fluid produced by the embryo. We have used chick embryos grown in shell-less culture to study the *in situ* handling of Ca^{++} by the allantoic epithelium. Between 8 d and 13 d of incubation (38°C , 5% CO_2), the $[\text{Ca}^{++}]$ of the allantoic sac fluid declines from about 1.5 mM to less than 0.3 mM, with most of this Ca^{++} reabsorption occurring between days 10 and 12. This is evidence for the developmental onset of a Ca^{++} reabsorption process in the allantoic epithelium. In 13 day-old embryos, the allantoic epithelium reabsorbs within 24 h over 90% of $^{45}\text{Ca}^{++}$ injected into the allantoic sac. The Ca^{++} is reabsorbed into the embryo's blood in which the serum $[\text{Ca}^{++}]$ is about 2 mM. Also, electrical potential profiles reveal that the serosal side of the allantoic epithelium is 5–30 mV positive compared to the mucosal (luminal) side. Thus, by electrochemical criteria this reabsorption process appears to be active. The allantoic epithelium may be a suitable model system for studying the development and regulation of Ca^{++} transport by the distal portions of the mammalian nephron.

M-AM-Pos94 MEMBRANE AREA ALTERATIONS ASSOCIATED WITH PROTON SECRETION IN TURTLE BLADDER

Chris Clausen, and Troy E. Dixon, SUNY Dept. of Physiology and Biophysics and Dept. of Medicine, Stony Brook, NY 11794.

The mechanism of proton secretion in turtle bladder appears to involve alterations in apical surface area resulting from fusion of intracellular vesicles with the apical membrane. In an attempt to quantify this in the living tissue, we have performed impedance analyses to measure the different membrane capacitances and conductances. Membrane capacitance has been shown to be proportional to exposed surface area. The bladders were pretreated with ouabain and amiloride to completely abolish Na^+ transport. Our results from 9 bladders are as follows. The apical-to-basolateral resistance ratio was 20 ± 2 and the capacitance ratio is 0.46 ± 0.04 , both of which are comparable to microelectrode data and micrographs, respectively. The base-line apical capacitance (C_a) started at $3.7 \pm 0.7 \mu\text{F}/\text{cm}^2$. Both C_a and the basolateral capacitance declined continuously throughout the experiment. The rate of decline of C_a , not C_a itself, was found to be related to the proton secretion rate. Inhibition of proton secretion with 0.5 mM SITS or 50 μM acetazolamide (AZ) increased the rate of decline of C_a from 0.35 ± 0.11 to $0.73 \pm 0.11 \mu\text{F}/\text{cm}^2/\text{hr}$ ($n=4$), and 0.68 ± 0.25 to $1.0 \pm 0.4 \mu\text{F}/\text{cm}^2/\text{hr}$ ($n=5$), respectively. In AZ-treated bladders, removal of AZ with addition of 10 mM bicarbonate plus 5% CO_2 restored proton secretion and reduced the decline in C_a to a near base-line level ($0.35 \pm 0.15 \mu\text{F}/\text{cm}^2/\text{hr}$). These studies indicate that proton secretion is associated with alterations in apical membrane area, but the observation is complicated by the finding of apical and basolateral area changes unrelated to the proton secretion process.

M-AM-Pos95 RABBIT CORNEA STROMAL HYDRATION MEASURED WITH PROTON NMR SPECTROSCOPY. B. R. Masters, V. Harihara Subramanian, and B. Chance. Johnson Research Foundation, University of Pennsylvania, Philadelphia, Pennsylvania 19104.

An index of corneal function is the degree of corneal swelling and concomitant loss of transparency. The water spin-lattice relaxation time (T_1) is sensitive to the local environment around the water molecule, and can be used to study corneal hydration. A corneal stromal preparation was made from the excised cornea of rabbit. The corneal hydration was varied by placing the preparation with the epithelium and the endothelium removed in isotonic saline (0.9%) at 23°C. for various periods of time. The water uptake for each period was determined gravimetrically, and the tissue was placed in a sealed chamber inside the NMR transceiver coil of a superconducting magnet. Proton NMR measurements were made at 60.01 MHz on a Johnson Research Foundation NMR spectrometer using the saturation recovery method. Signal to noise ratios of over 100 to 1 were obtained from a single free induction decay (FID) measurement of normal as well as swollen corneas of 1 cm^2 area. The T_1 value for the normal corneal preparation is 0.598 ± 0.01 s $N=6$, and increased to 1.220 ± 0.04 s $N=6$ for maximum hydration. A plot of $1/T_1$ versus (dry wt) / (wet wt - dry wt) is fit by the equation $y=0.220 + 5.07x$, $R^2=0.98$, $N=27$. This plot is based on the two compartment model of bound and free water, $1/T_1 = \theta_F / T_{1F} + \theta_B / T_{1B}$. The observed correlation between $1/T_1$ and the reciprocal of corneal hydration (wet wt - dry wt) / dry wt is consistent with the hypothesis that proton T_1 measurements could serve as an index of corneal dysfunction. In vivo studies would require the development of proton imaging techniques. Support: EY-02421 (BRM)

M-AM-Pos96 A GENERAL COMPUTER MODEL OF EPITHELIAL ION TRANSPORT AND CELL VOLUME REGULATION

R. Latta, C. Clausen, L.C. Moore (Intr. by P.G. LeFevre), Dept. of Physiology and Biophysics, SUNY Health Sciences Center, Stony Brook, NY 11794.

A general-purpose model has been developed to describe ion transport in a single representative cell within an epithelial layer. Any number of solutes of arbitrary valance (including zero) can be represented explicitly. Presently, Na^+ , K^+ , Cl^- , protein, and sucrose are included. Passive apical, basolateral, and paracellular fluxes of the solutes are assumed to obey the Goldman-Hodgkin-Katz flux equation. Basolateral membrane active transport follows experimentally observed saturable kinetics of Na-K ATPase. Both apical and basolateral membranes have finite water permeabilities. The solution of the model involves integrating a coupled set of differential equations, which express conservation of mass, yielding intracellular solute concentrations and cell volume as functions of time. Conditions of electroneutrality appropriate for the experimental situation being simulated (e.g., current- versus voltage-clamp) are imposed across each membrane utilizing a completely general iterative algorithm. The model is currently being used to investigate the transition between open- and short-circuit conditions, and to examine mechanisms of cell volume regulation, with the ultimate goal of obtaining transport parameter estimates from transient data. Comparison of model predictions with membrane potential transients measured in rabbit cortical collecting tubule shows excellent agreement, and indicates that basolateral membrane chloride permeability is an important determinant of the transient voltage response.

M-AM-Pos97 CHANGES IN INTRACELLULAR Cl ACTIVITIES WITH SECRETION IN CANINE TRACHEAL EPITHELIUM
S. R. Shorofsky, M. Field, and H. A. Fozzard. Department of Pharmacological and Physiological Sciences, University of Chicago, Chicago, Illinois 60637

The epithelium lining the canine trachea actively secretes chloride. Recently, it has been proposed that epinephrine and other cAMP-related stimuli activate this secretory process by increasing the apical membrane's simple diffusive permeability to Cl. To test this hypothesis, Cl-selective microelectrodes (Corning #477913 resin) were used to determine the intracellular Cl activity (a_{Cl}^i) of tracheal epithelial cells under open-circuited conditions (tissues bathed in HCO₃-free Ringer). Under control conditions when Cl secretion is minimal (Indomethacin 10⁻⁶M added), the transepithelial potential (V_{SM}) was 13.5 ± 2.2 mV (mucosal reference), the potential across the mucosal membrane (V_{cm}) was -49.1 ± 2.7 mV, the short-circuit current (I_{sc}) was 18.1 ± 1.9 μ amps-cm⁻², and a_{Cl}^i was 47.2 ± 1.9 mM (n=6 tissues). When Cl secretion was maximally stimulated with epinephrine (10⁻⁵M), V_{SM} was 31.4 ± 4 mV, V_{cm} was -43.5 ± 2 mV, I_{sc} was 160 ± 16 μ amps-cm⁻², and a_{Cl}^i was 32.2 ± 2.7 mM (n=6 tissues). The a_{Cl}^i values before and after epinephrine are 2.8 and 1.5 times those expected if Cl were passively distributed across the apical membrane. These findings indicate that Cl is accumulated above electrochemical equilibrium by the tracheal epithelial cell in both non-secreting and secreting states and are consistent with the hypotheses that Cl exit from the cell across the apical membrane is by simple diffusion and that epinephrine increases the Cl permeability of the apical membrane. (Supported by PHS grants 5T32GM07281 and HL26241)

M-AM-Pos98 Properties of Na⁺ channels in the apical membrane of rabbit urinary bladder. S.A. Lewis, M.S. Ifshin¹, D.D.F. Loo², and J.M. Diamond². Department of Physiology, Yale University, New Haven, CT. 06510. ¹Present address, Smith, Kline, Beckman, Philadelphia, PA. 19130. ²Department of Physiology, U.C.L.A. Medical School, Los Angeles, CA. 90024.

In a recent report Lewis and de Moura (Nature 297:685-688, 1982) demonstrated that the mammalian urinary bladder epithelium accommodates stretch by incorporating cytoplasmic vesicles into the apical membrane. This incorporation increases by a factor of 4 the amiloride sensitive apical Na⁺ permeability. In addition, both apical membrane and vesicles contain a non-selective cation pathway. In this report we use fluctuation analysis to study and compare the properties of apical Na⁺ channels and Na⁺ channels of vesicle origin. The apical membrane Na⁺ channels had single channel current of 0.65 pA, a forward (association) rate constant for amiloride binding (K_{01}) of 52.1 sec⁻¹ μ M and backward (dissociation) rate constant of 11.6 sec⁻¹. These parameters were also determined for Na⁺ channels of vesicle origin and were not different from the values obtained for apical Na⁺ channels. Decreasing mucosal Na⁺ from 136.2 to 30 mM resulted in a 2.3 fold increase in channel density, a finding consistent with previous reports that extracellular Na⁺ blocks amiloride sensitive channels. In addition to the amiloride induced fluctuations the power spectral density also possessed an amiloride insensitive component. The power at 1 Hz of this component was linearly correlated with the macroscopic amiloride insensitive current. This latter pathway was unstable in the membrane as replacing the mucosal solution caused both the macroscopic current and current fluctuations to decrease. This phenomenon will be discussed in terms of possible channel aging. (NIH grants GM-14772, AM-17328, AM-20851.)

M-AM-Pos99 Effects of sulfate and gluconate substitution to chloride on frog skin cell membranes
E. MINTZ & H. GOUDEAU, Dept. Biol., CEN Saclay, 91191 Gif/Yvette Cedex, France

Frog skin cell membranes were studied in the short-circuit state by microelectrode measurements. Apical and basolateral membrane resistances and emf's were evaluated from I_{Na} -V curves (I_{Na} is the amiloride inhibitable current). As previously shown (Goudeau & al. 1982. J. Memb. Biol. 66:Na123) these curves were non linear, especially the apical curve. Isoosmotic SO₄²⁻-Ringer was substituted to Cl⁻-Ringer, and I-V curves were done 20 min later. The short-circuit current I_{sc} had dropped from 39±6 to 22±4 μ A/cm²; the intracellular potential V_{sc}^o , initially highly hyperpolarized, had only slightly increased from -59±4 to -68±4 mV. Both apical slope resistance measured at V_{sc}^o (1.5 ± 0.2 k Ω cm²) and apical chord resistance (2.6±0.4 k Ω cm²) showed a 3fold increase. Neither of these resistances had changed at the basolateral membrane (1.3±0.2 k Ω cm²). A systematic increase in the apical emf E_o and a slight decrease of the basolateral emf E_i were observed: 39±8 versus 22±10 mV, and 93±3 versus 100±6 mV, respectively. The total resistance and the apical fractional resistance measured in the presence of amiloride were significantly higher. These results, as well as the increase in the apical resistance and emf, indicate a possible apical leak conductance depending on chloride presence and/or an effect of the anion on the sodium permeation mechanism. In another series of experiments, gluconate was substituted instead of sulfate. Although the same changes in I_{sc} , V_{sc}^o , and the resistances were observed, neither the apical fractional resistance, nor the apical emf showed any modification. This seems to rule out any chloride dependent apical leak conductance, unless such a conductance can be gluconate dependent. This microelectrode study suggests that anions affect the sodium permeation mechanism.

M-AM-Pos100 TWO PARALLEL DIFFUSION PATHWAYS ACROSS THE FROG GASTRIC MUCOSA. L. Villegas (Intr. by L. Sananes). IVIC, Apartado 1827, Caracas 1010A, Venezuela.

Water and graded size low lipid soluble non electrolytes are used for the operational characterization of the effect of tonicity changes at the mucosal surface on the restriction to the diffusion offered by the frog gastric mucosa. Fluxes were measured using isosmotic solution (220 mOsm/Kg water) at both surfaces in one period and with isosmotic solution at the serosal surface and hyperosmotic (524 mOsm/Kg water) at the mucosal surface in another period. The permeability coefficients calculated from the fluxes and concentration differences expressed in $\text{cm} \times 10^{-7}$, are:

	Serosal-to-mucosal		Mucosal-to-serosal	
	Isotonic	Hypertonic	Isotonic	Hypertonic
Inulin	2.0 ± 0.4	3.4 ± 0.5	2.4 ± 0.2	2.9 ± 0.2
Sucrose	4.7 ± 1.0	8.0 ± 1.2	3.1 ± 0.4	4.9 ± 0.6
Erythritol	10.8 ± 0.6	13.7 ± 0.8	11.6 ± 1.3	13.8 ± 3.0
Propionamide	132.8 ± 12.0	170.1 ± 11.9	115.1 ± 24.1	126.2 ± 42.2
THO	1019.4 ± 19.4	816.7 ± 17.7	983.3 ± 16.7	730.6 ± 13.9

Hyperosmotic solution increases inulin and sucrose diffusion, does not affect propionamide and erythritol diffusion and significantly reduces water diffusion. This reduction and the increase in the larger molecules fluxes in both directions corresponds to changes in the effective diffusion area of 20 to 70% for the inulin and 65 to 70% for the sucrose by effect of hyperosmolality. It is proposed that the small fraction of the diffusional area used by the larger molecules is more affected by the osmolality than the one used by the smaller molecules.

M-AM-Pos101 BASOLATERAL K EFFECT ON TOTAL CONDUCTANCE, OVERSHOOT RESPONSE TO APICAL Na AND AMILORIDE INHIBITION IN R. PIPIENS SKIN. T. HOSHIKO AND S. MACHLUP. Depts. of Physiol. and Physics, Case Western Reserve Univ., Cleveland, OH 44106. Study of epithelial transport is complicated by the presence of at least two membranes in series bounding intracellular compartment(s). In an effort to isolate the apical membrane, the basolateral surface was exposed to high $[K]_i$ by Fuchs, et al. (J. Physiol. 267:137, 1977) which was said to depolarize the basolateral membrane and reduce its resistance. Direct evidence in support of these effects has not appeared. Cuthbert and Wilson (J. Membr. Biol. 59:65, 1981) mention that cAMP may be doubled in the presence of $[K]_i$. In sulfate solutions, the short-circuit current (Isc) overshoots greatly in response to a sudden increase in $[Na]_o$, in the presence of $[K]_i$. Total skin conductance (Gt) after $[Na]_o$ increases by about 2.8 X with $[K]_i$ and about 1.8 X with $[Na]_i$. Gt and Isc typically increase with time in the presence of $[K]_i$. When $[Na]_i$ is replaced with arginine, the Isc transient after $[Na]_o$ is also much diminished compared to that in $[K]_i$, but Gt increases 3.3 X. In the presence of basolateral arginine, both Isc and Gt either remain constant or decrease with time. The apparent inhibition constant for amiloride is 2 X larger with $[K]_i$ than with $[Na]_i$, consistent with previous reports. In the absence of apical $[Na]_o$, Gt is higher in the presence of $[K]_i$ than of $[Na]_i$, Gt is dominated by apical conductance, and basolateral conductance changes would have little effect on Gt. Hence $[K]_i$ may affect shunt conductance and possibly the apical membrane conductance as well. These results suggest that $[K]_i$ is not a simple manoeuvre with effects on only the basolateral membrane and conductance. (Supported by grant from PHS AM 05865.)

M-AM-Pos102 COUPLED CELLULAR SALT ENTRY IN NECTURUS GALLBLADDER REQUIRES MUCOSAL Na, Cl, AND K. C. William Davis and Arthur L. Finn, Depts. of Medicine and Physiology, University of North Carolina School of Medicine, Chapel Hill, NC 27514.

Previous work in several laboratories has established that the first step in transepithelial solute transport in gallbladder involves the neutral coupled entry of Na and Cl into the cells. We have used a cell volume probe of net solute fluxes to investigate the possible K requirement for this solute entry process. Volumes of individual cells as a function of time were determined with an optical sectioning technique. Two experimental regimens were utilized. First, cell swelling was induced by the serosal addition of 0.1 M ouabain, a process which requires mucosal Na and Cl (Ericson, A.-C. and K.R. Spring, AJP, 243:C140, 1982); under these conditions the cells swelled at a rate of 1.2 ± 0.4 % original cell volume/min (n=3). When mucosal K was removed, cell swelling and, thus, net solute entry, was abolished. Second, following an initial exposure to mucosal low Na-Ringer (N-methyl-D-glucamine Cl replacing NaCl) cell swelling was induced by exposing the mucosal surface to high K-Ringer. With 10 mM Na the cells swelled in 97.5 mM K-Ringer at 2.5 ± 0.2 %/min (n=3). However, in a Na-free mucosal medium, there was no swelling when K was raised to 97.5 mM. Solute entry in 10 mM Na, 97.5 mM K-Ringer was completely inhibited by either replacing Cl with NO_3 , or by the addition of 0.1 M bumetanide to the mucosal solution. These results strongly suggest that the solute entry process in gallbladder requires the simultaneous presence of Na, Cl, and K. Supported by NIH grant AM25483.

M-AM-Pos103 VIRAL ENHANCEMENT OF HEMOGLOBIN INDUCTION IN A HUMAN ERYTHROLEUKEMIC CELL LINE (K562). Paul E. Wanda, Department of Biological Sciences, Southern Illinois University, Edwardsville, IL 62026.

The effect of viral infection on the expression of hemoglobin synthesis was investigated in a human erythroleukemic cell line K562. Induction of hemoglobin synthesis by 50 μ M bovine hemin was revealed by benzidine staining of cells and spectrophotometrically on cell lysates. It was found that infection of K562 cells by measles virus before the addition of hemin increased the rate and extent of hemoglobin synthesis. In infected cultures containing hemin, the increase in the number of induced cells (B+) was 2 to 3 fold greater than in uninfected cultures containing hemin, the most pronounced differences occurring between 12 and 36 hrs. after addition of hemin. When cells of a clone of K562 (B-1) were used, a similar increase in rate was noted, although it was less pronounced than with wild type K562 cells. This is consistent with other investigators who report quantitative variations in hemoglobin production among different clones of K562 cells. In cultures without hemin, whether or not infected, the percent of cells reactive with benzidine was minimal. Increase in benzidine-positive cells paralleled exactly the increments of chromogen measurable spectrophotometrically at 425 nm after reaction of the supernatants of cell lysates with benzidine reagent. Hemoglobin synthesis had no significant effect on the capacity of induced cells subsequently to synthesize virus. These results indicate a potential role of viral infection in enhancing erythroid differentiation in a leukemic cell already chemically stimulated to differentiate.

M-AM-Pos104 INDUCTION OF A LUMINAL ALKALINIZATION CURRENT BY CALCIUM IONOPHORE A23187 IN TURTLE BLADDER. G. Ehrenspeck. Dept. Zoological and Biomedical Sciences and Col. of Osteopathic Med., Ohio Univ., Athens, Ohio 45701.

The (ouabain + amiloride)-insensitive short-circuiting current (I_{SC}) across turtle bladders bathed by symmetrical Cl-free, ($HCO_3^- + CO_2$)-rich Na Ringer solution is generated by HCO_3^- absorption (or H secretion). Mucosal addition of ionophore A23187 (10 μ M) to bladders from post-prandial turtles changes the magnitude and direction of the I_{SC} from an initial value of -6 μ A/cm² (serosa negative to mucosa) to +4 μ A/cm² (serosa positive to mucosa) and decreases the trans-epithelial resistance (R) 40%. In bladders from HCO_3^- -loaded turtles, the I_{SC} is reversed from -3 to +15 μ A/cm² and R decreased 45% by the ionophore. The rate of alkali secretion (J_A) was estimated by pH-statting a HCO_3^- -free, Cl-free mucosal fluid at pH 4.5 while serosal pH and HCO_3^- were 7.6 and 20 mM. Under these conditions, A23187 elicits parallel increases in J_A and positive I_{SC} . Subsequent addition of the inhibitor of carbonic anhydrase, ethoxzolamide, induces parallel decreases in these parameters. The data suggest that electroneutral Cl: HCO_3^- exchange is not the sole process of luminal alkalization but that there also exists an electrogenic HCO_3^- secretion (or H absorption) mechanism which is influenced by changes in cytosolic Ca levels. (Supported in part by the Am. Heart Assoc., Central Ohio Heart Chapter, and the Ohio Univ. Baker Fund and Col. of Osteopathic Medicine.)

M-AM-Pos105 CHARACTERIZATION OF A NATURAL IONOPHORE DERIVED FROM ENTAMEBA HISTOLYTICA E. C. Lynch, I. Rosenberg, and C. Gitler, The Rockefeller University, N.Y., NY and The Weizmann Institute, Rehovot, Israel. (Intr. by M. Rubin)

E. histolytica kills host cells by mechanisms which include contact-induced damage of target cell membranes. Thinking that amoeba-derived substances might mediate membrane permeability changes, we exposed planar lipid bilayers and vesicles to material in which the amoeba had grown and observed spontaneous incorporation of ion-permeable channels into the artificial films. These stepwise conductance increments imparted to the membrane an irreversible permeability change. Membrane resistance decreased by up to 5 orders of magnitude when exposed to microgram quantities of amoeba derived substances. The channel is a protein with a subunit molecular weight of 13,000 Daltons in SDS. It associates with a particulate fraction obtained from high speed spins of both homogenized whole amoeba and the growth-conditioned media. The channel conductance is moderately cation-selective, voltage-dependent and displays a unit size of 1600 picoSiemens (pS) in 1 M KCl. In the bilayer, the amoeba-induced conductance exhibits an *in situ* sensitivity to protease.

We have discovered a channel-forming protein from *E. histolytica* with remarkable spontaneous activity in reconstituted systems. Our data suggest that the *in vivo* mechanism of cytotoxicity and cell lysis induced by *Entamoeba histolytica* may be initiated by the insertion of the parasite-derived channels into the host membranes.

(Supported in part by NIH Training Grant T32GM7288 and the Marine Biological Laboratory, Woods Hole, MA.)

M-AM-Pos106 A SURFACE CHARACTERIZATION OF COATED AND UNCOATED CHRYSOTILE UTILIZING AUGER ELECTRON SPECTROSCOPY.

L. D. McCormick, U.S. Department of the Interior, Bureau of Mines, Avondale Research Center, Avondale, MD 20782.

During the previous decade, research into asbestos carcinogenicity and cytotoxicity had been dominated by the "Stanton Hypothesis". This states that only the dimensions of a durable fiber are important in determining whether or not it will be carcinogenic. Thus neither composition, defects, crystal faces, nor surface charge would influence carcinogenicity. However, in recent years data have accumulated which indicate that surface properties of fibers are important in understanding the biological interaction of asbestos and cell membranes and therefore may be important in carcinogenicity as well. Recently fiber coating have been developed for the purpose of rendering asbestos fibers "biologically inert". Both of these developments have resulted in significant interest in the surface properties of asbestos and the asbestos-cell membrane interaction. Since surface characterization techniques have been widely applied to metals and minerals, asbestos would seem to be amenable to the numerous vacuum techniques which can be utilized to study surfaces of metals and semiconductors. Since these techniques depend upon charged particles for either excitation or signal detection (or both), and asbestos is a good insulator, their use has been minimal. Because of the need to study asbestos with Auger electron spectroscopy (AES), a procedure was developed which minimizes the problem of charge neutralization. Chrysotile fibers are dispersed in high purity water and then deposited onto indium foils. Indium was utilized because of its high purity, good conductivity, and softness. Even though the fibers are nonconducting, the conducting indium substrate prevents charging and allows the acquisition of AES spectra which can be utilized to study the top few monolayers of the fibers. Using this procedure, AES analyses of chrysotile fibers which were either coated for the purpose of yielding biologically inert fibers or uncoated were performed. This yielded both the composition of the coatings and with the use of inert gas sputtering a depth profile of the coating. The AES spectra on coated, uncoated, and sonicated and coated fibers will be presented. Some implications for cytotoxicity, haemolysis, and carcinogenicity will be discussed.

M-AM-Pos107 CALCIUM-DEPENDENT ACTIVATION OF CILIARY MOVEMENT: EFFECT OF CALMODULIN. Pedro Verdugo, Beat V. Raes and Manuel Villalon, Ctr. for Bioengineering and Dept. of Biological Structure, University of Washington, WD-12, Seattle, WA 98195

The frequency of ciliary beat (FCB) in tissue cultures of mammalian ciliated cells (MCC) from rabbit trachea and oviduct is dependent upon extracellular Ca^{2+} concentration. Also, in the presence of the Ca-ionophore A23187, the relationship between $[\text{Ca}^{2+}]$ and FCB is shifted towards the origin over approximately three orders of magnitude of Ca^{2+} concentration (Biophys. J. 16:115, 1976; J. Cell Biol. 75:293, 1977). Results presented here indicate that when MCC are demembrated by 0.01% Triton X and reactivated by 2.7 mM ATP and 5 mM Mg^{2+} the relationship between Ca^{2+} concentration and FCB is shifted towards the origin, as compared to intact cells, but the shift is smaller, and there is a 50% to 60% decrease in the response as compared to the effect observed in intact cells equilibrated in the presence of A23187. However, when demembrated cells are reactivated in the presence of Calmodulin ($2 \times 10^{-8}\text{M}$) it virtually restores the relationship between Ca^{2+} concentration and FCB to the curve observed in intact cells treated with A23187. We also have found that Trifluoroperazine (TFP), an inhibitor of Calmodulin, in concentrations as low as 10^{-6}M can arrest ciliary movements in both intact MCC and demembrated MCC. In each case, TFP-induced inhibition can be reversed by either 1 μM A23187 or 1 μM calmodulin respectively. Also ATP-calmodulin-reativated models arrested by 1 mM Ca^{2+} , can be transiently reactivated by addition of 1 μM TFP.

Supported by HL-29908

M-AM-Pos108 CONTRIBUTION OF JUNCTIONAL CONDUCTANCE TO THE CELLULAR VOLTAGE DIVIDER RATIO. Wolfram Nagel, Fernando J. Garcia-Diaz and Alvin Essig, Department of Physiology, Boston University School of Medicine, Boston Ma. 02118

It has been suggested that distribution of lateral interspace resistance in association with a highly conductive junction can significantly affect the measurement of voltage divider ratios, F_o ($\equiv \Delta V_o / \Delta V_t$), thereby leading to erroneous inferences regarding the actual cellular membrane resistance ratios (Boulpaep and Sackin 1980, Essig 1982). We present here experimental support for this view. During seasons when frog skins were highly permeable to Cl, transepithelial conductance, g_t , often exceeded 2 mS/cm^2 . High concentrations of amiloride rapidly blocked cellular transport completely, but g_t remained initially high and F_o remained appreciably less than 1.0. Although such values of F_o are generally attributed to residual ionic conductance of the mucosal membrane, they were here found to result from large junctional conductance, g_j : Lowering g_j (e.g. by removal of mucosal Cl) consistently led to a concomitant increase of F_o to near 1.0, without effect on either membrane potential or short circuit current. Similarly, when the microelectrode tip was located in the lateral interspace immediately beyond the first cell layer, F_o was less than unity; lowering g_j again increased F_o to a value of 1.0. (Supported by USPHS grant AM 20068 and Deutsche Forschungsgemeinschaft.)

M-AM-Pos109 INCREASED GAP JUNCTION AREA IMPROVES CELL-TO-CELL DIFFUSION OF ^3H -2-DEOXYGLUCOSE BETWEEN UTERINE SMOOTH MUSCLE CELLS Cole, W.C., R.E. Garfield, J.S. Kirkaldy*, Dept. of Neuroscience and the Institute for Energy Studies*, McMaster University, Hamilton, Ontario, Canada.

The precipitous appearance of gap junctions (GJ's) between the smooth muscle cells of the myometrium is thought to synchronize and coordinate metabolic and electrical activity in the uterus facilitating effective labour. To determine whether there is a change in intercellular communication between uterine smooth muscle cells at parturition we have determined the apparent diffusion coefficient (D) for phosphorylated ^3H -2-deoxyglucose (2DG) in myometrial strips from Day 17-20 pregnant (FEW GJ's) and parturient (MANY GJ's) rats. Values of D were determined from the longitudinal distribution of radioactivity in the strips after exposing one portion of the strip to the tracer in a two-compartment bathing chamber. Extracellular movement of tracer was studied with ^3H -sucrose and ^3H -mannitol. The area of GJ's as a % of the cell membrane increased from <0.005% in Day 17-20 pregnant rats to 0.25% at parturition as measured by transmission EM morphometry. D was at least ten-fold larger in tissues from parturient rats ($1.69 \pm 0.06 \times 10^{-6} \text{ cm}^2 \text{ sec}^{-1}$) than in tissues from Day 17-20 pregnant rats ($1.70 - 0.4 \times 10^{-7} \text{ cm}^2 \text{ sec}^{-1}$). The longitudinal distribution of the extracellular markers was considerably less than and, hence, could not account for that of 2DG. The concomitant increase in the area of GJ's between smooth muscle cells and the value of D for 2DG diffusion in strips of uterine muscle from parturient rats suggests; (i) that GJ's represent an intercellular pathway of low resistance for the direct exchange of small molecules between smooth muscle cells and, (ii) that there is a substantial increase in the ability of these cells to communicate during parturition. Supported by MRC and a Can. Heart Found. scholarship to W.C.C.

M-AM-Pos110 ELECTRICAL COUPLING AND FLUORESCENT DYE SPREAD BETWEEN CULTURED VASCULAR SMOOTH MUSCLE CELLS. M. S. Kannan, M. G. Blennerhassett, R. E. Garfield and S. Caveney. Department of Neurosciences, McMaster University, Hamilton and Department of Zoology, University of Western Ontario, London, Ontario, Canada.

Primary cultures of smooth muscle cells of rat aorta and portal vein were used to test the hypothesis that gap junctions mediate electrical coupling and spread of fluorescent dye. Thin-section and freeze-fracture electron microscopy of aortic cells revealed gap junctions as the only junctional specializations. Cells in sparse regions of the culture were impaled with two microelectrodes. Cells had a mean membrane potential (V_m) of -30 mV and showed no rectification to cathodal currents. Current-voltage relationship was linear when anodal pulses were used. There was spatial decay of electrotonic potential elicited by injecting current with one electrode and measuring the voltage with a second electrode. The coupling ratio of cell pairs was 0.29 and it decreased to 0.14 after exposure to Ca^{2+} ionophore A23187. The input resistance of single cells was 10 M Ω and of cells in cluster 1.5 M Ω . The initial V_m was more negative than the value at steady state, suggesting a Ca^{2+} -activated K^+ conductance. When 6-carboxy fluorescein (MW376) was iontophoretically injected into a cell, it spread quickly to other cells. Dye coupling was consistently demonstrable at high ambient temperature (30°C) and at pH 7.4 of medium. These results suggest that smooth muscle cell gap junctions are permeable to dyes and intracellular Ca^{2+} appears to regulate electrical coupling.

Supported by M.R.C. and the Ontario Heart Foundation.

M-AM-Pos111 THE TEMPERATURE DEPENDENCE OF THE KINETICS OF LYMPHOCYTE PROLIFERATION FOR CELLS IN SUSPENSION AND AFTER AGGREGATION INTO A PELLET. D. J. Hall, J. J. O'Leary, and A. Rosenberg, Dept. of Laboratory Medicine and Pathology, University of Minn., Mpls., Mn., 55455.

It has been shown that a population of mitogen stimulated lymphocytes exit G0 phase in a first order fashion, showing a lag phase (the time until the first cells enter S-phase), t_0 , a first order entry rate constant for entry into first and subsequent S-phases, k' & k'' respectively, as well as the numbers of cells initially stimulated to respond, $N_A(t_0)$. Provided that the first order model is permissible, the temperature dependence in the form of an apparent activation energy (E_a) can be used to characterize the details of the entry process. We have determined the E_a of t_0 , k' , k'' and k_D (the slope of a log-linear growth curve) for mitogen stimulated lymphocytes in suspension and in naturally settled pellets. It was found that when cells were kept in suspension the E_a for k' was 37.2 kcal while that for the reciprocal of the lag phase duration ($1/t_0$) was approx. 16 kcal suggesting that the rate limiting event for entry into first S-phase, reflected by k' , is more energy dependent and separate from that event that fixes the lag phase duration. When the cells were allowed to pellet, however, the E_a for k' dropped dramatically to approx. 3 kcal. The E_a for k'' and k_D remained high at about 40 kcal while that for $1/t_0$ remained within the range of 10-20 kcal for cells in a pellet. Thus, cells in suspension have to traverse a very energy dependent step in order to enter first S-phase, reflected by k' , while a second process, reflected by t_0 , is not rate limiting. However, when cell to cell contact is increased in the pellets, t_0 may become rate limiting while k' is not. This suggests that cell to cell contact, by an as yet unknown mechanism, is intimately involved in the process that determines k' .

M-AM-Pos112 THE CYTOPLASMIC MATRIX; ITS STRUCTURE, VOLUME, SURFACE AREA AND SPACE FOR DIFFUSION. N.D. Gershon⁺, K.R. Porter⁺⁺, B.L. Trus⁺, DCRT, NIH, Bethesda, MD 20205, ⁺⁺Univ. of Colorado, Boulder, CO 80309.

Small molecules in the cytoplasm diffuse a few times slower than in aqueous solutions, while fluorescent proteins (BSA or IgG) in human diploid fibroblasts at 22°C diffuse about 70 times slower than in buffer solution (1). To determine whether the cytoplasmic matrix (the microtrabecular lattice (2) or MTL and the cytoskeleton) has a structure that might retard the diffusion to that extent, we developed a novel image analysis method to measure the volume fraction it occupies. We digitize electron micrographs of frozen dried cells, find the area occupied by the structure using a video frame buffer, and correct for the thickness of the cell and the directions of the strands in space. The measured values of the fractional volume of the cytoplasmic matrix in PTK and NRK cells cytoplasm are only 10-21%, which cannot explain the slow cytoplasmic diffusion of proteins. It is possible that the diffusing fluorescent proteins are entangled with, adsorbed or attracted chemically by the network. For the simplest adsorption model, where the concentration of the adsorbed protein is proportional to its concentration in the aqueous space, we obtained a binding free energy of about -2.4 kcal/mole for the MTL and filaments volume fraction of 0.1 in the cytoplasm. The amount of surface associated with the MTL and the cytoskeleton is quite high (our measurement yields estimated values of 50,000 - 100,000 μm^2 in a cytoplasm of a cell of 16 μm in diameter with a 10 μm nucleus). Similar measurements on cells responding to different osmotic environments will be presented.

1. Wojcieszyn, J.W. et al. (1981). PNAS U.S.A. 78,4407-4410. 2. Wolosewick, J.J., and Porter, K.R. (1979). J. Cell Biol. 82, 114-139.

M-AM-Pos113 MONITORING CELLS IN TISSUE CULTURE WITH AN ELECTRIC FIELD, I. Giaever and C.R. Keese, General Electric Research & Development Center, P.O. Box 8, Schenectady, NY 12301

We have cultured both normal and transformed fibroblasts on evaporated Au electrodes inside tissue culture dishes. By using one large and one small area electrode, the measured impedance is, for practical purposes, dominated by the small electrode. An electrical signal at 4000 Hertz is applied and changes, caused by the cells, in both the in-phase (resistive) and out-of-phase (capacitive) signal are recorded. The current density, a few $\mu\text{amps/cm}^2$, has no detectable effect on the cells. The cells, however, have a large influence on the measured in-phase signal and a somewhat lesser effect on the out-of-phase signal. When the cells are first seeded in the tissue culture dishes, they attach and then spread on the electrodes blocking out large areas of the electrodes. This process causes an increase by about 100% in the resistive part, and about a 25% increase in the capacitive part, depending on cell density. After the initial spreading the cells are in more or less continuous motion that causes fluctuating changes in the measured impedance. Preliminary experiments show that cancer cells are noisier than their normal counterpart. By using this method the effect on the cells of various drugs can be monitored as a function of time. By making very small electrodes ($\sim 10^{-4}\text{cm}^2$) it is possible to observe changes in the impedance arising from a single cell.

(Supported, in part, by a grant from the National Foundation for Cancer Research, Bethesda, MD.)

M-AM-Pos114 PHOTOELECTRON MICROSCOPY AND IMMUNOFLUORESCENCE MICROSCOPY OF CYTOSKELETAL ELEMENTS IN THE SAME CELLS. Karen K. Nadakavukaren¹, Lan Bo Chen¹, Douglas L. Habliston² & O. Hayes Griffith². ¹Sidney Farber Cancer Institute, Harvard Medical School, 44 Binney St., Boston, MA 02115, and ²Institute of Molecular Biology, University of Oregon, Eugene, OR 97403.

Electron microscopy (photoemission electron microscopy) has recently emerged as a new, surface sensitive electron microscope technique with interesting potential applications in cell biology. In order to aid the interpretation of these new images and explore the possible applications of photoelectron microscopy in cell biology, immunofluorescence and photoelectron microscopy were performed on the same cells. PtK2 kangaroo epithelial cells and RAT-1 fibroblasts were grown on conductive glass discs and permeabilized, and the cytoskeletal elements actin, keratin, and vimentin visualized by indirect immunofluorescence. After the fluorescence microscopy, the cells were post-fixed and dehydrated for photoelectron microscopy. By comparison with fluorescence micrographs obtained of the same cells, actin-containing stress fibers, keratin tonofilaments and vimentin filaments were identified in the photoelectron micrographs. The apparent volume occupied by the cytoskeletal network in the cells as judged from the photoelectron micrographs is much less than it appears to be from the fluorescence micrographs because the higher resolution of PEM shows the fibers at closer to their true dimensions. PEM is a surface technique and the images highlight the exposed cytoskeletal structures and suppress those extending along the substrate below the nuclei. The photoelectron micrographs reported here demonstrate the marked improvement in image quality and shows that this technique has the potential of contributing to higher resolution studies of cytoskeletal structures. This work was supported by PHS Grant No. CA11695 from the National Cancer Inst.

M-AM-Pos115 MAPs MEDIATE ASSOCIATION OF MICROTUBULES AND NEUROFILAMENTS IN VITRO. Eric Aamodt and Robley C. Williams, Jr., Department of Molecular Biology, Vanderbilt University, Nashville, TN 37235.

Runge *et al.* (1981, PNAS 78:1431) have described the association in vitro between microtubules and neurofilaments prepared from bovine brain. We have extended their findings by investigating the association of microtubules with neurofilaments prepared from bovine spinal cord (Delacourte *et al.*, 1980, Biochem. J. 191:543). This preparation was found, by SDS-PAGE, to consist of fewer detectable proteins than the neurofilaments prepared from brain. In particular, high molecular weight microtubule-associated proteins (HMW-MAPs) were apparently absent. When neurofilaments were centrifugally removed from mixtures that also contained HMW-MAPs, HMW-MAPs were enriched in the neurofilament-containing pellets. The apparent viscosities of mixtures of microtubules with neurofilaments, measured with a falling-ball viscometer, were the same, within experimental error, as those of microtubules without neurofilaments (~500 cp). Mixtures that contained HMW-MAPs formed a gel (>12,000 cp). Measurement of the dependence of observed viscosity on concentration of HMW-MAPs showed a maximum. We interpret these results to mean that HMW-MAPs bind to spinal cord neurofilaments, that HMW-MAPs mediate formation of a viscous complex between microtubules and neurofilaments, and that a limited number of sites is present on microtubules and neurofilaments for the binding of MAPs. These results suggest that one or more HMW-MAPs may serve as a link between the two filamentous structures. Previous results of Runge *et al.* showing association in the absence of added MAPs can be explained by the presence of small amounts of contaminating HMW-MAPs in the neurofilaments prepared from brain. Supported by grant GM 29834 of the NIH.

M-AM-Pos116 HUMAN PLATELET P235: A HIGH M_r CYTOPLASMIC PROTEIN WHICH MODULATES ACTIN POLYMERIZATION. Nancy C. Collier and Kuan Wang (Intr. by Dawn Palter), Clayton Foundation Biochemical Institute and Department of Chemistry, University of Texas, Austin, Texas 78712.

P235, a large (2 X 235,000 M_r) cytoplasmic protein which contributes 3-8% of total platelet protein, has recently been purified and characterized (J. Biol. Chem. (1982) 257 6937). It is distinct from spectrin, filamin, myosin and fibronectin. To explore the potential involvement of P235 in platelet contractility, we have been investigating its interaction with actin in solution. It was observed that the presence of substoichiometric amounts of P235 during salt-induced actin polymerization resulted in a lowered low shear viscosity and shortened actin filaments (FEBS Lett. (1982) 143 205). Currently, studies of P235-actin interaction are being performed with pyrene-conjugated actin which exhibits a ~25-fold increase in fluorescence emission at 386 nm upon polymerization (Kouyama and Mihashi, Eur. J. Biochem. (1982) 114 33). This sensitive fluorescence technique allows the kinetics of actin polymerization to be followed continuously without subjecting the sample to mechanical shearing which alters the rate of polymerization. We observed that P235 alters the initial rate of actin polymerization in a Mg^{2+} -dependent manner. For example, a decrease in the initial rate of polymerization occurred at high $[Mg^{2+}]$ (>1 mM); at low $[Mg^{2+}]$ (<10 μM), an increase occurred; at intermediate $[Mg^{2+}]$ (~50 μM), no change was observed. However, P235 caused no significant change in the final steady state fluorescence of actin at any $[Mg^{2+}]$. These preliminary results suggest that P235 modulates the rate of actin polymerization in a Mg^{2+} -sensitive manner, but has no effect on the extent of polymerization. (Supported in part by NIH AM20270, NIH CA09182 and American Heart Association, Texas Affiliate, Inc.)

M-AM-Pos117 THE PURIFICATION AND INITIAL CHARACTERIZATION OF A HIGH MOLECULAR WEIGHT ACTIN BINDING PROTEIN FROM HUMAN PLATELETS. Mark A.L. Atkinson, Yale University School of Medicine, New Haven, CT 06510 (Current Address: Bldg. 3, Room B1-22, NIH, Bethesda, MD 20205).

I report a method to purify a protein of approximate molecular weight 255,000 daltons from the cytoskeleton of human platelets by which 30 units of outdated platelets (from the American Red Cross) yielded approximately 5 mg of purified protein. This procedure involves the extraction of a Triton X100 insoluble cytoskeleton, formed from washed platelets, by dialysis against a large excess of 1 mM EDTA at pH 8.0. The extract is then chromatographed on a column of Sepharose CL-4B in low ionic strength buffer at pH 7.6. Under these conditions the 255K protein is separated from most of the cytoskeletal components but co-elutes with a fraction of the total cellular actin to which it appears to be tightly bound. It has proven possible to separate the putative actin binding protein from actin only under mild denaturing conditions by anion exchange on a column of DEAE-Sephacel in the presence of 3 M urea. The purified protein has an amino acid composition similar to that reported for other high molecular weight actin binding proteins but differs significantly from that reported for human erythrocyte spectrin. The molecule appears to self-associate to form dimers and may form higher order oligomers. Rotary-shadowed replicas of the molecule indicate an extended structure. Limited tryptic digestion and two-dimensional IEF/SDS gel electrophoresis of the tryptic peptides suggest that the protein has a multi-domain structure and that this structure is able to reform when the molecule is dialyzed out of urea. Two-dimensional mapping of these peptides labelled with I^{125} in stained gel slices has yielded a preliminary structural map of the molecule. [Supported by the James Hudson Brown and Alexander B. Coxe Research Fellowship.]

M-AM-Pos118 MOTILITY OF MOUSE FIBROBLASTS: THERMOTAXIS AND MAGNETOTAXIS.

W. C. Parkinson, Department of Physics, The University of Michigan, Ann Arbor, Michigan 48109.

The motility of mouse fibroblasts is a function of the phase of the cell cycle, and for approximately the first one-eighth of the cycle can be described in terms of a random-walk¹). A question of interest, for which the answer is not yet known, is why they move. Do they move in response to external stimuli? It is known that certain simple cellular structures such as the pseudoplasmodia of dictyostelium discoideum and the nematode caenorhabditis elegans exhibit not only a thermotactic response, but migrate toward the temperature at which they have been cultivated²). Preliminary measurements of the motion of mouse fibroblasts under a temperature gradient of 5° C/cm centered on 35° C indicate a small positive thermotactic effect. However, at present a directional correlation with thermal streaming can not be ruled out. Measurements of the motility in a uniform magnetic field of 30 gauss indicate no magnetotactic response. Quantitative results of further measurements will be reported.

- 1) W. C. Parkinson, Biophysical Journal (in press).
- 2) Whitaker, B. D. and Poff, K. L. (1980) Exp. Cell. Res. 128, 87.

M-AM-Pos119 ELECTRON MICROSCOPY OF THE CORE FRAGMENTS OF KERATIN AND NEUROFILAMENTS REVEALS A MAJOR GLOBULAR DOMAIN. Leslie Milam and Harold P. Erickson, Department of Anatomy, Duke University Medical Center, Durham, North Carolina 27710. (Introduced by Emma R. Jakoi).

Intermediate filament structure has been studied by limited proteolysis followed by biochemical characterization of the fragments (Skerrow et al., JBC 248: 4820-4826, 1973; Steinert, J. Mol. Biol. 123: 49-70, 1978; Geisler et al., Cell 30: 277-286, 1982). We have digested whole keratin filaments and neurofilaments using similar methods. Gel filtration chromatography on Sepharose 6B yields 3 peaks other than the void and included volume peaks. Electron microscopy of shadowed specimens shows rod shaped particles averaging 40 nm and 20 nm in length, for Peaks 1 and 2, as described previously by Skerrow and by Steinert. However, the particles seen in shadowed specimens appear much more heterogeneous in both length and thickness than those described before. Peak 3 contains a particle eluting at $K_{av} = .77$ (corresponding to a globular protein of 55,000 daltons) which has not been previously described. CD of the peak fraction indicates low α -helix content. Electron microscopy of shadowed specimens shows that Peak 3 does consist of globular particles, about 6 nm in diameter. Limited proteolysis of neurofilaments also yields long rods (34 nm average length) and globular particles, but no short rod. The spheres eluted later than those of keratin, but appeared similar by EM.

Models for IF protofilament structure include 40 nm long regions of helix divided at the ends by globular regions. However, the globular domains in Peak 3 are larger than depicted in previous models. Supported by NIH grant GM-28553.

M-AM-Pos120 TOPOGRAPHICAL FLUORESCENCE MICROSCOPY OF OXYNTIC CELL MICROFILAMENTS. C. Okamoto, J.M. Wolosin, T.M. Forte and J.G. Forte. Dept. of Physiology-Anatomy and Donner Lab, Lawrence Berkeley Laboratory, Univ. of California, Berkeley, CA 94720.

In rabbit gastric glands, actin comprises 4% of the total protein with 60% of it existing in the F (filamentous)-form. Topographical fluorescence microscopy with 7-nitrobenz-2-oxa-1,3 diazole-phalloidin (Barak et al., PNAS USA 77,980) revealed that the majority of this F-actin is predominantly located in the apical pole of the HCl secreting parietal cell. No significant F-actin levels were detectable in the other main gland component, the chief cell. The spatial distribution of F-actin was dependent upon the cell secretory state. In non-secreting parietal cells, the fluorescence tended to be confined to the area in close proximity to the glandular lumen. Upon stimulation (histamine or dibutyryl cAMP), there was an increase in fluorescence intensity and distribution, F-actin expanded throughout the cytoplasm in a distribution consistent with that of the expanded apical membrane. The isolated, (H⁺+K⁺)-ATPase-rich, apical membrane obtained from secreting cells contained F-actin (10% of the total protein) arranged as single microfilaments. The microfilaments, isolated by sedimentation after detergent solubilization of 85% of the protein contained actin and 3 other polypeptides (MW's 100K, 82K and 78K). All four peptides were present also in highly pure apical membranes obtained by immunopurification. They were not present, in contrast, in (H⁺+K⁺)-ATPase-rich membranes obtained from non-secreting cells, suggesting that a transient interaction between cytoplasmic microfilaments and the (H⁺+K⁺)-ATPase-rich membrane occurs during the stimulation cycle. (Supported by USPHS Grant #AM10141)

M-AM-Pos121 RANDOM WALK DESCRIPTION OF RELEASE, UPTAKE AND PULSE CHASE OF LABELED SUBUNITS OF F-ACTIN OR A MICROTUBULE THAT UNDERGOES TREADMILLING. Takashi Tsuchiya, NIADDK, NIH, Bethesda, MD 20205, Yoshinori Nagai, Dept. of Applied Physics, and Hiroshi Asai, Dept. of Physics, Waseda Univ., Tokyo 160, Japan. (Intr. by Yi-der Chen)

Head-to-tail polymerization or treadmilling of actin or microtubules attract considerable attention recently. We describe this phenomenon as a random walk problem and present exact formulas for the amount of release and uptake of labeled subunits. This is done by applying the results for the quantity called the average number of distinct sites visited by a random walker, or for brevity, the number of once-visited sites. Each end of a polymer is regarded as a random walker with asymmetric transition probabilities which are determined by the rate constants of polymerization and depolymerization and the concentration of free subunits in the solution. Our formulas cover not only asymptotic and steady states but also arbitrary transient states. If we assume the length of a polymer is very long, calculation of the quantity of interest for the walker at one end of the polymer can be done independently of the walker at the other end and various asymptotic expressions are derived for all the possible sets of the rate constants and the concentration. We also treat the number of remaining labeled subunits observed in pulse chase experiments. Numerical calculations are done using hypothetical and experimentally measured values of the rate constants. For a finite-length polymer, calculations of the quantities of interest becomes quite complicated. We study the limiting length of the polymer at which the infinite-length model ceases to be valid.

M-AM-Pos122 PURIFICATION OF A PROTEIN PHOSPHATASE FROM ACANTHAMOEBA ACTIVE AGAINST MYOSIN II. Joseph A. McClure and Edward D. Korn, LCB/NHLBI, NIH, Bethesda, MD 20205.

The actomyosin ATPase activity of myosin II from Acanthamoeba castellanii is inhibited by phosphorylation of three serine residues on the tail of the heavy chain of the molecule. We have purified a phosphatase from Acanthamoeba using myosin II as a substrate. The phosphatase has a molecular weight by SDS-PAGE of 39,000 daltons. It is active against intact myosin II and also dephosphorylates the purified 9,000-dalton piece of the tail shown previously to contain all three phosphorylation sites. In preliminary experiments, the three phosphorylation sites on myosin II appear to be dephosphorylated simultaneously by the phosphatase. The phosphatase also dephosphorylates turkey gizzard smooth muscle myosin light chains, microtubule-associated protein II from bovine brain, and a seven-amino acid synthetic peptide which is a cAMP-dependent protein kinase substrate. The phosphatase activity is completely inhibited by 100 μ M pyrophosphate, 50 mM NaF, and by 0.5 mM ATP, but is not affected by 0.5 mM AMP, Ca^{2+} , EGTA, EDTA, or Ca^{2+} -calmodulin. Although the enzyme activity as isolated is not dependent on the addition of $MgCl_2$ or $MnCl_2$, the protein is considerably more stable in the presence of 5 mM $MnCl_2$. The Mg^{2+} -dependent actomyosin ATPase activity of myosin II is activated by dephosphorylation by the phosphatase, which has no ATPase activity of its own. Myosin II activated by the phosphatase can be inhibited by phosphorylation with a partially purified myosin II kinase, repurified over gel filtration in its inactive form, and reactivated by the phosphatase. This 39,000-dalton protein phosphatase is a useful tool for studying the regulation of the actomyosin II ATPase activity in this non-muscle system and may represent the physiologic myosin II phosphatase in Acanthamoeba.

M-AM-Pos123 HETEROGENEITY IN MACROPHAGE MYOSIN DEMONSTRATED BY THREE DIFFERENT ELECTROPHORETIC TECHNIQUES. J.A. Trotter, S.P. Scordilis, and S.S. Margossian. Univ. of New Mexico School of Medicine, Albuquerque, NM 87131; Smith College Dept. of Biological Sciences, Northampton, MA 01063; and Montefiore Hospital Division of Cardiology, Bronx, NY 10467.

It has been shown previously (Trotter, J.A., *J. Cell Biol.* 91, 295a) that myosin from rabbit alveolar macrophages and from two macrophage-like murine tumor cell lines, when analyzed by high resolution SDS-PAGE, contains two components of the 20KD light chain. The heavier component (LC₂₀₋₁) is present in approximately twice the concentration of the lighter component (LC₂₀₋₂). Macrophage myosin-light-chain-kinase (MLCK) phosphorylates both LC₂₀₋₁ and LC₂₀₋₂ to 1 mol/mol. We now demonstrate that 2D electrophoresis of macrophage myosin resolves LC₂₀₋₁ and LC₂₀₋₂ as spots of different molecular weight (MW) and isoelectric point (IEP) as follows: LC₂₀₋₁: MW=20,600; IEP=5.16. LC₂₀₋₂: MW=19,300; IEP=5.26. Phosphorylation of this myosin by MLCK from rabbit back and leg muscles results in a shift of the IEP of LC₂₀₋₁ and LC₂₀₋₂ to 5.13 and 5.22, respectively. Electrophoresis in the presence of 40mM sodium pyrophosphate resolves native macrophage myosin into predominately two major bands. The faster migrating band is present in approximately twice the concentration of the slower migrating band, as estimated from quantitative densitometry of stained gels. We interpret these results to mean that each macrophage must contain at least two myosins, one of which must be homodimeric for LC₂₀₋₁. We are presently attempting to analyze the polypeptide composition of the different bands from the native gels to determine directly the light-chain composition of each macrophage myosin. (Supported by grants from the ALA to J.A.T., from the MDA and Blakeslee fund of Smith College to S.P.S., and from the N.I.H. (HL26569) to S.S.M.)

M-AM-Pos124 POSSIBLE MECHANISMS BY WHICH CALMODULIN ANTAGONISTS ALTER SWIMMING IN PARAMECIUM. Tim Otter, Birgit H. Satir and Peter Satir, Department of Anatomy, Albert Einstein College of Medicine, Bronx, New York 10461

We have investigated in detail how trifluoperazine (TFP) and W7, drugs that inhibit calmodulin (CaM), alter swimming behavior in both living and reactivated, Triton-extracted *P. caudatum*. Living paramecia slow forward swimming speed reversibly and concurrently shorten when incubated in standard medium containing 10 μ M TFP or 40 μ M W7. Preincubating cells in TFP or W7 blocks the repetitive reversals that normally occur in Ba²⁺-medium; instead there are infrequent but prolonged reversals. At 50 μ M, W5 does not affect swimming behavior. In living cells, drug effects are consistent with inhibition of the removal of Ca²⁺-ions from the ciliary matrix by a CaM-mediated membrane Ca²⁺-pump. Triton-extracted paramecia reactivated with 4 mM ATP swim forward at ca. 0.3 mm/sec at pCa 7. When the pCa is lowered to 6.3 they slow down. At pCa 6, average forward progression ceases and the cells rock in place. Addition of up to 40 μ M TFP does not alter the behavior of extracted cells reactivated at pCa's > 6. However, below pCa 6, TFP affects the behavior of such cells: when reactivated at pCa 5.7 they swim slowly backward, but TFP blocks the reversal so that they swim slowly forward. We conclude that in Triton-extracted paramecia at low pCa's, TFP alters axonemal rather than membrane function. We propose a model that reconciles the responses to TFP in extracted paramecia with the effects of TFP on the Ca²⁺-dependent arrest of lamellibranch gill cilia. In this model, three different Ca²⁺-binding states of an axonemal Ca²⁺-CaM complex in paramecium correspond to forward, "neutral", and reversed ciliary beat. Supported by USPHS and ACS PF-2130.

M-AM-Pos125 CILIARY TWIST ARISING FROM INTERNAL FORCES IN THE PRESENCE OF A 5-6 BRIDGE. Michael Hines & J. J. Blum. Department of Physiology, Duke University Medical Center, Durham, N. C. 27710.

It has been shown that, for a strict sliding filament model, interdoublet links which cannot transmit bending moments (i.e. pinned links) also cannot cause twisting of the axoneme. (Hines & Blum, Biophys. J. In press)

It has proved difficult to extend the analysis to moment bearing links with the usual methods of equilibrium mechanics since a moment bearing link is not describable solely in terms of a shear force. A conceptually simple reformulation of ciliary mechanics in terms of a minimum potential energy principle provides a more direct and more easily understandable procedure for developing the three-dimensional equilibrium equations.

The fixed 5-6 bridge seen in some cilia and flagella has been modeled as a structure whose energy of distortion depends on the angle the bridge makes with its doublets. Computer simulations of the sliding filament model with such bridges show that axoneme twist is generated when the 5-6 bridge is subject to shear forces.

Graphs of curvature (including twist) and of ciliary shape will be presented for several distributions of internal shear force and as a function of rigidity of the 5-6 bridges.

When bending resistance and bridge rigidity is such that sliding is primarily limited by the bridge, then, for a given active shear force, a change in bridge rigidity will cause a corresponding change in sliding with no change in total twist.

M-AM-Pos126 CALCIUM ACTIVATION OF THE ABRONTAL GILL CILIA OF *MYTILUS EDULIS*. E. W. Stommel (Intr. by E. R. Baylor), Marine Biological Laboratory, Woods Hole, MA 02543.

The cilia of extracted cell models of the abfrontal cells of *Mytilus edulis* gill filaments start beating when the Ca concentration of an ATP reactivating solution is increased to 20 μ M. This phenomenon is quite unlike the well-studied effects of Ca on the lateral cells, which are arrested at a Ca concentration of 1 μ M. The cilia of the frontal cells beat well in a large range of Ca concentrations, from 0.1 μ M-0.2 mM, with a peak frequency at about 50 μ M. In intact cells, the abfrontal cilia are quickly arrested in artificial sea water containing 20 mM Co or 2 mM La and quickly resume beating when these ions are washed out. Artificial seawater in which the Na is replaced by Li increases the beat frequency of the abfrontal cilia. In seawater containing 50 μ M Ca ionophore A23187, the beat frequency of the abfrontal cilia is also increased. If 50 μ M trifluoperazine is added to the 20 μ M Ca reactivating solution, the abfrontal cilia of cell models stop beating. Using fluorescent or ferritin labeled secondary antibodies and cells incubated in rabbit calmodulin antiserum, there appears to be a higher level of calmodulin in the abfrontal cilia than in the cilia of other cells of the gill filament. A new isolation procedure separates lateral cilia from cilia of other cell types. SDS polyacrylamide gel electrophoresis shows no detectable calmodulin in either the membrane-matrix or axoneme fractions of the lateral cilia. I conclude that calmodulin plays a role in activating ciliary beat in the abfrontal cells. Dynein of the abfrontal cilia may be unique, requiring calmodulin directly or indirectly to be an active or functional ATPase. Ca may also inhibit dynein above calmodulin's buffering capacity since these cilia are arrested at very high calcium levels. Supported by NIH Grant GM 29,503.

M-AM-Pos127 CALCIUM BASED MECHANOSENSITIVITY IN CILIATED ABFRONTAL CELLS OF MYTILUS EDULIS GILLS. E. W. Stommel (Intr. by Lionel F. Jaffe), Marine Biological Laboratory, Woods Hole, MA 02543.

There is no detectable voltage noise to correlate with beating abfrontal cilia (cirrus cells not included). However, if the cilia of a quiescent cell are stimulated mechanically, receptor potentials as high as 5-10 mV can be obtained. These same quiescent cells consequently start to beat when mechanically stroked. There is good evidence for gap-junctions between adjacent abfrontal cells, for the receptor potentials elicited by the stimulating electrode can be recorded with a diminishing magnitude the further one records from the stimulated cell. In artificial seawater containing 20 mM Co, or in Ca-free seawater, these receptor potentials can be completely eliminated and there is consequently no elicitation of ciliary beat with mechanical stimulation. As in lateral cells (Murakami and Machemer, *J. Comp. Physiol.* 145: 351-362, 1982), the velocity of the stimulation is the most effective parameter and the direction of stimulation has little effect on the magnitude of the response. Depolarization of the abfrontal cells with 1-2 nA of current also elicits ciliary beating. The cilia of adjoining cells are also caused to beat, the effect of which diminishes with distance. When either artificial seawater containing 20 mM Co or Ca-free seawater is applied to the cells, the response to the depolarization is eliminated. Small spontaneous action potentials have been recorded from these cells, but they do not correlate with receptor potentials or with depolarizations. I conclude that mechanical and voltage sensitive Ca channels exist in the abfrontal cilia or cell bodies; these may be the same or different channels. As explained in an accompanying abstract, an increase in intracellular Ca increases the motility of these cells.

Supported by NIH Grant GM 29,503.

M-AM-Pos128 THERMODYNAMIC ASPECT OF THE LOCKED CELL HYPOTHESIS. Ezzatollah Keyhani. Inst. Biochem. Biophys., University of Tehran, P.O. Box 314-1700, Tehran, Iran.

The locked cell hypothesis postulates that mutated anaerobic (energy sufficient) and aerobic (energy efficient) sporulating prokaryote cells blocked at stage 3 or 4 were the precursor of eukaryotic cells (1,2,3). The locked cell is essentially in a metastable state both structurally and functionally. It has either to revert or evolve. Moreover the presence of two sets of information (nuclear and cytoplasmic DNA), increases further the entropy and facilitates the cell to undergo non-equilibrium phase transition. Such system may become "spontaneously inhomogeneous and present an ordered distribution of the chemical constituents in space" (4,5). The instability of a homogeneous system has been also postulated as a chemical basis for morphogenesis (6). Thus the non-equilibrium state and large scale fluctuation in locked cell may be a source of order, promoting compartmentalization and specialization of function within the cell. For example in aerobic system, this instability promotes the evolution toward the formation of mitochondria as a center for efficient energy production. Environmental constraint and gene rearrangement (including gene flow) orients the cell toward adaptation to a given ecological niche. (1) Keyhani, E. (1976) *J. Cell Biol.* 70, 81a; (2) Keyhani, E. (1981) *Ann. N.Y. Acad. Sci.* 361, 376-396; (3) Keyhani, E. (1982) *J. Cell Biol.* 95, 475a; (4) Prigogine, I. et al. (1972) *Physics Today* 25, 23-28 and 38-44; (5) Prigogine, I. (1978) *Science* 201, 777-785; (6) Turing, A.M. (1952) *Phil. Trans. Roy. Soc. (London)* B237, 37-72.

M-AM-Pos129 INITIAL ATTEMPTS TO IDENTIFY COMPONENTS OF THE SPERM PLASMA MEMBRANE WHICH ARE INVOLVED IN THE EGG JELLY INDUCED ACROSOME REACTION. A. Darszon, L. De Delatorre, I. Varga, P. Alvarez, M. Gould-Somero, and N. Cross. CINVESTAV de IPN, Mexico City; Biology Dept., UCSD, La Jolla, CA.

The sea urchin acrosome reaction is induced by a glycoprotein "jelly" surrounding the egg and is accompanied by changes in sperm plasma membrane ion permeability. We are interested in what membrane components are involved. Jelly in seawater at concentrations that induce the acrosome reaction did not significantly change $^{45}\text{Ca}^{++}$ uptake of sonicated unilamellar vesicles made with soybean lipid only (ratio jelly:control uptake = 1.08 ± 0.36 SD, $n=21$). Experiments with pure lipid planar bilayers held at various voltages have also not revealed substantial permeability increases at comparable jelly concentrations. In contrast, significant ($p < 0.005$, t test for two sample means) $^{45}\text{Ca}^{++}$ uptake was observed with vesicles made by cosonating soybean phospholipids and Strongylocentrotus purpuratus sperm membranes isolated by the procedure of Cross (*J. Cell Sci.*, in press) (ratio jelly:control uptake = 1.45 ± 0.66 , $n=21$). Egg jelly also induces increased permeability to $^{22}\text{Na}^{+}$ in these mixed vesicles. In an attempt to isolate a putative jelly receptor, we used affinity chromatography. Purified FS-1 factor from jelly (Kopf and Garbers, *Biol. Reprod.* 22:1118) was bound to CnBr activated Sepharose and Triton extracts from sperm labeled with sulpanilic-iodine or ^{125}I plus iodogen were added to the column in seawater followed by elution with increasing [NaCl]. Elution with 3 M NaCl 0 Ca^{++} yielded a fraction enriched for a labeled protein (~80 kd) on SDS-PAGE. Our interest is to determine if this protein is the postulated jelly receptor in order to use it in reconstitution studies where the molecular mechanism of the acrosome reaction can be examined. Supported by grants from NSF, CONACyT.

M-AM-Pos132 EPR STUDIES OF CONFORMATIONAL STATES IN A MULTIFILAMENT PROTEIN ARRAY: CROSSBRIDGE TRANSIENTS IN MUSCLE FIBERS. C.J. Ritz-Gold, CVRI, Univ. of Calif., San Francisco, CA 94143

Transient changes in crossbridge (actin-myosin head) conformational state were observed in muscle fibers following incubation with a substrate analog. Rabbit psoas fibers were labeled with a maleimide spin probe attached at a fixed angle to myosin heads. Uniformly aligned bundles of fibers supported by the surface of the sample holder were incubated for 5-10 min at 0 deg in the absence of Ca⁺⁺ and presence of different concs of MgPPi. Fibers were then scanned at 5 min intervals to monitor changes in the distribution of crossbridges between RIGOR (myosin head immobilized; probe orientation ordered) and PSEUDORELAXED (myosin head mobile; probe orientation disordered) states.

Crossbridges in untreated fibers were found to exist largely in the immobilized, ordered state. Following incubation, a rapid rise in the mobile, disordered state was observed that increased linearly over several time points. This was followed by a rapid recovery phase that either a) continued linearly until the final extent of crossbridge order recovery was achieved or b) was interrupted by an intervening plateau phase of variable duration. All transients exhibited similar waveform characteristics, with variability in the specific rates and relative contributions of the component phases. These results will be discussed in terms of a model based on the concepts of catastrophe theory and known mechanical properties of organelles such as muscle fibers in which a multifilament protein array mediates a dynamic mechanochemical response. (Supported by NIH HL07192).

M-AM-Pos133 CALCIUM SENSITIVE BINDING OF HEAVYMEROMYOSIN TO REGULATED ACTIN. Paul Wagner and Deborah Stone, Cardiovascular Research Institute, University of California, San Francisco, San Francisco, Ca 94143

The binding of heavymeromyosin, HMM, to regulated actin in the presence of MgATP was examined using a preparative ultracentrifuge. One-third of the HMM bound independent of the calcium concentration. The rest bound much more weakly to regulated actin in the absence of calcium than in its presence. Removal of LC2 by incubation at 37° C in EDTA or cleavage of LC2 to a 17,000 dalton fragment destroyed this calcium sensitivity. Cleavage of LC2 accounts for most of the HMM with calcium insensitive binding. The binding of single-headed HMM to regulated actin is similarly calcium sensitive.

M-AM-Pos134 MICROTUBULES IN HEART MUSCLE OF THE POSTNATAL AND ADULT RAT. Joiner Cartwright, Jr. and Margaret A. Goldstein, Section of Cardiovascular Sciences; Departments of Medicine and Cell Biology; Houston, Texas 77030.

In the postnatal rat heart muscle cells continue to divide as well as increase in size. At the same time cells in the soleus muscle do not divide, though they continue to grow in size. Since microtubules have a role in orienting intracellular structures in muscle, we determined the numbers of microtubules per μm^2 cross sectional area in rat heart muscle during development. We have previously determined that in the soleus muscle (a slow skeletal muscle) microtubule number per μm^2 increased to a maximum at five to nine days of age, after which there is an abrupt decrease to a steady level characteristic of the adult (J. Ultrastr. Res. 79: 74, 1982). We have counted the microtubules per μm^2 in cross sections of rat heart (papillary) muscle. The numbers of microtubules per μm^2 in heart were similar to those in the soleus muscle at the same age. The numbers of microtubules per μm^2 increased from birth to a maximum at nine days, then decreased to a steady state. This decrease in microtubule number in heart muscle occurred at nine to eleven days as in the soleus muscle. The distributions of microtubules are thus similar for cardiac and slow skeletal muscle, suggesting similar function(s) in these different muscle types.

M-AM-Pos135 A STEADY STATE KINETIC ACTIVE SITE TITRATION FOR MYOSIN ATPase, David D. Hackney and Patrick K. Clark, Department of Biological Sciences, Carnegie-Mellon University, Pittsburgh, PA 15213.

The slow turnover rate of myosin with $Mg \cdot ATP$ and the low K_m for ATP can be used to produce a steady state kinetic active site titration for myosin in the presence of the active regenerating system for ATP of pyruvate kinase and phosphoenolpyruvate. With micromolar concentrations of myosin in 0.5 M KCl or with the myosin subfragments, the rate of the steady state ATPase reaction increases linearly with addition of ATP until a sharp break occurs after which no further increase in rate is observed on further addition of ATP. This equivalence point represents saturation of the myosin ATP binding site responsible for the steady state ATP hydrolysis and is usually observed to occur at 0.7-1.0 ATP per myosin head with the higher range more characteristic of highly purified myosin and its subfragments. For each preparation the same equivalence point is also found when titrating for excess free ATP by the luciferase method (Furukawa, *et al.*, *J. Biochem.* **88**, 1629 (1980)). These results are similar to those reported recently by Ikebe, *et al.* (*J. Biochem.* **91**, 1855 (1982)) regarding these two types of titration, but they are only consistent with two classes of active site under a restrictive set of circumstances. Two types of ATPase site can only be accommodated if the nonburst site also binds ATP tightly and has the same turnover rate or if the nonburst head has the same K_m as the burst head independent of their relative steady state rates.

Supported by Grant AM 25980 from the USPHS.

M-AM-Pos136 CONFORMATIONAL TRANSITIONS OF SMOOTH MUSCLE TROPOMYOSIN. D.L. Williams, Jr.* AND C.A. Swenson, NIH, Bethesda, MD 20205 and Dept. of Biochem., Univ. Iowa, Iowa City, IA 52242.

Tropomyosin of smooth muscle may have a different role in the regulation of smooth muscle contraction than tropomyosin of skeletal muscle does in the regulation of skeletal muscle contraction. Functional changes are determined by changes in primary protein sequence. This allows altered stability in various regions of the structure and altered interactions with other proteins (actin and troponin) of this complex allosteric system. To probe these altered stabilities we have investigated the thermally induced transitions of smooth muscle tropomyosin in a differential scanning calorimeter and compared the results with those of skeletal muscle tropomyosin for which the amino acid sequence is known. Measurements were made on tropomyosin isolated from turkey gizzard as a function of pH in the presence and absence of dithiothreitol (DTT). At pH 7.0 a single endotherm with a T_m of 42°C is observed in the presence and absence of DTT. As the pH is decreased to 6.5 the T_m of this endotherm increases to 43°C and a shoulder appears on the high temperature side. This shoulder is resolved as a broad endotherm with a T_m of 58°C as the pH is decreased to 6.0. The results at each pH are the same in the presence and absence of DTT. This is in marked contrast to results on skeletal muscle where one endotherm is shifted from 50°C to 42°C when DTT is present. The absence of any changes when DTT is added suggests that no disulfide is present to link the chains in smooth muscle tropomyosin. The small pH dependence of the endotherm at 42°C suggests that it may arise from the same region of the structure as the only transition with these properties in reduced skeletal tropomyosin. In skeletal tropomyosin this endotherm is assigned to the unfolding of the region of the molecule which includes CYS-190. (NIH grants, HL 14388 and AM 27554.)

M-AM-Pos137 PHOSPHORYLATION AND ACTIVATION OF SMOOTH MUSCLE MYOSIN BY MYOSIN I HEAVY CHAIN KINASE ISOLATED FROM *ACANTHAMOEBA CASTELLANII*. John A. Hammer III (Intr. by P. Riesz), NHLBI, NIH, Bethesda, MD 20205.

Myosin I heavy chain kinase (MIHCK) is a myosin kinase which has recently been purified to homogeneity from the soil amoeba *Acanthamoeba castellanii*. MIHCK phosphorylates the heavy chain, but not the two light chains, of the single-headed *Acanthamoeba* myosin I isoenzymes, MIA and MIB, resulting in a 10- to 20-fold increase in their actin-activated Mg^{2+} ATPase activities. MIHCK phosphorylates MI at a rate of about 4 $\mu\text{mol}/\text{min} \cdot \text{mg}$ (2.5 μM MI, 30°C) and does not require Ca^{2+} for activity. MIHCK was found to phosphorylate isolated turkey gizzard smooth muscle light chains (SMLC), gizzard smooth muscle heavy meromyosin (HMM), and intact gizzard smooth muscle myosin (SMM), all in the absence of Ca^{2+} and with specific activities close to those measured for purified Ca^{2+} and calmodulin-dependent gizzard smooth muscle light chain kinase (SMLCK). MIHCK incorporated a maximum of 2 moles of phosphate/mole HMM, both by itself and together with SMLCK (SMLCK alone incorporated 1.6 moles of phosphate/mole HMM). SDS-PAGE and autoradiography of HMM and SMM phosphorylated by MIHCK to near maximal extent showed essentially all the phosphate to have been incorporated into the 20,000-dalton SMLC. Preincubation of HMM with MIHCK resulted in full activation of HMM actin-activated Mg^{2+} ATPase. These results support the conclusion that MIHCK phosphorylates gizzard SMM at the same site within the 20,000-dalton SMLC as does SMLCK. The results suggest that the phosphorylation site within the heavy chain of *Acanthamoeba* MI isoenzymes may have a similar sequence to the phosphorylation site in the 20,000-dalton SMLC.

M-AM-Pos138 PURIFICATION AND PHYSICAL CHARACTERIZATION OF CHICKEN GIZZARD SMOOTH MUSCLE MYOSIN LIGHT CHAINS. Walter F. Stafford, Department of Muscle Research, Boston Biomedical Research Institute, Boston MA 02114.

Gizzard myosin light chains were obtained by urea treatment of myosin followed by chromatography on DEAE Biogel A and hydroxylapatite. Myosin, prepared by ammonium sulfate fractionation, was taken up in 8 M urea, 20 mM MOPS, 0.1 mM EGTA, 1 mM $MgCl_2$, 1 mM DTT, pH 5.8 and applied to a DEAE Biogel A column to separate the light chains from myosin heavy chains and a nucleic acid component. Both light chains were eluted stepwise with 0.2M NaCl. The pooled light chain peak was applied to a hydroxylapatite column in 1 mM sodium phosphate, 1 mM EDTA, 1 mM DTT, pH 6.0 at 4°C and then eluted with a gradient (0-0.4M sodium phosphate, pH 6.0). Two peaks, well separated, were obtained, with LC₁₇ eluting before LC₂₀. Both light chains were free of kinase, phosphatase and calmodulin. The size and shape of the light chains were determined by sedimentation velocity measurements, analytical gel filtration and sedimentation equilibrium. Secondary structure was studied by circular dichroism measurements. These light chains were similar in structure to those of invertebrate and vertebrate striated muscle myosin (W.F. Stafford and A.G. Szent-Gyorgyi, (1978), *Biochemistry* 17,607).

This work was supported by NHLBI grant HL-26229.

M-AM-Pos139 REGULATION OF ACTIN-ACTIVATED ATPase ACTIVITY IN SMOOTH MUSCLE BY PHOSPHORYLATION OF MYOSIN LIGHT CHAIN WITH A Ca^{2+} -INDEPENDENT PROTEASE ACTIVATED KINASE, P.T. Tuazon and J.A. Traugh (Intr. by D. F. Bocian), Department of Biochemistry, University of California, Riverside, 92521.

The 20,000 dalton light chain of myosin from chicken gizzard has been shown to be phosphorylated in a Ca^{2+} and calmodulin-independent manner by the activated form of a protease activated kinase from chicken gizzard and rabbit reticulocytes. The protease activated kinase incorporates phosphate into the P-light chain in isolated myosin light chains and actomyosin stoichiometrically. Phosphorylation of the P-light chain by the proteolytically-activated protein kinase stimulates the actin-activated Mg-ATPase activity of myosin in the absence of Ca^{2+} . The extent of stimulation of the ATPase activity is similar to that observed upon phosphorylation of actomyosin by the Ca^{2+} -dependent myosin light chain kinase. The same serine residue appears to be phosphorylated by the protease activated kinase and the Ca^{2+} -dependent myosin light chain kinase. This conclusion is based on results from two-dimensional peptide maps of the chymotryptic and tryptic digests of the phosphorylated P-light chain and from phosphoamino acid analysis of acid hydrolysates. Protease activated kinase I has been shown to be distinct from the Ca^{2+} -dependent myosin light chain kinase by the mode of activation and specificity with other substrates, including phosphorylation of a different site on myosin P-light chain from skeletal muscle (P. T. Tuazon, J. T. Stull and J. A. Traugh, *Biochem. Biophys. Res. Commun.* 108, 910-917, 1982). Differences in the sites phosphorylated by the protease activated kinase in smooth and skeletal muscle are due to differences in the primary sequence of the P-light chains.

M-AM-Pos140 SUBSTRATE INHIBITION OF Ca^{2+} -ATPase OF MYOSIN, HMM AND S-1 ISOZYMES. Balish, M., and Dreizen, P. Biophysics Graduate Program and Department of Medicine, SUNY Downstate Medical Center, Brooklyn, N.Y.

Concentrations of ATP in excess of Ca^{2+} are known to inhibit myosin-ATPase, but the mechanism of substrate inhibition has been ambiguous. Avena and Bowen (JBC, 1971) concluded that substrate inhibition of Ca^{2+} -ATPase is non-competitive, with cooperative inhibition by two moles of ATP per active site; however, Bocharnikova and Samorukova (Biokhimiya, 1975) interpreted substrate inhibition in terms of essential activation by Ca^{2+} . We have re-examined this question, extending the analysis to myosin, HMM, and the chymotryptically prepared subfragment-1 isozymes of rabbit fast muscle myosin. Studies were done with Tris-ATP rather than K^+ -ATP in order to minimize variations in cationic environment. In all cases, free ATP in the millimolar range acts as an inhibitor of Ca^{2+} -ATPase. Analysis by conventional Dixon plots, at Ca^{2+} concentrations from 0.5mM to 3mM, reveals simple competitive inhibition with a single ATP binding site. The inhibitory constant, K_{ATP} , is approximately the same before and after chromatographic purification on DE-52, and is unaffected by treatment with Chelex. K_{ATP} is considerably stronger for HMM ATPase and S-1 ATPase than for myosin ATPase, but no significant differences are found between the light chain isozymes, S1-L1 and S1-L3. The overall findings may be interpreted in terms of competition between free ATP and $CaATP$ substrate at the hydrolytic site of myosin, HMM, and S-1. Unexpectedly, the interaction appears to be somewhat different in the case of myosin as compared with HMM and S-1. (Supported by grants from N.Y. Heart Association, N.I.H., and a fellowship from Insurance Medical Scientist Scholarship Fund).

M-AM-Pos141 EFFECTS OF SALTS ON THE REACTIVITY OF A FAST REACTING THIOL OF MYOSIN IN MUSCLE FIBERS. M.S. Crowder, M. Kwok, and R. Cooke, Department of Biochemistry/Biophysics and CVRI, University of California, San Francisco, California 94143 (Intro. by D. Warnock).

Electron paramagnetic resonance (EPR) has been used to examine the influence of ions on the specificity of the reaction between spin-labels (maleimide and iodoacetamide) and the fast reactive sulfhydryl (SH_1) of myosin. The EPR spectrum of spin-labeled muscle fibers in rigor is characterized by three spectral components: a highly mobile component, a rigidly bound component which is randomly oriented and a highly oriented spin which represents spin labels bound to SH_1 on myosin. Analysis of EPR spectra intensities indicate that the percentage of spin labels bound to SH_1 is highly dependent upon the anion present and follows the series (in order of increasing specificity): $\text{KF} < \text{KI} < \text{KCl} < \text{KCH}_3\text{COO}$. KF is .1x, KI is .5x and KCH_3COO is 1.5x as effective as KCl in enhancing SH_1 specificity. Potassium propionate and butyrate are only slightly more effective than acetate. Cations showed no such effects. Potassium and tetramethylammonium ions were equally effective. Duke et al. (PNAS, 1976, 73:302), demonstrated that the reactivity of SH_1 in glycerinated muscle fibers is dependent upon the state of the cross bridge, being more reactive when actin and myosin are disassociated. These results suggest that salt effects on proteins can also increase SH_1 reactivity. The anion effect follows the Hofmeister series and may reflect the ability of these anions to stabilize protein structure. Alternatively, these effects may reflect differences in electrostatic shielding of positive charges in the vicinity of SH_1 which cause its pK to shift relative to other sulfhydryl groups. This work was supported by grants from the USPHS AM00479 and AM 30668.

M-AM-Pos142 MgATP-INDUCED FLUORESCENCE ENHANCEMENT IN MYOFIBRILS, Howard D. White, Department of Biochemistry, University of Arizona, Tucson, AZ 85721

A four to six percent maximum enhancement of the tryptophan fluorescence occurs upon the addition of MgATP to stirred suspensions of bovine cardiac and rabbit psoas myofibrils. Approximately one mole of MgATP per myosin head is required to obtain the maximum fluorescence enhancement (Conditions: 100 mM KCl, 5 mM MgCl_2 , 10 mM MOPS, 100 μM EGTA, pH 7, 20°C). Upon the addition of MgATP at a stoichiometry greater than one mole per mole myosin head the fluorescence enhancement rapidly increases (< 1 sec) to a steady state, which lasts for a period that is proportional to the amount of MgATP added. The fluorescence then decays to the initial level with a half time of ~30 sec. The fluorescence enhancement can be repeated up to ten times by the addition of subsequent aliquots of MgATP. Rate constants for the formation of the steady state fluorescence intermediate were measured at [MgATP] from 1 to 5 μM by averaging 5 to 10 transients. The k_{obs} of the transient is proportional to [MgATP] and has a second order rate constant of $4 \times 10^5 \text{ M}^{-1}\text{s}^{-1}$. The kinetics of the fluorescence enhancement observed in myofibrils during ATP hydrolysis is qualitatively very similar to that observed for myosin, myosin-S1, and actomyosin-S1, and actomyosin-S1 in solution and suggests that the same mechanism of ATP hydrolysis that has been well established by studies in solution also occurs in myofibrils, although the rate constants are two- to three-fold slower. The same general pattern of a rapid fluorescence enhancement followed by a decay to the initial level of fluorescence is observed at identical conditions except that [Calcium] is 10^{-4} M . However, [ATP] >> [myosin heads] is required to obtain the maximum enhancement and the duration of the enhancement is twenty-fold less than observed at [Calcium] $\leq 10^{-7} \text{ M}$. (Supported by grants from the Muscular Dystrophy Assoc., Az Heart Assoc., & PHS HL 20984).

M-AM-Pos143 UV SPECTROSCOPIC STUDIES OF THE TWO STATES OF HEAVY MEROMYOSIN AND MYOSIN SUBFRAGMENT-1. Nader Moaven, Kathy Cunningham, Steve Wilson, John Shriver; Department of Medical Biochemistry and Department of Chemistry and Biochemistry, Southern Illinois University, Carbondale, IL 62901.

We have initiated a study of the UV difference spectra induced by the binding of nucleotides to rabbit skeletal muscle myosin fragments. As demonstrated by Morita (J. Biochem. 81, 313 (1977)), AMP-PNP induces a heavy meromyosin (HMM) difference spectrum at 25°C essentially identical to that observed for ATP. However, the difference spectrum is highly temperature dependent, and at 1°C the AMP-PNP induced spectrum is similar to that induced by ADP at 25°C. The HMM data can be described by a two-state equilibrium with an apparent van't Hoff enthalpy difference of 34 kcal/mole and $\Delta S = 120 \text{ eu}$. Thus these data imply that the HMM•AMP-PNP complex can exist in two states, one resembling the 25°C ATP state and the other the 25°C ADP state. This is consistent with the model recently proposed (Shriver and Sykes, Biochemistry 20, 2007 (1981)) in which myosin heads may exist in two fundamental states with the preferred state being a function of the nucleotide in the active site and the temperature. Although the AMP-PNP induced difference spectra of the limiting high and low temperature states appear identical for HMM and subfragment-1, there is a significant difference between the temperature dependence of the spectra for the two species. For S-1, preliminary studies indicate that the apparent van't Hoff enthalpy difference and ΔS are roughly half that seen for HMM. These results are reminiscent of data obtained without nucleotides using ^{19}F NMR (Shriver et al., Biophysical J. 37, 54a (1982)). (Supported by the Muscular Dystrophy Association).

M-AM-Pos144 EVIDENCE FOR A MONOMER ACTIVATION STEP IN ACTIN POLYMERIZATION. Lewis C. Gershman, Lynn A. Selden, James E. Estes, Research Service, Veterans Administration Medical Center, Albany, and Department of Physiology, Albany Medical College, Albany, NY 12208; and Jay Newman, Department of Physics, Union College, Schenectady, NY 12308.

The polymerization of actin induced by low concentrations of $MgCl_2$ occurs after a lag phase. This lag phase is usually attributed to a slow nucleation reaction. In studying actin polymerization kinetics at low $MgCl_2$ concentrations (0.3-0.5 mM) using N-(1-pyrenyl)iodoacetamide (N-P) labelled actin, we noted that if phalloidin-stabilized actin nuclei are added simultaneously with $MgCl_2$ (to eliminate the effect of the nucleation step), the lag phase, although somewhat shorter, is still present. Light scattering measurements also show no intensity change during this lag phase. If incubation of monomer actin with $MgCl_2$ is started before the addition of nuclei, this lag phase is shorter or absent, and the initial rate of polymerization is increased. These experiments indicate that a monomer activation step is required for elongation. Monomer actin labelled with 1,5-I-AEDANS (Friedan, J. Biol. Chem., 1980,1981) has been shown to undergo a conformational change having a similar time course as the lag period after $MgCl_2$ addition. With mixtures of both N-P labelled monomer and I-AEDANS labelled monomer, the fluorescence change with the I-AEDANS labelled monomer occurs during the lag phase and precedes the fluorescence change in the N-P labelled monomer. This suggests that a conformational change may be associated with the activation step reported here. Supported by the Veterans Administration.

M-AM-Pos145 EVIDENCE FOR OLIGOMER FORMATION BY MONOMER ACTIN AT LOW $MgCl_2$ CONCENTRATIONS. Jay Newman Department of Physics, Union College, Schenectady, NY 12308; Lynn A. Selden, Lewis C. Gershman and James E. Estes, Research Service, Veterans Administration Medical Center, Albany, and Department of Physiology, Albany Medical College, Albany, NY 12208.

In the absence of $MgCl_2$, the translational diffusion coefficient (D_{20}) of column-purified monomer actin extrapolated to zero concentration was determined by intensity fluctuation spectroscopy to be $7.88 \pm 0.11 \times 10^{-7}$ cm²/sec. This value decreased after incubation of monomer actin, at concentrations below the critical concentration, with added $MgCl_2$ (100-200 μM) at 25°C for 24 h. The decrease in D_{20} from control values was 20% with 150 μM $MgCl_2$ added and was larger at higher $MgCl_2$ concentrations (actin always below the critical concentration). The apparent diffusion coefficient for actin incubated in 150 μM $MgCl_2$ is much more dependent on scattering angle than actin in the absence of $MgCl_2$, indicating that larger scattering units are formed upon incubation in $MgCl_2$. Further evidence for the presence of oligomers was obtained using fluorescent-labelled (N-(1-pyrenyl)iodoacetamide) monomer actin added to demonstrate that monomer actin incubated with $MgCl_2$ polymerized more rapidly than control actin incubated without $MgCl_2$, but assayed under identical conditions in the presence of added equimolar phalloidin to stabilize any oligomer formed. Titration of the actin SH groups during incubation with $MgCl_2$ indicated there was no significant disulfide bond formation to account for the observed decrease in D_{20} , and the actin population remained fully polymerizable by viscosity measurements. These data suggest that at actin concentrations below the critical concentration, and in the presence of low $MgCl_2$ concentrations, a portion of the monomer actin population aggregates to form small amounts of oligomer. Supported by the Veterans Administration and the Research Corporation.

M-AM-Pos146 STRUCTURE OF TARANTULA AND SCORPION THICK FILAMENTS. Robert W. Kensler, Rhea J. C. Levine, Mary Reedy*, and Waltraud Hoffmann.* Department of Anatomy, The Medical College of Pennsylvania, Phila., PA 19129 and Department of Anatomy, Duke University, Medical Center, Durham, NC 27710.

The thick filaments from the tarantula and scorpion appear very similar in both negatively stained and platinum shadowed preparations to the thick filaments from *Limulus*. The filaments appear periodic with a helical repeat of ~ 43.8 nm. Optical diffraction patterns of the micrographs are detailed showing a series of layer lines which index as orders of a 43.9nm helical repeat. Meridional reflections occur on the third and sixth layer lines indicating that the crossbridge arrays have a 3-fold screw symmetry. Qualitatively the patterns are very similar to our previously published optical diffraction patterns from *Limulus* (Kensler and Levine, 1982, J. Cell Biol. 92:443-451) and the X-ray diffraction results of Wray et al. (1975, Nature 257: 561) on *Limulus*. Complete analysis of the diffraction patterns indicates that these filaments like those of *Limulus* most likely have 4 myosin cross-bridges extending axially from the backbone every 14.6nm, with a helical array similar to that previously described for *Limulus*. Optical filtrations of micrographs of both the negatively stained and shadowed filaments support this conclusion.

Supported by USPHS Grants: AM30442 (to RWK), HL15835 to the Pennsylvania Muscle Institute (RJCL), and AM14317 (MR).

M-AM-Pos147 STRUCTURE OF THE FROG THICK FILAMENT. Robert W. Kensler and Murray Stewart. Department of Anatomy, The Medical College of Pennsylvania, Phila., PA 19129 and MRC Laboratory of Molecular Biology, Cambridge, England.

A procedure has been developed for the isolation of frog thick filaments such that the helical arrangement of the myosin crossbridges is better preserved than has been previously reported for vertebrate skeletal muscle thick filaments. The filaments in negatively stained preparations appear periodic and at high magnification it can be seen that the pattern is due to the projection of the myosin crossbridges from the backbone with an apparent helical repeat distance of 42.9nm. The crossbridges appear to be only slightly tilted from the filament axis and extend to a radius of 14.5nm. Optical diffraction patterns of micrographs of the filaments are detailed and qualitatively similar to previously published X-ray diffraction patterns, except that the 1/14.3nm⁻¹ meridional reflection is weaker than expected. The patterns typically extend to at least the 6th layer line, and frequently to the 11th. Additional meridional reflections not expected from the helical symmetry are typically present on the 5th, 8th and 11th layer lines, and less frequently on the 2nd, 4th, 7th, 8th and 10th layer lines. Analysis of computed fourier transforms of the images demonstrates the phases of the inner maxima on the 1st layer line to be 180° out of phase and thus consistent with an odd number of helical strands. Computer filtrations of the images demonstrate a 3-stranded arrangement of the myosin crossbridges in the filaments. Platinum shadowing of the isolated filaments demonstrates the crossbridges to be arranged on right-handed helices.

Supported by USPHS Grant AM30442.

M-AM-Pos148 TITIN IS AN EXTRAORDINARILY LONG AND FLEXIBLE MYOFIBRILLAR PROTEIN. Kuan Wang and Ruben Ramirez-Mitchell, Clayton Foundation Biochemical Institute, Department of Chemistry and Cell Research Institute, University of Texas, Austin, Texas 78712.

We have proposed that titin ($M_r \sim 1 \times 10^6$) and nebulin ($M_r \sim 5 \times 10^5$) are major components of a set of elastic longitudinal filaments which span from Z disc to Z disc from within the sarcomere of striated muscles (Biophys. J. (1981) 33 21a). To evaluate this proposal, we have studied the morphology of titin molecules. Rotary and unidirectional shadowing of native titin dried from glycerol according to the technique of Tyler and Branton (J. Ultra. Res. (1980) 71 95) revealed images that are extremely long (400-1000 nm) and flexible. A significant degree of polymorphism of fine structures was apparent; the thickness along the length of the strand varied somewhat without obvious regularity and some molecules even possessed a few globular domains at either end or along the length. Metal casting under conditions which favored the decoration effect (but not the shadowing effect) revealed the presence of somewhat regular, periodic structural domains along the strand. The observations that titin is an extraordinarily long and flexible molecule possibly with periodic domains suggest that this novel molecule may be ideally suited to form a flexible cytoskeletal filament with which other periodic assemblies such as thick filaments may interact. (Supported in part by NIH AM20270, CA09182 and American Heart Association, Texas Affiliate, Inc.)

M-AM-Pos149 PHOSPHORYLATION OF TITIN AND NEBULIN IN VITRO AND IN VIVO. Laura L. Somerville and Kuan Wang (Intr. by Andrew T. C. Tsin), Clayton Foundation Biochemical Institute and Department of Chemistry, University of Texas, Austin, Texas 78712.

Three approaches were taken to examine the phosphorylation of the recently described giant myofibrillar proteins titin (PNAS (1979) 76 3698) and nebulin (PNAS (1980) 77 3254): (1) Incubation of rabbit skeletal myofibrillar preparations with [γ -³²P]ATP resulted in radiolabeling of titin, nebulin, tropomyosin and myosin P-light chain. Phosphorylation was enhanced by adding cAMP-dependent protein kinase to the incubation mixture; (2) Injection of [³²P]phosphate into the dorsal lymph sacs of *Xenopus laevis* resulted in the preferential labeling of these high molecular weight proteins, as well as myosin P-light chains of the gastrocnemius muscle. Autoradiography of paper electrophoretograms of partially hydrolyzed proteins purified by gel filtration indicated the presence of phosphoserine; (3) Determination of protein-bound phosphate by the method of Stull and Buss (J. Biol. Chem. (1977) 252 851) indicated that purified rabbit titin and nebulin contained 2 to 3 moles of phosphate per mole of protein. These findings indicate that titin and nebulin are phosphoproteins and suggest that protein phosphorylation may play either a structural or a regulatory role in titin and nebulin-containing structures. (Supported in part by NIH AM20270, CA09182 and American Heart Association, Texas Affiliate, Inc.)

M-AM-Pos150 THE HIERARCHICAL ARRANGEMENT OF INTER- AND PERI- CELLULAR CONNECTIVE TISSUE STRUCTURES IN HEART MUSCLE. T.F. Robinson, L. Cohen-Gould, and S.M. Factor. Albert Einstein College of Medicine, Bronx, New York 10461

We present an integrated description of extracellular matrix of mammalian cardiac muscle using LM and EM. The skeletal framework of the heart is organized in a hierarchical system of structures. Components include unit fibrils of collagen, 30-70 nm in diameter; elastin fibers, 1 μ m wide; microfibrils, 15-20 μ m in diameter, with periodicity, hollow profile, and fibrous subunits; polyanionic microthreads, with 4 nm cores and 2-3 nm side chains; polyanionic granules, 10-40 nm in diameter; "amorphous" ground substance; lamellar bodies; external glycocalyx-like sheets; and polyanionic extracellular sacs. Cardiac myocytes are enveloped by a collagen weave and inter-connected by collagen struts, <0.3-2.5 μ m in diameter, often with twisted configuration, probably for enhanced tensile strength. The collagen weave is criss-crossed at sarcomere lengths of 1.8-2.0 μ m in papillary muscle, and is aligned with the muscle long axis at the tensile limit at 2.4-2.5 μ m. Elastic fibers inter-connect cells and helically wind around myocytes. Circumferential forces from elastin stretched about shortened, thickened myocytes in systole should promote elongation in tandem with intra-myocyte forces of elongation. In contracted muscles festoons of sarcolemma are attached to Z bands, thus forming regions for lateral, trans-sarcolemmal force transmission. Superimposed on large extracellular structures is a polyanionic-rich matrix of unit collagen fibrils, microthreads, and granules. Amorphous ground substance forms a matrix in which collagen fibrils of struts are embedded and is continuous with the cell coat. Supported by NIH HL-24336, NY Hrt.Assoc.Grant-in-Aid, and NIH RCDA HL-00568 (TFR).

M-AM-Pos151 STRUCTURAL STUDIES OF THE OUTER REGION OF NATIVE THICK FILAMENTS Kathy Riley and Jane F. Koretz, Biology Dept., RPI, Troy, NY 12181 (Introduced by Joseph V. Landau.)

AMP deaminase, a tetrameric enzyme of 320K MW, has been shown to bind specifically to the sub-fragment-2 region of rabbit skeletal muscle myosin. When mixed with isolated native thick filaments, AMPD binds along the entire length of the filament except for the bare zone. Because of its large bulk relative to the number of available binding sites, it binds at each subunit level with a symmetry less than or equal to the symmetry of the myosin heads. This, combined with the immobilization of the heads by AMPD decoration, aids in the structural analysis of thick filament symmetry. Electron microscopy and optical diffraction of the outer region of decorated and undecorated thick filaments were performed, and the results compared with those obtained for the banded region (Koretz, PNAS, 1982). The undecorated outer region exhibits both orders of 43 nm, including a weak meridional 14.3nm reflection, and orders of 57.2 nm (4×14.3), the latter and its second order generally visible; these results are similar to those within the banded region. In the decorated structure, these periodicities are enhanced and other reflections related to them become visible; the latter reflections depend on the binding pattern of the deaminase on the backbone of the filament, and would not be observed if the deaminase could bind with the same period as the myosin molecules themselves in a symmetric structure. The reflections observed are thus similar in both regions, and inconsistent with a simple symmetric two-fold or three-fold model. A distorted four-fold model has been suggested; that, and other consistent models will be presented. Research supported by a grant from the Muscular Dystrophy Association.

M-AM-Pos152 STRUCTURAL STUDIES OF MYOSIN ROD AGGREGATES WITH AMP DEAMINASE AND/OR C-PROTEIN Mark S. Goldberg and Jane F. Koretz, Biology Dept., RPI, Troy, NY 12181 (Introduced by Robert H. Parsons)

Myosin rod (MW 200K) is the largest aggregating proteolytic fragment of myosin. When the papain product from rabbit skeletal myosin is dialyzed against low ionic strength (0.10M KCl, 10 mM imidazole, pH 6.5), it forms ordered sheetlike structures which appear to curl at the edges. The sheets exhibit stripes perpendicular to the long axis at 14.3 nm intervals, and optical diffraction also reveals a 7.2 nm period. AMP deaminase, a 320K MW tetrameric enzyme which has been shown to bind specifically to the S-2 region of myosin and rod, completely decorates the already formed rod sheet at 14.3 nm intervals all the way out to both ends, but seems to obscure the 7.2 nm period. When added to rod before dialysis, AMPD appears to interfere with aggregation; the resultant structures are short and blunt-ended, show a 14.3 nm period (but not a 7.2 nm period), and sometimes exhibit bare zones free of AMPD decoration. When C-protein, a thick filament protein of MW 140K that has been shown to bind to both the S-2 and light meromyosin regions of the rod, is mixed with rod before aggregate formation, sheets are formed; these sheets, however, have more diffuse stripes and do not exhibit a 7.2 nm period with optical diffraction. Further, these sheets cannot be decorated with AMPD. When both C-protein and AMPD are mixed with rod before dialysis, the resultant structure shows length and organizational characteristics intermediate between either of the two-protein mixtures. AMPD decoration to both ends of the rod sheets indicates bipolar organization within the sheets, as does the presence of a bare zone when the two are mixed before dialysis. C-protein appears to block the AMPD binding site on the S-2 region of the rod. Research supported by a grant from the Muscular Dystrophy Association.

M-AM-Pos153 FLUORESCENCE ENERGY TRANSFER MEASUREMENTS OF SH₁ TO SH₂ DISTANCES IN MYOSIN SUBFRAGMENT ONE (SF₁), Ross Dalbey, Biochemistry/Biophysics Program, Washington State University, Pullman, WA 99164-4630

Myosin contains two reactive thiols, designated SH₁ and SH₂, which can be crosslinked in the presence of MgADP by various bifunctional reagents with crosslinking spans of 2 to 14 Å [Wells et al. (1980) *J. Biol. Chem.* 255, 11135]. Efficient crosslinking requires addition of Mg-nucleotides and these nucleotides are stably trapped at the active site with half-lives of hrs to days at 0°C. It has been proposed that nucleotide binding juxtaposes SH₁ and SH₂ to enhance their crosslinking which would stabilize a conformation favoring bound nucleotide. This proposal has been tested using Förster energy transfer techniques. SH₁ was labeled with the dansyl derivative, 1,5 IAEDANS and SH₂ with the chromophoric acceptor, N-(4-dimethylamino-3,5-dinitrophenyl)maleimide (DDPM). Peptide studies indicated that [³H]IAEDANS specifically labeled SH₁ while [¹⁴C]DDPM modified both SH₂ and the alkali light chains. The [¹⁴C]DDPM modified alkali light chains were replaced with unmodified light chains by the exchange procedure of Wagner and Weeds [*J. Mol. Biol.* (1977) 109, 455]. SF₁ labeled with IAEDANS and then with DDPM exhibited two fluorescence lifetimes, 20.6 ns (SF₁-AEDANS unquenched) and 9.28 ns (SF₁-AEDANS, quenched by DDPM). The latter lifetime changed to 2.8 ns on addition of MgPP, MgAMP-PNP or MgADP (but not MgAMP) indicating that the donor-acceptor pair moved closer to each other. An R₀ of 29 Å was calculated for the AEDANS/DDPM system assuming K² = 2/3. The change in lifetimes observed is consistent with the donor/acceptor pair moving from 28 Å to 21 Å on addition of Mg-nucleotides. Other explanations are possible and will be discussed. Support by MDA and NIH grants to R. G. Yount.

M-AM-Pos154 CROSS BRIDGES IN VERTEBRATE MUSCLE. C. Franzini-Armstrong, E. Varriano-Marston, J. C. Haselgrove. Depts. Anatomy, Biology, Biophysics, Univ. of Pennsylvania, Philadelphia, Pa. 19104.

We have analyzed shape and disposition of X-bridges in freeze-fractured, deep-etched fish muscle in rigor. We use the terms target zone to indicate attachment sites of X-bridges along single actin strands, and crown for the 14.3 axial repeat of myosin filaments. Shadowing reveals two shapes of X-bridges attached to actin. Some are uniformly narrow (3nm diam), others are narrow near the myosin shaft and wide near the actin (3 to 10 nm diam). Using the negatively stained images of Craig et al. (*J. Mol. Biol.* 140, 35, 1980) for comparison, we interpret the narrower X-bridges as a single S₁ and the wider X-bridges as two S₁ from the same myosin, attached to two adjacent actin monomers. On this basis we count approximately 12% single headed, and 88% double headed-X bridges. In the 1,0 fracture plane the visible bridges attached to an actin filament come from the two adjacent myosin filaments. Counts from three experiments give an average of 8.3 cross bridges every 6 actin target zones (112.5 nm), in agreement with image averaging of the same micrographs, showing a 1,1,2 pattern of bridge attachment to adjacent target zones. Detached cross bridges are visible in relaxed sarcomeres, but none are present in rigor muscle. From these data we calculate an average of 3.2 cross bridges and 5.9 S₁ (or 3 myosin molecules) per crown, and conclude that myosin filament in these muscles is three stranded. Computer modelling, based on the above information, on the known helical parameters of actin and relaxed myosin filaments in vertebrate muscles and on the trigonal position of actin filaments, is used to determine the factors that allow this pattern of decoration of the actin filament in the rigor condition. Supported by NIH (HL 15835-09) and MDA.

M-AM-Pos155 DNase I-ACTIN INTERACTIONS IN THE Z LATTICE OF SKELETAL MUSCLE. Danna B. Zimmer*, Robert L. Pardue[†] and M. A. Goldstein*. *Dept. Med. and Cell Biol., Baylor Coll. Med. and [†]Dept. Int. Med., Div. Endocrinol., Univ. Texas Hlth. Sci. Ctr., Houston, Tx. (Intr. by Laurel Treager)

The recent use of DNase I as an actin specific probe in nonmuscle cells suggests that it may be useful in studying the arrangement of actin and its associated proteins in skeletal muscle cells. DNase I-actin interactions in muscle fibers were studied by incubating glycerinated muscle fibers for one hour at 37°C in 20 mM tris 5 mM MgCl₂ containing various concentrations of DNase I and processing the treated fibers for electron microscopy. Electron micrographs of muscle fibers treated with buffer only demonstrated the presence of axial filaments in the lattice which were continuous with but thicker than the thin filaments of the adjacent sarcomeres. In addition, small diameter cross-connecting filaments were also present in the Z lattice. When avian fast and slow muscles and rat fast and slow muscles were treated with 1 mg/ml DNase I, electron micrographs revealed that the substructure of the Z lattice had been completely destroyed. The axial filaments were present in the Z lattice, however they were thinner and less organized than those of control fibers. The small diameter cross-connecting filaments were not present. Indirect immunofluorescence microscopy has demonstrated the presence of DNase I in the I and Z bands of treated fibers. The effect of DNase I could be abolished by lowering the DNase concentration (0.1 mg/ml or less) or by preincubating the enzyme with purified actin. These data suggest that DNase I interacts with actin in the Z lattice and this interaction causes the subsequent release of the Z band proteins associated with the axial and cross-connecting filaments.

M-AM-Pos156 LOCALIZATION OF α -ACTININ IN THE Z LATTICE OF ADULT SKELETAL MUSCLE. Danna B Zimmer, Departments of Cell Biology and Medicine, Baylor College of Medicine, Houston, Texas.

α -Actinin is a structural protein which has been localized at the Z band by indirect immunofluorescence and immunoelectron microscopy. Due to the size of the probes used in these studies, it is not clear if α -actinin is diffusely located in the matrix material of the lattice or discretely localized as a component of the axial or cross-connecting filaments. In this study direct immunoelectron microscopy techniques have been used in order to determine the specific location of α -actinin in the Z lattice. An α -actinin specific antibody was raised in sheep and characterized by indirect immunofluorescence microscopy, "Western" transfer techniques and immunodot assays. Fab fragments of the anti- α -actinin were used to label muscles which were permeabilized by glycerination. Glycerination extracted the dense amorphous material of the lattice. However, the dimensions and the arrangement of the axial and cross-connecting filaments were not altered. When purified α -actinin was incubated with glycerinated fibers, the density of the lattice was unchanged suggesting that α -actinin was not a component of the dense amorphous matrix. Incubation of fibers in buffer containing anti- α -actinin Fab fragments resulted in an increase in the density of the Z lattice demonstrating that α -actinin was present in the lattice after extraction of the amorphous material. These data suggest that α -actinin is a component of the axial and/or cross-connecting filaments. Labeling of the lattice did not alter the arrangement of the structural components or the dimensions of the lattice. Thus it may be possible to more precisely determine the location of α -actinin in the Z lattice.

M-AM-Pos157 THREE-DIMENSIONAL IMAGE RECONSTRUCTION OF RIGOR CROSSBRIDGES IN THE INSECT FLIGHT MUSCLE "MYAC" LAYER. K. Taylor, L. Cordova, M.C. Reedy and M.K. Reedy. Anatomy Department, Duke University Medical Center, Durham, N.C. 27710

We have obtained a preliminary model of the 3-dimensional structure of the MYAC single filament layer of rigor insect flight muscle by using Fourier image analysis methods applied to electron micrographs of tilt series taken of thin sections. Our specimens were prepared for E.M. using glutaraldehyde-tannic acid-osmium fixation. Continuous x-ray monitoring allowed selection of specimens which showed the best preservation of native order. The Fourier transforms of the individual images contained good quality data for reflections on layer lines which were orders of the 385Å repeat. Data for other layer lines which were orders of the 1160Å axial repeat were of only marginal quality (with the exception of the 145Å meridional reflection). We have combined the data in space group P12 with acceptable results. The 3-D map when viewed down the filament axis shows an actin filament which is clearly resolved as a 2 stranded filament along about 2/3 of the 385Å repeat. Each of the presumed actin strands has a diameter in cross section of 50-60Å. Both the rear and lead members of the double chevrons are clearly distinguishable. The double stranded actin filament is clearly resolved at the point where the lead chevron binds to it. The binding geometry in this case is clearly that described by Taylor and Amos (*J. Mol. Biol.* 147, 297 (1981)). Supported by NIH grant GM 30598 and a grant from the Muscular Dystrophy Association of America.

M-AM-Pos158 PHOSPHORYLATION OF A 140,000 DALTON PROTEIN OF SKELETAL MUSCLE.

Krystyna Kasman and Carl Moos, Biochem. Dept., SUNY, Stony Brook, NY 11794.

It has been reported that cardiac C-protein can be phosphorylated by cAMP-dependent protein kinase [Jeacocke & England (1980), *FEBS Lett.* 122: 129; Hartzell & Titus (1982), *JBC* 257: 2111]. We have now observed phosphorylation of a 140,000 dalton C-protein-like component in skeletal muscle as well. When crude C-protein, separated from myosin on a DEAE-Sephadex column, is incubated with 32 P-ATP in 0.5 M NaCl, 12.5 mM MgCl₂, 0.1 mM CaCl₂, 20 mM K-Phosphate, pH 7, 32 P is incorporated into a protein of about 140,000 molecular weight. This labeled protein is not the C-protein of white muscle, however, because it is not precipitated by antibodies against purified white C-protein. Hydroxylapatite (HAp) chromatography of the phosphorylated mixture clearly separates the labeled protein from white C-protein; the protein-bound 32 P elutes with the X-protein of Starr, Offer & Bennett [*J. Muscle Res. Cell Mot.* 1:205 (1980)]. We have previously shown that X-protein is very similar in primary structure, although not identical, to the C-protein of red muscle, [Yamamoto & Moos (1981), *JGP* 78: 31a]. After separation on HAp, neither white C-protein nor X-protein incorporates 32 P, but when the two protein fractions are mixed, phosphorylation of X-protein is again possible, indicating that the kinase involved is present in the white C-protein peak from the HAp column. Further work is directed toward identifying the kinase, clarifying the conditions for phosphorylation, and investigating the effect of phosphorylation on the functional properties of X-protein. (Supported in part by NIH Grant AM-28028.)

M-AM-Pos159 FLUORESCENCE OF ACTIN-BOUND HYDROPHOBIC PROBES. L.D. Burtnick and K.W. Chan, Department of Chemistry, University of British Columbia, Vancouver, B.C., Canada V6T 1Y6.

2-(*N*-methylanilino)naphthalene-6-sulfonic acid (MANS) binds to actin in a noncovalent manner at a single site characterized by $K_d = 41 \mu\text{M}$. The emission spectrum of MANS-G-actin exhibits two peaks, one near 430 nm and the other near 490 nm. This double-peaked emission spectrum can be mimicked by placing MANS in a variety of nonpolar solvents. Salt-induced polymerization of MANS-G-actin results in a general enhancement of sample emission at all wavelengths. At 430 nm, the enhancement factor for KCl-induced MANS-F-actin is 2.3, while that for MgCl_2 -induced MANS-F-actin is 2.0. Polymerization of MANS-G-actin in the absence of agitation results in fluorescence polarization values of 0.33 at 430 nm. However, subsequent mixing of the sample results in a dramatic reduction in the polarization value to 0.14. These results suggest that, concurrent with filament growth, side-by-side interactions between F-actin filaments yields a relatively ordered array of filaments in the sample. Mixing the sample disrupts the network in such a way that the time-dependent reformation of side-by-side contacts between F-actin filaments does not produce an array having the same degree of order as did the undisturbed array. 9-anthroyl choline (9AC) also binds to G-actin in a noncovalent manner at a single hydrophobic site. For this site, $K_d = 68 \mu\text{M}$. The single emission peak has a maximum near 490 nm. KCl-induced polymerization of 9AC-G-actin causes a drop in the emission intensity at 490 nm to 70% of its initial value. MgCl_2 -induced polymerization, on the other hand, results in a 30% increase in fluorescence. These results again suggest that the MgCl_2 and KCl-induced forms of F-actin are structurally different. (Supported by NSERC and BCHCRF.)

M-AM-Pos160 PRODUCTION AND CHARACTERIZATION OF A MONOCLONAL ANTIBODY TO SKELETAL MUSCLE TROPONIN I (STnI). Saleh El-Saleh and James D. Potter, Section of Contractile Proteins, Department of Pharmacology and Cell Biophysics, University of Cincinnati College of Medicine, 231 Bethesda Avenue, Cincinnati, Ohio 45267.

A monoclonal antibody (IgG- κ_2 - γ_2) to STnI has been produced using the somatic cell fusion of spleen cells from $\text{CB}_6\text{F}_1/\text{J}$ mice immunized with STnI with cells of the myeloma cell line SP2/O-Ag-14. The reaction of this antibody (Cl35) towards STnI has been determined using a) the ELISA technique b) a triple sandwich immunodot technique, and c) by immunoblot on nitrocellulose after gel electrophoresis of skeletal myofibrils. Cl35 also interacts with cardiac TnI (CTnI) suggesting that both STnI and CTnI share a common antigenic determinant. The effect of Cl35 on the Ca^{2+} -dependence of the myofibrillar ATPase activity was also investigated. At low Ca^{2+} concentrations, where the ATPase was inhibited, the antibody had no effect. However, in the presence of Ca^{2+} , where the myofibrils were fully activated, the antibody greatly inhibited the ATPase activity. These results suggest that the binding of the antibody to STnI in the myofibrils "locks" the conformation of this troponin subunit in an inhibitory state, similar to the one in which STnI is still bound to actin in the absence of Ca^{2+} . Work is in progress to determine the binding site of Cl35 on fragments of STnI generated by CNBr cleavage. Supported by grants from the NIH (HL 22619-III-A) and the Muscular Dystrophy Association.

M-AM-Pos161 ^{113}Cd NMR STUDIES OF TROPONIN C. James D. Potter¹, Priscilla Strang-Brown¹, and Paul D. Ellis² (1) Section of Contractile Proteins, Department of Pharmacology and Cell Biophysics, University of Cincinnati College of Medicine, Cincinnati, Ohio 45267, (2) Department of Chemistry, University of South Carolina, Columbia, South Carolina 29208.

The binding of cadmium to skeletal TnC (STnC) has been measured by equilibrium dialysis. The equilibrium binding experiments have shown that there are 2 cadmium binding sites on STnC with a high affinity for Cd^{++} ($K_d \sim 10^{-10} \text{M}$) and 2 binding sites with a lower affinity for Cd^{++} ($K_d \sim 10^{-3} \text{M}$). The former binding constant is comparable to Ca^{++} binding to the Ca^{++} - Mg^{++} (structural) sites and the latter is about 100 times less than the Ca^{++} binding to the Ca^{++} -specific (regulatory) sites. The ^{113}Cd NMR spectrum is shown to be temperature dependent. At 20° the spectrum consists of 2 resonances at -107.8 and 112.7 ppm with respect to Cd (ClO_4)₂. This spectrum is similar to that shown by Forsen et al. (FEBS Lett. 104, 123, 1979). Lowering the temperature to 4° alters the cadmium exchange and results in a four line ^{113}Cd spectrum. The two new resonances at -103.1 and -109.8 ppm are due to cadmium binding to the regulatory (Ca^{++} -specific) sites on STnC, whereas, the resonances at -107.8 and -112.7 ppm correspond to cadmium binding at the structural (Ca^{++} - Mg^{++}) sites. These resonances were assigned based on ^{113}Cd titrations and on Ca^{++} displacement titrations of bound ^{113}Cd . These studies also show a temperature dependent conformational change in some of the Ca^{++} binding sites. In addition, it is demonstrated that an allosteric coupling network exists between the two classes of sites and this may be important physiologically depending on whether Ca^{++} or Mg^{++} are bound to the Ca^{++} - Mg^{++} sites. Supported by grants from the NIH GM 26295 (PDE), HL 22619-III-A (JDP), NSF CHE 78-18723 (PDE) and the Muscular Dystrophy Association (JDP).

M-AM-Pos162 ASSEMBLY OF LC₂-DEFICIENT RABBIT SKELETAL AND DOG CARDIAC MYOSINS. S. S. Margossian¹, T. W. Huiatt² and A. Bahn^{1*}, Dept. of Biochem., A. Einstein Col. Med. and Montefiore Medical Center¹, Bronx, NY 10467 and Muscle Biology Group, Iowa State Univ.², Ames, IA 50011.

The possible role of the LC₂ light chains in assembly of rabbit skeletal and dog cardiac muscle myosins was examined by formation of synthetic filaments from control and LC₂-deficient myosins and from LC₂-deficient myosin reconstituted with excess purified LC₂. LC₂ was removed by using a pro²⁺tease from a genetic strain of myopathic hamsters. LC₂-deficient and reconstituted myosins had Ca²⁺ and K⁺-EDTA ATPase activities comparable to controls, and exhibited little aggregation in 0.6 M KCl by sedimentation velocity. Filaments were formed by dilution of myosin solutions (0.5 mg/ml) from 0.5 M to 0.15 M KCl over 5 min by addition of buffer without KCl, and were examined in the electron microscope by negative staining with 2% uranyl acetate. Buffers used were: 20 mM imidazole; 20 mM imidazole, 5 mM ATP; and 20 mM imidazole, 5 mM ATP, 5 mM MgCl₂, all at pH 7.0. Skeletal myosin filaments formed in imidazole buffer alone were bipolar, tapered at both ends, and about 1.6 μm long. Inclusion of ATP in the buffer disrupted the filament structure, resulting in irregular, short filaments (< 0.6 μm); inclusion of both ATP and MgCl₂ largely reversed the effects of ATP alone. No differences in filament morphology between control, LC₂-deficient and reconstituted myosins were seen. Similar results were obtained with dog cardiac myosin. These results suggest that removal of LC₂ does not affect synthetic filament structure. However, removal of LC₂ light chains may affect the stability of filaments formed in different buffer conditions or the equilibrium between different assembly states resulting from the addition of ATP. Supported by NIH Grant HL-26529 (S.S.M.) and American Heart Assn., Iowa Affiliate (T.W.H.)

M-AM-Pos163 ISOLATION OF HIGH MOLECULAR WEIGHT FORMS OF MYOSIN LIGHT CHAIN KINASE. Michael P. Walsh, Susan Hinkins and David J. Hartshorne, Dept. of Medical Biochemistry, University of Calgary, Calgary, Alberta, Canada T2N 1N4, and Dept. of Nutrition and Food Science, University of Arizona, Tucson, AZ 85721.

During attempts to purify turkey gizzard MLCK, we consistently observed two distinct forms of the kinase which are separable on columns of DEAE-Sephacel, Affi-Gel blue or DEAE-Affi-Gel blue. The two forms of MLCK are denoted MLCK I and MLCK II by their order of elution from DEAE-Sephacel. Purification of MLCK II to homogeneity showed it to be the well-characterized 130,000-dalton enzyme (Adelstein and Klee, J. Biol. Chem. 256, 7501 (1981)). MLCK I was purified by affinity chromatography on calmodulin-Sepharose and found to consist of a doublet of M_r = 136,000 and 141,000. MLCK II may arise from MLCK I by proteolysis.

Bovine rumen has a low level of protease activity which prompted us to purify MLCK from this tissue. The bovine stomach kinase was purified by a simple and rapid procedure. The stomach enzyme shares many properties with the gizzard kinase: dependence on Ca²⁺-calmodulin (K_d = 1.3 nM); Ca²⁺-dependent interaction with immobilized calmodulin; phosphorylation of the same site on myosin; phosphorylation by cAMP-dependent protein kinase; similar amino acid composition. The major difference between the two kinases is their molecular weight, the stomach MLCK having M_r = 155,000.

These observations are consistent with the hypothesis of Walsh and Guilleux (Adv. Cyclic Nucleotide Res. 14, 375 (1981)) that all mammalian MLCKs may be structurally homologous and subject to similar regulation by Ca²⁺ and cAMP.

M-AM-Pos164 IMMUNOLOGICALLY DISTINGUISHABLE PARAMYOSINS. S.M. Goldfine, B.D. Gaylinn, M.M. Dewey and B. Walcott. Department of Anatomical Sciences, School of Medicine, S.U.N.Y., Stony Brook, N.Y. 11794

To test for immunological similarities between paramyosins in a variety of invertebrate muscles, we have used electrophoretic immunoblotting from SDS-polyacrylamide gels (Towbin, et al., PNAS 76:4350, 1979). A polyclonal mixture of antibodies to Limulus telson muscle paramyosin was used as the probe. Paramyosin was isolated according to the method of Merrick and Johnson (Biochem. 16:2260, 1977). It was further purified by SDS-polyacrylamide gel electrophoresis. The main band from these SDS-gels was excised and injected into rabbits. The IgG fraction of the anti-serum obtained was purified by ammonium sulfate fractionation and was absorbed against purified Limulus myosin and tropomyosin. This resulted in a probe which specifically bound to only the paramyosin band in immunoblots of Limulus muscle homogenate and stained only the A band in isolated Limulus myofibrils as judged by indirect immunofluorescence microscopy. The experimental results show an immunologically similar polypeptide of approximately 100,000 daltons in eight out of thirteen different muscle homogenates tested. These muscles were obtained from organisms in three different phyla: Arthropoda, Annelida and Sipunculida. Of those paramyosin-containing muscles which showed no cross-reactivity, three were from Mollusca and one was from Arthropoda, Homarus. We, therefore, conclude that there are antigenic differences between paramyosins. (Supported by NIH Grants: GM 28804, GM 26392, and AM 30053).

M-AM-Pos165 ENDOGENOUS PROTEIN KINASE SUBSTRATES IN CHICKEN SKELETAL MUSCLE, HEART, AND GIZZARD. L.H. Schliselfeld, M. Bárány, and S.R. Hager Department of Biological Chemistry, College of Medicine, University of Illinois at Chicago, Chicago, IL 60612

Endogenous phosphorylation of proteins in chicken breast muscle, heart, and gizzard homogenates were studied at 37° in 0.14–0.25 M NaCl, 0.14 M TrisHCl, 5 mM DTT, 14 mM MgAc₂, 4.3 mM EGTA, 10 µg/ml insulin, and 4.8 mM [³²P]ATP at pH 7.4. Activation of protein phosphorylation was tested with 0.4 mM cAMP or 4.1 mM CaCl₂ (free Ca²⁺ about 2 µM). The reactions were stopped after 1 min by an appropriate means. The homogenates were fractionated by differential centrifugation and analyzed by SDS-urea gel electrophoresis. Skeletal muscle homogenate yielded 4 [³²P]proteins (214182 cpm/g muscle). Addition of cAMP had little effect on the total incorporation (258360 cpm/g muscle) but an extra [³²P]protein appeared. Addition of CaCl₂ caused a tripling of the radioactivity incorporated (774070 cpm/g muscle) and the formation of at least six distinct [³²P]proteins. Myosin light chain (LC) is phosphorylated only in the presence of CaCl₂. Heart homogenates yielded 5 [³²P]proteins (264358 cpm/g heart). Addition of CaCl₂ had little effect on the total incorporation (281896 cpm/g heart) but an extra [³²P]protein appeared. Surprisingly no significant phosphorylation of the heart LC was detected without or with CaCl₂. Addition of cAMP tripled the total incorporation (771446 cpm/g heart) and produced about 12 [³²P]proteins. The phosphorylation of gizzard homogenate by this procedure yielded a very radioactive LC only in the presence of CaCl₂. Thus protein phosphorylation in skeletal muscle and heart differ in their most potent activator of protein phosphorylation and in their ability to catalyze Ca²⁺-dependent phosphorylation of LC. (Supported by Shriner's Hospitals and NIH NS-12172).

M-AM-Pos166 SPECTRAL STUDIES ON THE CALCIUM BINDING PROPERTIES OF BOVINE BRAIN S-100b PROTEIN.

R.S. Mani, J.G. Shelling, B.D. Sykes and C.M. Kay. MRC Group in Protein Structure and Function, Department of Biochemistry, University of Alberta, Edmonton, Alberta.

The effect of Ca²⁺ binding on the circular dichroism (CD) and 270 MHz proton nuclear magnetic resonance spectrum of brain specific S-100b calcium binding protein has been examined at two pH values, 8.5 and 7.5. At pH 8.5, S-100b protein binds two Ca²⁺ per monomer with K_d values of 6 x 10⁻⁵ M and 2 x 10⁻⁴ M, whereas at pH 7.5 the protein binds only one Ca²⁺ per monomer with K_d 2 x 10⁻⁴ M. The presence of K⁺ inhibits the binding of Ca²⁺ to the higher affinity site at pH 8.5, and the affinity for calcium is lowered to K_d 8.5 x 10⁻⁴ M. Mg²⁺ has no effect on protein conformation. In the absence of Ca²⁺, S-100b undergoes a conformational change when the protein is titrated from pH 8.6 to 6.0. Addition of Ca²⁺ perturbed the environment of tyrosine and phenylalanine residues as measured by ultraviolet difference spectroscopy and ¹H NMR. CD melt experiments and far ultraviolet CD studies at alkaline pH and NMR experiments suggest that the protein is more stable in the presence of Ca²⁺. The single tyrosine residue in the protein ionizes only after the protein is denatured by exposure to high pH.

(Supported by MRC, Canada)

M-AM-Pos167 TRYPTIC DIGESTION OF MYOFIBRILS AS A PROBE OF MYOSIN S-1 CONFORMATION. T. Chen and E. Reisler, (Intr. by J. Horwitz, Jules Stein Eye Institute, UCLA), Department of Chemistry and Biochemistry and the Molecular Biology Institute, UCLA, LOS Angeles, CA 90024.

Tryptic digestion of rabbit skeletal myofibrils at physiological ionic strength and pH was employed as a probe of the myosin S-1 conformation in the presence of nucleotides and pyrophosphate. Under rigor conditions proteolysis of myofibrils at room temperature results in production of three major bands, 110K (HMM), 70K (LMM) AND 25K. In the presence of sodium pyrophosphate, when the myosin heads are dissociated from actin, the main digestion reactions proceed at two sites, 25K and 75K from the N-terminal end of myosin, yielding the 25K, 50K and 150K species. The rate of formation of the 50K species in the presence of MgATP, MgAMPPNP and Mg pyrophosphate is consistent with their effectiveness in dissociating myosin from actin. Similar digestions carried out in the presence of MgADP produce myosin fragments corresponding to a mixed population of rigor and relaxed myofibrils. These results are discussed in terms of conformational changes in S-1 due to ADP binding. Tryptic digestions of myofibrils carried out at 0°C lead to qualitatively similar fragmentation of the S-1 moiety. However, under rigor conditions and at low temperature the rate of proteolytic cleavage at the LMM/HMM junction is greatly reduced. This research was supported by USPHS grant 22031.

M-AM-Pos168 EVIDENCE FOR A ROLE OF THE COOH-TERMINAL REGION OF MYOSIN SUBFRAGMENT 1 HEAVY CHAIN IN THE BINDING OF ALKALI LIGHT CHAIN. Morris Burke, Mathoor Sivaramakrishnan and Vedhachalam Kamalakannan. Department of Biology, Case Western Reserve University, Cleveland, Ohio 44106.

Removal of the alkali light chain from the heavy chain of myosin SFl by the thermal ion-exchange procedure exposes additional sites on the latter that are rapidly cleaved by trypsin and chymotrypsin. An examination of the course and extent of these digestions indicates that the initial cleavage occurs close to one or both ends since SDS PAGE analysis shows that the residual heavy chain is about 3,000 daltons smaller than the undigested form. Sequential (double) digestion studies, however, establish that these sites are confined to the COOH terminal region and are responsible, on further digestion, for the formation of a tryptic COOH-terminal fragment of 18,000 daltons rather than the 21,000 daltons fragment obtained by digestion of SFl. The ability of the 'truncated' heavy chain and 'native' heavy chain to reassociate to alkali light chain at 0° in the presence of 10mM MgATP was investigated by examining mixtures of these proteins by gel electrophoresis under non-denaturing conditions. The results obtained show that this initial cleavage(s) at the COOH-terminus essentially abolishes the ability of the heavy chain to reassociate with the alkali light chain. This finding together with the observation that digestion of reconstituted SFl, formed by reassociation of 'native' heavy chain with alkali light chain, does not occur at these sites suggests that the integrity of the COOH-terminal region of the heavy chain is crucial for light chain attachment. Supported by grants from the National Institutes of Health, National Science Foundation and Muscular Dystrophy Association.

M-AM-Pos169 ON THE THERMAL STABILITY OF THE NON-COVALENT INTERACTIONS WITHIN THE HEAVY CHAIN OF MYOSIN SUBFRAGMENT 1. Morris Burke and Vedhachalam Kamalakannan. Department of Biology, Case Western Reserve University, Cleveland, Ohio 44106.

Recent studies from this laboratory have shown that ion-exchange chromatography of subfragment 1 at 37°C in the presence of 10mM MgATP is capable of stripping the alkali light chain subunit from subfragment 1 thereby demonstrating the lability of this interaction. In the present study we have sought to employ this procedure to determine whether the non-covalent interactions between the segments of the heavy chain subunit, produced by prior digestion with trypsin, are stable under the same conditions and whether the functional integrity of the 'fractured' heavy chain is maintained in the absence of the alkali light chain subunit. The data obtained show that at 39° in the presence of MgATP a protein fraction can be isolated by DEAE-cellulose chromatography of tryptic digested SFl devoid of alkali light chain. This fraction moves as a single protein band on polyacrylamide gel electrophoresis under non-denaturing conditions. SDS-PAGE analysis showed that it is a complex comprised of equimolar amounts of the NH₂-terminal (27,000 daltons), middle (50,000 daltons), and COOH-terminal (18,000 daltons) fragments of the heavy chain. This free 'fractured' heavy chain exhibits Ca⁺⁺ ATPase and K⁺/EDTA ATPase activities. These studies show that the stability of the intrachain interactions within the heavy chain is significantly greater to temperature perturbation than that between the alkali light chain and the heavy chain and, moreover, the functional integrity of the heavy chain is retained in the fractured heavy chain in the absence of the alkali light chain. Supported by grants from the National Institutes of Health, National Science Foundation and Muscular Dystrophy Association.

M-AM-Pos170 MYOSIN, ACTIN AND TROPONIN CONTENT IN RABBIT SKELETAL MUSCLE AND MYOFIBRILS. Lawrence D. Yates and Marion L. Greaser, Muscle Biology Laboratory, University of Wisconsin, Madison, WI 53706.

The content of myosin, actin, troponin-T(Tn-T), troponin-I(Tn-I), and troponin-C(Tn-C) of rabbit psoas muscle and purified myofibrils was determined. Myofibrils were purified using Percoll density gradients which allowed rapid separation from nuclei and connective tissue proteins. Proteins were separated on polyacrylamide gels in the presence of sodium dodecyl sulfate. The quantities of the separated proteins were determined directly from the gel slices by amino acid analysis after correction for losses and background. The Tn-I bands of whole tissue were not fully resolved from adenylate kinase and myosin light chain-I while the Tn-T bands contained glyceraldehyde-3-phosphate dehydrogenase. The troponin subunit content, however, could be calculated using regression analysis of the amino acid compositions. Muscle tissue contained 102, 610 and 91 nMol/g wet weight of myosin, actin and troponin respectively, while myofibrils possessed 0.90, 5.37 and 0.77 μMol/g protein. The molar ratio of Tn-T, Tn-I and Tn-C was found to be the same in muscle tissue and isolated myofibrils, namely 1.02:1.01:0.97. The molar ratio of myosin to actin was 0.168 ± 0.014 and the number of myosins per thick filament was 320 ± 24 as calculated from the unit mass of a sarcomere determined from the density of myofibrils in Percoll density gradients. These values were only compatible with models of thick filament assembly containing three myosins per 14.3 nm axial repeat. From the contents of these proteins in muscle tissue and myofibrils, it was calculated that rabbit psoas muscle contains 11.6% (w/w) myofibrils. The proteins of the myofibril and their content, as determined here and from data found in the literature, accounted for greater than 98% of the myofibrillar proteins. (Supported by NIH HL 18612 and the Wisconsin Heart Association.)

M-AM-Pos171 STRUCTURAL COMPARISON OF THREE VARIANTS OF MYOSIN LIGHT CHAIN-1 FROM FAST WHITE CHICKEN FIBERS. Julie Ivory Rushbrook¹, Axel Georg Wadewitz¹ and Ralph G. Somes, Jr.² (intr. by E. McGowan), SUNY-Downstate Medical Center, Brooklyn, N.Y. 11203¹ and College of Agriculture and Natural Resources, The University of Connecticut, Storrs, CT 06268².

Recently we reported the existence of two forms of myosin light chain-1 (LC-1), type I and type II, differing in electrophoretic mobility and peptide maps, in the fast white fibers of domestic chickens (Rushbrook, J.I., Yuan, A.I and Stracher, A. (1982) *Muscle and Nerve* 5, 505). The distribution of the two forms differed in several commercial chicken strains. The forms did not vary during development and appear to be related as allelic variants.

While conducting a genetic linkage study of the two LC-1 species and avian dystrophy, we became aware of a third LC-1 variant. 50% of the progeny from the cross between a certain male and female were found to possess two LC-1 forms separating only on high resolution SDS-gels (a characteristic of the type I+II LC-1 mixture), while the remaining 50% contained two forms separating readily on routine analytical SDS gels, and even further on high resolution gels. Other results indicated that the male of the cross was homozygous for the type II LC-1 form. Scrutiny of the gels revealed that, in addition to the type I form, the female possessed a new form migrating faster than type I which we have called type III.

A procedure has been developed to purify LC-1 and LC-3 from a mixture of myosin light chains using reverse phase HPLC. The differences in the types I, II, and III LC-1 species will be further analyzed by comparison of their cyanogen bromide peptide maps and that of LC-3 using HPLC. Supported by grants from NIH (R23 HL 27883) and MDA.

M-AM-Pos172 EVIDENCE FOR THE LACK OF LOCALIZED MELTING AND CHAIN SEPARATION AT CYSTEINE IN GIZZARD TROPOMYOSIN. D.Betteridge, P.Graceffa, S.Lehrer and J.Seidel, Boston Biomedical Research Institute, Boston Ma. 02114.

Previous studies have shown that the 2-chain rabbit skeletal tropomyosin (RS-Tm) molecule exists in 2 states in solution; a "chain-closed" and a "chain-open" locally melted state, predominating at low and physiological temperatures, respectively. This was indicated by the ability of Nbs₂ to produce an interchain S-S crosslink, by the ability of pyrenemaleimide-labeled RS-Tm to exhibit excimer fluorescence, and by the presence of a long-lived fluorescence component in didansylcysteine-labeled RS-Tm whose contribution correlates with a helix pretransition (25°-40°) (Ann.N.Y.Acad.Sci., 366, 285, 1981). In the case of gizzard tropomyosin (G-Tm) studied under the same conditions as RS-Tm, it was found that Nbs₂ reacts with 1 Cys/chain without producing a S-S crosslink, that no excimer was observed for pyrene-G-Tm, and that dansyl-G-Tm did not show a long-lived fluorescence component whose intensity increased at temperatures preceding the major unfolding transition. G-TM's Cys groups are located closer to the chain ends as compared to RS-Tm from studies of the relative mobility on PAGE-SDS gels of fragments made by cleavage at Cys. No obvious pretransition was observed in the G-Tm thermal helix unfolding profile, however, in agreement with Woods (Aust.J.Biol.Sci., 29, 405, 1976), indicating that localized melting does not occur at a region not containing Cys. Thus, in contrast to RS-Tm, G-Tm does not undergo localized melting at Cys, nor probably in any other region of the molecule.

(Supported by NIH HL-22461,-15391 and the MDA)

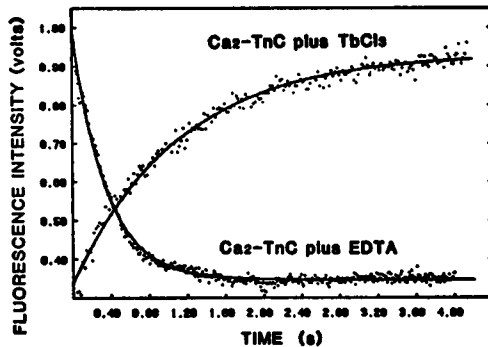
M-AM-Pos173 ACTIVITY STUDIES ON GLUTARALDEHYDE-CROSSLINKED RABBIT SKELETAL F-ACTIN-TROPOMYOSIN THIN FILAMENTS. S.S.Lehrer, Boston Biomedical Research Institute, Boston Ma. 02114.

Previous activity studies showed that tropomyosin caused an inhibition of the acto-myosin subfragment 1 (acto-S1) Mg²⁺-ATPase that approached 100% as the [S1] approached zero. We concluded that in the absence of S1, the F-actin-tropomyosin (FTm) thin filament is in an inhibited state (Lehrer and Morris, JBC, 257, 8073, 1982). To test this, FTm was "fixed" by crosslinking with glutaraldehyde (Ga) to form GaFTm, (Lehrer, JCB, 90, 4059, 1981), and the [S1] dependence of activity was measured. PAGE-SDS gels indicated that >90% of the actin and Tm was crosslinked into a very high Mw complex excluded from a 5-15% acrylamide gradient gel. Control FTm samples showed strong inhibition of specific activity (per S1) at low [S1], with marked upward curvature beginning at ~3uM S1. In contrast, in the presence of GaFTm the specific activity was constant and strongly inhibited at least up to 8 uM S1. Highly crosslinked F-actin samples (GaF) showed only a small inhibition indicating that the presence of the crosslinks, per se, did not inhibit acto-S1 activity. Previous studies indicated that Ga crosslinking stabilizes actin against denaturation (Lehrer, BBRC, 48, 967, 1972), and does not appreciably affect the position of Tm nor the actin filament helix symmetry (Lehrer and O'Brien, J.Musc.Res.and Cell Motility, 1, #2, 1980). Thus the FTm filament appears to be in an inhibited state in the absence of S1 and Ga crosslinking prevents the S1-induced transition to the activated state.

(Supported by NIH HL 22461 and the MDA)

M-AM-Pos174 KINETICS OF CALCIUM RELEASE FROM HIGH AFFINITY SITES SHOW INTERACTIONS BETWEEN THE TWO CLASSES OF SITES OF TROPONIN-C. C.-L.A. Wang, P.C. Leavis and J. Gergely, Dept. of Muscle Research Boston Biomedical Research Institute, Dept. of Biological Chemistry and Neurology, Harvard Medical School, Dept. of Neurology, Massachusetts General Hospital, Boston, MA 02114

The kinetics of Ca^{2+} -release from the two high affinity sites of troponin-C (TnC) were studied by the stopped-flow technique following rapid mixing with (1) EDTA or (2) Tb^{3+} . The first method, monitored by the decrease of tyrosine fluorescence, yields an off-rate of 2.8 s^{-1} ; the second,



which depends on the binding of Tb^{3+} following the displacement of Ca^{2+} , monitored by either the decrease of tyrosine fluorescence or the increase of Tb^{3+} luminescence, gives a slower rate of 0.7 s^{-1} . With the use of the tryptic fragment (TR2C) of TnC, that contains only the C-terminal half of the molecule both methods generate the same rate constants of $2.7 \pm 0.4 \text{ s}^{-1}$. These results are consistent with the following interpretations: Tb^{3+} binds to the two low affinity sites of TnC before Ca^{2+} is displaced from the high affinity sites; binding of Tb^{3+} to the low affinity sites enhances the affinity of Ca^{2+} for the two high affinity sites resulting in a lower dissociation rate. This, in turn, suggests interactions between the two halves of the TnC molecule.

M-AM-Pos175 AN EPR STUDY OF THE INTERACTIONS OF TROPONIN SUBUNITS. C.-L.A. Wang, P.C. Leavis and J. Gergely. Dept. of Muscle Res., Boston Biomed. Res. Inst., Dept. of Biol. Chem. and Neurology, Harvard Med. School, and Dept. of Neurology, Mass. Gen. Hospital, Boston, MA 02114

We have used a maleimide spin label (MSL) attached to Cys-98 of troponin-C (TnC) to study the interaction between TnC and the other subunits of the troponin complex, troponin-T (TnT) and troponin-I (TnI). In the presence of Ca^{2+} , the formation of complexes between MSL-TnC and TnT or TnI is accompanied by the appearance of additional peaks in the EPR spectra at both high and low fields; the separation of these peaks indicates a substantial immobilization of the spin label. We have carried out Ca^{2+} titrations of a 1:1 mixture of MSL-TnC and TnI in an EGTA-NTA buffered system monitoring both the weakly and strongly immobilized peaks of the EPR signal. Two transitions were observed: one occurs at pCa^{-8} , the other at pCa^{-6} . Although each component has a different contribution to the two transitions, both exhibit the same midpoints. Computer fitting of the titration data yields the following apparent Ca^{2+} -binding constants: $1.12 \times 10^8 \text{ M}^{-1}$ and $8.3 \times 10^5 \text{ M}^{-1}$ by monitoring the EPR signal at the field corresponding to the weakly immobilized peak, and $1.81 \times 10^8 \text{ M}^{-1}$ and $9.2 \times 10^5 \text{ M}^{-1}$ by monitoring the high-field strongly immobilized peak. The first transition, associated with the high affinity sites of TnC, occurs both in TnC alone and in its binary complex and probably reflects a Ca^{2+} -induced conformational change in the C-terminal half of the TnC molecule. The second transition suggests a structural rearrangement resulting from Ca^{2+} binding to the two low affinity sites. The fact that the latter effect is not observed in TnC alone suggests that binding of Ca^{2+} to the low affinity sites influences in the complex of TnC with other subunits the region containing Cys-98 and one of the two high affinity sites. Similar results have been obtained with the complex of MSL-TnC and TnI.

M-AM-Pos176 KINETICS OF CALCIUM DISPLACEMENT FROM CALMODULIN BY TERBIUM. Marcia A. Tudor and Howard D. White, Department of Biochemistry, University of Arizona, Tucson, Az. 85721

The rate constant for the dissociation of calcium from calmodulin was measured by the appearance of energy transfer from tyrosine to terbium. Upon mixing terbium with calcium-saturated calmodulin in a stopped-flow fluorometer, terbium emission increases with a rate constant of $9.5 \pm 0.5 \text{ s}^{-1}$ at 20° C and $2.8 \pm 0.3 \text{ s}^{-1}$ at 2° C ($\lambda_{\text{exc}} = 280 \text{ nm}$, $\lambda_{\text{emiss}} = 550 \text{ nm}$, 0.1 M KCl , 20 mM Mes , $\text{pH } 6.5$). The observed rate constant is independent of terbium concentration above an eight-fold molar excess of terbium to calmodulin, conditions under which the dissociation of calcium is rate limiting for terbium binding. Measurement of calcium dissociation from calmodulin by the decrease in tyrosine emission ($\lambda_{\text{exc}} = 280 \text{ nm}$, $\lambda_{\text{emiss}} = 313 \text{ nm}$) observed upon mixing EDTA with calcium-saturated calmodulin gives rate constants of $9.3 \pm 0.6 \text{ s}^{-1}$ and $2.7 \pm 0.1 \text{ s}^{-1}$ at 20° and 2° C , respectively.

There is considerable evidence in the literature¹ that the tyrosine emission enhancement is dependent upon metal binding to sites I and II and the tyrosine-terbium energy transfer is associated with sites III and IV, thus the equality of the rate constants measured by direct tyrosine emission and energy transfer to terbium is somewhat surprising. The results reported here are, however, consistent with the spectroscopic assignment of binding sites if calcium dissociation from both classes of sites is limited by a common rate determining step. Support by research grants from the Arizona Heart Association and the Muscular Dystrophy Association.

1. C. A. Wang, R. Aquaron, P. Leavis, J. Gergeley, EJB, 124, 7, 1982.

M-AM-Pos177 HIGH YIELD PURIFICATION OF M-LINE PROTEIN FROM RABBIT MUSCLE. T. William Houk and Sondra Karipides, Department of Physics, Miami University, Oxford, Ohio 45056.

The purification of the 165,000 dalton component of the M-line of striated muscle conventionally follows two very different paths depending on whether proteins are extracted with high or low salt concentration buffers. Each method, as commonly applied, has difficulties which lead to relatively low yields of this protein. We report a simple procedure using low ionic strength extraction which considerably increases the yield of M-line protein. Our procedure eliminates the low pH precipitation step following the low ionic strength extraction. [Morimoto, K. and W. F. Harrington, *J. Biol. Chem.*, 247, 3052 (1972), and Mani, R. S. and C. M. Kay, *Biochem. Biophys. Acta*, 533, 248 (1978).] The crude extract is subjected to a 25% ammonium sulfate fractionation and the M-line protein is purified by anion exchange and affinity chromatography.

M-AM-Pos178 MYOSIN AND TROPOMYOSIN IN MALE AND FEMALE GUINEA PIG TEMPORALIS MUSCLE. A. Kelly, G. Lyons and N. Rubinstein, University of Pennsylvania, Philadelphia, PA.

Testosterone influences the metabolic properties and the size of myofibers in the guinea pig temporalis (*Histochemie* 24:287, 1970). The adult male contains large, fast white fibers (60 μ mean x diameter); the adult female has fast red fibers (40 μ mean x diameter). Before puberty the temporalis in both sexes is fast red in type and at 45 days fiber x diameters are the same (30 μ m). At this stage myosin isozymes from the male and female have similar mobilities when run on pyrophosphate gels, the light chains are indistinguishable on two-dimensional SDS gels and the α and β forms of tropomyosin in both sexes are distributed in equal proportions. Peptide maps of the heavy chain, though similar, have some minor differences. By 75 days, sexual distinctions in myofiber metabolism and size are evident. The mobility of myosin isozymes from the female is the same as at 50 days but in the male there is a shift to a more slowly migrating complement of isozymes. Heavy chain distinctions are greater than at 50 days. The subunits of tropomyosin also reveal sexual dimorphism; in the female the α and β subunits continue in the ratio of 1:1; in the male the ratio is now 1.5:1. This distinction is accentuated in the sexually mature male (120 days), in which the ratio of α : β subunit is approximately 4:1. Sexual differences in the mobility of myosin isozymes are also more evident. This maturation correlates with clear sexual differences in peptide maps of the heavy chain whereas the light chain complements remain identical. Thus distinct forms of myosin and of tropomyosin occur in fast red and fast white fibers of the guinea pig temporalis. This diversity appears to be regulated by testosterone.

M-AM-Pos179 REEVALUATION OF TROPONIN-I/TROPONIN-T BINDING, AND EFFECTS OF TROPONIN-I ON TROPONIN-T/TROPOMYOSIN BINDING: Ca^{2+} -SENSITIVITY AND COOPERATIVITY. Joyce R. Pearlstone and Lawrence B. Smillie, MRC of Canada Group in Protein Structure and Function, Department of Biochemistry, University of Alberta, Edmonton, Canada T6G 2H7.

The binding of troponin-I (Tn-I) of two chymotryptic fragments of troponin-T (Tn-T), T1 (residues 1-158) and T2 (residues 159-259), was investigated by gel filtration on Sephadex G-75 using pH 7.0 buffer containing 0.1 M versus 0.5 M NaCl. In 0.1 M NaCl buffer, complete binding was observed between T2 and Tn-I, but none between T1 and Tn-I. In 0.5 M NaCl buffer, the T2/Tn-I binding was weaker, while T1/Tn-I binding was strong. Whereas the former interaction appears to be genuine, the latter binding involving the NH_2 -terminal region of Tn-T with Tn-I appears to be an anomaly caused by the non-physiological, high-salt conditions. In view of these findings, previous studies on Tn-T/Tn-I interaction, carried out in high-salt buffer for solubility reasons, should be reevaluated.

The binding of Tn-I to tropomyosin (TM), and its effects on the two sites of Tn-T binding to TM, were studied using immobilized α -TM. When applied alone, Tn-I, intact Tn-T, T1 (at site 1) and T2 (at site 2) were eluted with a NaCl gradient at 0.12 M, 0.40 M, 0.32 M and 0.22 M NaCl respectively. However, the simultaneous presence of Tn-I and T2 resulted in a strong ternary complex (Tn-I/T2/TM) at site 2 (which was Ca^{2+} -sensitive) such that elution of Tn-I/T2 now occurred at 0.45 to 0.5 M NaCl. Binding of Tn-I at site 2 also strengthened T1/TM interaction at site 1, such that T1 was now eluted at 0.45 to 0.5 M NaCl. Tn-I binding to TM may, therefore, result in a conformational change in Tm, such that cooperativity between the two sites is induced. (Supported by MRC of Canada)

M-AM-Pos180 CALCIUM DEPENDENT INHIBITORY REGION OF TROPONIN: A ^1H NMR STUDY ON THE INTERACTION BETWEEN TROPONIN C AND THE SYNTHETIC PEPTIDE, N^α -ACETYL-[F Phe^{106}]-TnI AMIDE.

P. J. Cachia, B.D. Sykes and R.S. Hodges. Department of Biochemistry and Medical Research Council Group in Protein Structure and Function, University of Alberta, Edmonton, Alberta T6G 2H7.

The synthetic analogue, N^α -acetyl-[F Phe^{106}]-TnI amide, of the troponin I inhibitory region, has been made by solid phase peptide synthesis. This region represents the minimum sequence necessary for inhibition of actomyosin ATPase activity in the presence of tropomyosin. Conformational changes induced by synthetic peptide-troponin C complex formation are followed by ^1H NMR spectroscopy. Difference spectra indicate that hydrophobic (Leu, Val and F Phe) and charged (Arg) peptide residues are perturbed by interaction with troponin C. Charged Lys residues are unaffected by this interaction. Peptide-protein interaction results in redistribution of the troponin C Phe envelope, together with perturbations associated with the protein's aliphatic region. The observed effects on the protein resonances are in agreement with proposed peptide-protein interaction in the N-terminal region of site III in troponin C. In the absence of calcium, this region of troponin I (104-115) is bound to actin tropomyosin inhibiting actomyosin ATPase activity (Talbot and Hodges (1981) *J. Biol. Chem.* 256, 2798). Interpretation of our results suggests that in the presence of calcium, the binding site for region 104-115 of troponin I is induced in troponin C and a troponin IC complex is formed between the N-terminal region of site III in troponin C and troponin I residues 104-115, releasing actomyosin ATPase inhibition. (Supported by MRC and AHFMR)

M-AM-Pos181 COMPARISON OF ISOMYOSIN DISTRIBUTION IN SKELETAL MUSCLES OF NORMAL AND MYOTONIC GOAT. A.F. Martin, S.H. Bryant, and F. Mandel. Department of Pharmacology and Cell Biophysics, University of Cincinnati College of Medicine, Cincinnati, Ohio 45267.

Myosin isoforms were examined in hindleg muscles isolated from normal and myotonic goat. The muscles studied were the soleus, gastrocnemius, gluteus, semitendinosus, semimembranosus and adductor. The myosin isoforms were analyzed by pyrophosphate polyacrylamide gel electrophoresis. The relative proportions of slow and fast myosin isoforms present were determined by densitometric scanning of Coomassie Blue stained gels. All muscles contained three fast myosin isoforms and either one of two slow myosin isoforms. In normal goat, the soleus and gastrocnemius, containing 70-75% slow myosin isoforms were representative of slow muscle. The semimembranosus, semitendinosus and the adductor, with less than 50% slow myosin, represented a predominantly fast muscle group. The gluteus, with approximately 55% slow myosin isoforms, was intermediate between the other two groups. In the myotonic goat, a consistent increase in the proportion of fast myosin isoforms was observed for all the muscles studied. The largest change occurred in the gastrocnemius where the percentage of slow isoforms decreased from 70 ± 4 to 38 ± 6 ($p < 0.01$). In contrast to the gastrocnemius, only a slight decrease ($\sim 10\%$) in slow myosin content was observed for the soleus. All the other muscles examined showed a moderate decrease ($\sim 15\% - 20\%$) in slow myosin content. A significant decrease in slow myosin isoforms (from 57 ± 4 to 37 ± 3 , $p < 0.001$) was observed for the average of the six muscles studied. These results suggest that the abnormal skeletal muscle repetitive excitability of myotonic goats leads to a redistribution of the myosin isoforms. This research was supported by grants from the MDA, by NIH grants HL22651 (AFM), NS03178 (SHB), HL26049 (FM), and by RCDAs to AFM (HL00487) and FM (HL00789).

M-AM-Pos182 MATURATIONAL CHANGES IN MYOSIN ISOZYMES IN THE REGENERATING RAT SOLEUS. G. Lyons, A. Kelly and N. Rubinstein, University of Pennsylvania, Philadelphia, PA.

Myosins of the regenerating rat slow twitch, soleus muscle were examined after marcain destruction of preexisting muscle fibers. We asked (1) whether regeneration recapitulated the developmental sequence of myosin types, (2) whether the synthesis of adult slow myosins in this muscle was endogenously programmed or neurally dependent, and (3) whether the thyroid played a role in myosin transitions during muscle regeneration. Myosins were analyzed by pyrophosphate gel analysis of whole isozymes, peptide mapping of myosin heavy chains, and 2D electrophoresis of light chains. When regeneration proceeded in the presence of soleus motoneurons, the myosins recapitulated development: several days after regeneration had begun, the muscle synthesized fetal and neonatal myosins plus a significant amount of adult slow isozymes. With time, slow myosins became the dominant isozymes of the muscle. In the absence of the nerve, no slow isozymes were seen, and after 18 days of regeneration, the denervated soleus synthesized fetal and neonatal myosin plus adult fast isozymes. If regeneration occurred in the absence of motoneurons and in the presence of PTU to block thyroid action, the soleus synthesized only the fetal and neonatal isozymes. We conclude that, in terms of myosin isozymes, regeneration does mimic development in this slow muscle. The results support our earlier hypotheses that the synthesis of adult slow myosin in the soleus is dependent on innervation. In the absence of innervation, muscles converge to the synthesis of an adult fast myosin. Synthesis of adult fast myosin is dependent on adequate levels of thyroid hormones. Finally, the synthesis of fetal and neonatal myosin isozymes appear to be independent of both innervation and thyroid status.

M-AM-Pos183 ORIENTATION AND INTERACTION ENERGY PROFILE OF THE SERINE PROTEASES. T. F. Kumosinski and M. N. Liebman. Eastern Regional Research Center, USDA, Philadelphia, PA 19118; Mt. Sinai School of Medicine, CUNY, New York, NY.

The relationship of structure and function in biologically active molecules is dependent on a number of parameters which describe shape and organization of the molecules and the energy components which hold them together. Small drug molecules may be readily represented by van der Waal's surfaces, electrostatic potential fields, dipole moment vectors, conformational energy analysis, etc. Biological macromolecules are more difficult to analyze in similar, simple terms because of their structural complexity. We have previously developed techniques which permit rapid correlation of energetics with the various levels of structural organization using the distance matrix approach (Liebman, Amato and Kumosinski). We now extend this energetic profile analysis to the serine proteases and their protein inhibitors in order to study the relationship of structure and function in terms of limited proteolysis. This approach is used to facilitate examination of the internal energetics, (e.g., dipole alignments, dipole-dipole, charge-dipole and charge-charge interaction potentials, weighted hydrophobicity indices, etc.), in terms of domain-domain interactions, enzyme-substrate/inhibitor complexes and macromolecular recognition (see Liebman, Kumosinski and Brown) as well as to monitor the effects of evolutionary changes in amino acid sequence. The ability to portray such calculations in the form of a distance matrix provides a rapid and more objective means of correlating structure-function parameters for this important class of enzymes.

M-AM-Pos184 MODELLING THE FUNCTIONAL ASPECTS OF SUBSTRATE SPECIFICITY IN CARBOXYPEPTIDASE A, Carol A. Venanzi*, Harel Weinstein[†] and Michael N. Liebman[†], *Dept. of Chemical Engineering and Chemistry, N.J. Inst. of Technology, Newark, N.J., and [†]Dept. of Pharmacology, Mt. Sinai School of Medicine, CUNY, New York, N.Y.

We examine the relationship between structure and function in active sites of metalloenzymes by the techniques of computational chemistry. Using the X-ray results of Lipscomb, et al., we study the complementarity between Carboxypeptidase A and peptide inhibitors, including glycylytyrosine and a potato inhibitor. We seek to determine the criteria for molecular interactions and recognition, as well as the changes in molecular properties induced upon complexation of the individual components. The properties we examine are the electrostatic potential (EP) throughout the active site region and the EP surrounding the inhibitor, the penetration of van der Waals surfaces, the conformational perturbations which accompany complexation, and the potential accessibility of the active site by solvent molecules (e.g., water) which might participate in the hydrolysis mechanism. EP maps calculated from various point charge assignments were compared, and contrasted with those obtained directly from quantum mechanical calculations of small fragments of the active site.

To establish criteria for our computational studies, we have also undertaken comparative analyses of various proton-positioning techniques used in completing protein structures derived from X-ray analysis. The comparisons make use of the high-resolution X-ray data and the independent neutron structural determinations of ribonuclease (Moss, et al.; Wlodawer).

Supported by USPHS grant DA-00060 (H.W.) and a Revson Foundation Fellowship (M.N.L.).

M-AM-Pos185 HINGE-BENDING IN L-ARABINOSE-BINDING PROTEIN. Boryeu Mao and J. Andrew McCammon, Department of Chemistry, University of Houston, Houston, TX 77004.

The hinge-bending flexibility of L-arabinose-binding protein (ABP) is analyzed theoretically by altering the width of the sugar-binding cleft and then carrying out "difference" energy refinement of the heavy atom coordinates of the protein. This procedure minimizes extraneous contributions due to structural relaxation unrelated to bending. Calculated from an empirical potential energy function, the adiabatic energy cost for bending ABP is found to be modest for bending angles from -20° to 40° . Changes in protein-solvent interactions during the opening and closing of the cleft as well as upon ligand-binding are estimated to be significantly larger than the internal energy changes. These effects will stabilize the open conformation in the unliganded protein and the closed conformation in the liganded protein.

Analyses of the structural changes associated with the bending show that strains in the molecular hinge are delocalized over several dihedral angles in each of the polypeptide strands that connect the globular domains of ABP. When the cleft is closed, atoms on opposite lobes are brought into close contact and the resulting stresses are relieved by local dihedral angle changes.

Supported by grants from the NIH, NSF, Welch Foundation and Sloan Foundation.

M-AM-Pos186 PREDICTION OF PROTEIN STABILITY FROM X-RAY DATA. Alexander A. Rashin and Barry Honig - Department of Biochemistry, Columbia University, 630 West 168th Street, New York, N.Y. 10032

We argue that the stability of proteins and their fragments is given by the difference between free energy equivalent of the buried area and the loss of the conformational entropy due to folding. The loss of conformational entropy ΔS^0 is calculated from the data on protein stability, disulfide bonding pattern and buried surface area for a limited number of proteins. It is shown that ΔS^0 can be very accurately approximated by three linear functions of the molecular weight (MW), the first one for α -helices, the second one for proteins with MW below 10000 D, and the third one for those with MW above this value. Stabilities predicted for more than 20 proteins and fragments are in a good agreement with the experimental data available. Special attention is paid to α -helices in proteins. Contributions of different interactions to stability are discussed.

We gratefully acknowledge receiving computer programs from F.M. Richards, J.A. Rupley and J.B. Matthews. This work is supported by NIH Grant GM 30518.

M-AM-Pos187 ANTIQUITY OF VERTEBRATE PROTEINS. W.C. Barker and M.O. Dayhoff. National Biomedical Research Foundation, Georgetown University Medical Center, 3900 Reservoir Road N.W., Washington, D.C. 20007

When all of the sequenced proteins are categorized into superfamilies of recognizably related sequences, only 10 of these superfamilies contain both vertebrate and prokaryote sequences. These include proteins involved in mitochondrial electron transport, ATP synthesis, and steroid hydroxylation, some enzymes of glycolysis and purine metabolism, and serine proteases and their inhibitors. These protein types must be considered essential to cellular function, though some have specialized functions in the vertebrate body. Some enzymes have been sequenced from other eukaryote groups and prokaryotes and may someday be characterized also from vertebrates. Other superfamilies contain proteins from vertebrates and at least one other major group of eukaryotes but not yet from prokaryotes. For some of these, e.g., actin or calmodulin, we expect to easily recognize prokaryote homologs once sequence data are available. In other cases, evidence of relatedness may be found only in essential portions of the sequence or in the tertiary structure. We have surveyed the proteins sequenced from vertebrates for evidence of sequence relationships to proteins from other eukaryotes and prokaryotes. Where possible we have made alignments and evolutionary trees from the sequences and have estimated rates of change for the proteins and the approximate times of major gene duplications. Supported by NIH grant HD-09547.

M-AM-Pos188 PROTEIN IDENTIFICATION THROUGH ACTIVE SITE PATTERNS. M.O. Dayhoff, L.-S. Yeh, and W.C. Barker National Biomedical Research Foundation, Georgetown University Medical Center, 3900 Reservoir Road N.W., Washington, DC 20007

We are constructing distinctive sequence patterns that will be sufficient to identify homologous proteins of similar chemical function in all (or most) organisms. Useful patterns are derived from highly conserved sequences around catalytic sites or cofactor and substrate binding sites. For the serine proteases related to trypsin, 23 sequences are known, including 4 from bacteria. These function as digestive enzymes and clotting factors. Two highly conserved sequences surrounding the active serine and histidine residues characterize these proteins. A sequence of 500 residues that contains both of these sequences is extremely unlikely to occur by chance ($P = 6 \times 10^{-6}$, on the basis of amino acid frequencies in proteins). Even if the whole human genome could be examined, we would not expect to find such a combination by chance. A search of the current database of 340,000 amino acids for the sequence surrounding the serine active site, Gly-Asp-Ser-Gly-Gly, retrieves all of the active serine proteases related to trypsin and no other segments. Many other proteins also contain distinctive sequences that may serve to identify them. A number of the characteristic patterns will be shown.

This work was supported by NASA contract NASA3317 and NIH grant GM08710.

M-AM-Pos189 RELATIVE INVARIANCE OF PROTEIN CONFORMATION TO INTER-SPECIES SEQUENCE CHANGES.

R. L. Jernigan, W. R. Church and S. Miyazawa, Lab. of Math. Biol., DCBD, Natl. Cancer Inst., NIH, Bethesda, MD 20205 and Dept. of Immunology, Scripps Clinic and Res. Foundation, La Jolla, CA 92037

To avoid dependences on statistics derived from X-ray crystallographic data, we have devised a semi-empirical method for calculating approximate conformational energies of regions of regular secondary conformation. For fixed backbone conformations and average side chain conformations taken from crystallographic data, approximate energies are calculated. Backbone-side chain and side chain-side chain electrostatic energies are calculated explicitly, in the point charge approximation. The energies of backbone-backbone and backbone-C^β atom interactions are approximated by means of parameters, one for each standard backbone conformation. Results indicate the special importance of the position of polar residues within regular helices. Energies of all possible helices and beta strands are calculated for every location within a protein. The total energy, as the sum of these, is minimized. This method has previously been applied to a series of globular proteins [Macromolecules, 13, 518, 1980]. In the present case, parameters have been varied within small ranges to obtain the best agreement in conformation among the members of a family of proteins. Five species of β₂-microglobulins have been considered; results agreed in suggesting 2 helix regions and ten β strands, with an average content of 14% α-helix and 64% β-strand. The average agreement for the conformations of all residues in comparisons of pairs of molecules was 88%; whereas agreement of sequences was only 70%. This provides evidence of the expected relative invariance of conformation in spite of substantial numbers of amino acid substitutions. Results for other families of proteins will be reported.

M-AM-Pos190 RELATIVE EXPOSURE AND DYNAMICS OF LYSINE RESIDUES IN GLOBULAR PROTEINS. E. M. Brown,

T. F. Kumosinski and P. E. Pfeffer. Eastern Regional Research Center, USDA, Philadelphia, PA 19118.

To study the environment of lysine residues in globular proteins by ²H NMR, acetone-d₆ was used to reductively alkylate lysine residues in α-lactalbumin, β-lactoglobulin, lysozyme and ribonuclease, resulting in the addition of a hexadeutero-isopropyl group at the ε-amino position. The number of lysine residues modified was determined by amino acid analysis. The ²H NMR spectra at 9.17 MHz of the alkylated proteins in neutral buffer gave lower apparent deuterium concentrations than those calculated from amino acid analysis. However, in 6M guanidine the expected integrated responses, corresponding to amino acid analysis, were obtained. Line-width, spin-lattice and spin-spin relaxation values exhibited by the observable lysine-d₆ residue resonances translated into effective C²H₃ correlation times in the range of 40 psec (qQ/h = 170kHz). Those lysine-d₆ residues not observable at 9.17 MHz were assumed to have motions slower than 5n sec (instrumental dead-time-50 μsec). The results suggest the existence of three populations of lysine residues in these native globular proteins: unmodifiable, buried residues; fully exposed, fast tumbling residues; and residues with motions not faster than those predicted from the rotatory diffusion coefficient of the protein. Correlation of these results with X-ray crystallographic data for some of these proteins is being used to locate lysine residues exhibiting different degrees of exposure.

M-AM-Pos191 PREDICTION OF THE THREE-DIMENSIONAL STRUCTURE OF PLANT LECTINS, Kenneth W. Olsen, Department of Biochemistry, The University of Mississippi Medical Center, Jackson, MS 39216

The circularly permuted sequence homology that relates Concanavalin A to the other leguminous plant lectins can be explained by an evolutionary model that requires three exons. The identification of these potential exons from the amino acid sequence data allows the prediction of three domains in the three-dimensional structure of Con A. The predicted domains are reasonably functional and structural units in Con A, demonstrating the correspondence of exons and domains. Slight modifications to the three-dimensional structure of Con A produces a model which is consistent with the sequence data for the other plant lectins, such as those found in peanuts, peas, fava beans and the sanfoin. To make the predicted structure the local conformations at the amino and carboxyl termini were changed to bring them close enough to form the new peptide bond. This was easy to do since both residues are on the surface and only 17 Å apart. When the peptide bond between residues 122 and 123 was cleaved to form the new termini, the local conformation of the new carboxy terminal pentatide was modified to preserve a compact structure. The predicted conformation can be used to explain the changes in the carbohydrate-binding specificity of the various lectins. (This work was supported by grants from the Division of Research Resources, NIH, for the PROPHET Computer Network, from the Biomedical Research Support Program (SO 7 RR05386-20) and from the American Heart Association - Mississippi Affiliate).

M-AM-Pos192 COMPARISON OF *E. COLI* AND HIGHER PLANT CYTOPLASMIC AND CHLOROPLAST RIBOSOMAL PROTEINS BY PATTERN RECOGNITION TECHNIQUES. Malcolm Capel & Don Bourque. Dept. of Biochemistry, University of Arizona.

Ribosomal proteins of *E. coli* and tobacco (*Nicotiana tabacum*) chloroplasts and cytoplasm have been resolved by two-dimensional (2D) polyacrylamide gel electrophoresis. Sets of 2D absolute electrophoretic mobilities from a large number of separations have been processed to compensate for systematic inter-run variation in 2D absolute electrophoretic mobility in order to produce average 2D electrophoretic mobility maps of constant scale and origin (1,2). A variety of pattern recognition methods were employed to compare the average mobility maps of the proteins of all three types of small and large ribosomal subunits and to suggest possible homologies between *E. coli* and *N. tabacum* chloroplast ribosomal proteins.

- 1) Capel, M.S., Redman, B., & Bourque, D.P. (1979) *Analyt Biochem.* 97, 210-228.
- 2) Capel, M.S., & Bourque, D.P. (1982). *J. Biol. Chem.* 257, 7746-7755.

M-AM-Pos193 PROGRESS TOWARD THE 3-DIMENSIONAL STRUCTURE OF THE POLYPEPTIDE HORMONE HUMAN CHORIONIC SOMATOMAMMOTROPIN. R.E. Hunt, J.A. Bell, D.M.E. Szebenyi, K. Moffat, Section of Biochemistry, Molecular and Cell Biology, Clark Hall, Cornell University, Ithaca, NY 14853.

We have purified the large polypeptide hormone human chorionic somatomammotropin to near electrophoretic homogeneity by a new purification scheme. The hormone crystallized from polyethylene glycol in a form suitable for high resolution x-ray analysis; crystals are monoclinic, space group C2, $a = 124.7$, $b = 30.5$, $c = 54.3$ Å, $\beta = 119^\circ 30'$, with one molecule/asymmetric unit. The growth promoting activity of homogeneous hormone and of dissolved crystals, measured by their effect on committed erythroid precursor cells in tissue culture assays, was comparable to hormone purified by standard procedures. The latter preparation yielded either no crystals or disordered crystals unsuitable for x-ray analysis¹. Using radiation from the Cornell High Energy Synchrotron Source, we collected a native data set to 3.3 Å resolution and identified two isomorphous heavy atom derivatives, K_2HgI_4 and $K_2UO_2F_5$. We collected a native 3.5 Å resolution diffractometer data set that scaled to the film data with an overall R-factor of 5% on $|F|$, and one derivative data set (K_2HgI_4) to 3.5 Å resolution. A difference Patterson map for this derivative reveals one major site. Isomorphous replacement phases from this derivative yield an electron density map that distinguishes solvent channels and protein molecules. We are employing a density modification algorithm to flatten the solvent electron density and locate the molecular boundary. Combination of density modification, higher resolution data, and data on the second derivative may yield the alpha carbon backbone and preliminary side chain location.

¹Hunt, R.E., Moffat, K., and Golde, D.W. *J. Biol. Chem.* 256, 7042-7045 (1981).

M-AM-Pos194 CONFORMATIONAL ANALYSIS OF ACTIVE SYNTHETIC ANALOGS OF HUMAN C3a, Zi-xian Lu, Kam-Fook Fok,* Bruce W. Erickson,* and Tony E. Hugli "Introduced by Donald W. Jacobsen." Scripps Clinic and Research Foundation, La Jolla, Ca. and *Rockefeller University, New York, N.Y. The anaphylatoxin C3a is a 9000 m.w. fragment released during activation of the third component of the complement system. C3a is a potent spasmogen that contracts smooth muscle and enhances vascular permeability. Previous studies suggested that a C-terminal segment of C3a constitutes the essential active site of the C3a molecule. Recently, it was observed that a synthetic monocosapeptide (C3a 57-77, 21 residues), mimicking the C-terminal portion of C3a exhibits biological activities nearly equivalent to those of natural C3a. The CD spectra of the monocosapeptide, trideca- and pentapeptides (based on the C-terminal sequence of human C3a) were measured in aqueous and in trifluoroethanol (TFE) solutions. The far UV CD indicates that the monocosapeptide exists in aqueous solution as a random coil with little α -helical content. In TFE the monocosapeptide assumes a largely α -helical conformation. The tridecapeptide C3a 65-77 and the pentapeptide C3a 73-77 assume conformations that appear to be β turns according to CD analysis. The crystalline structure of C3a indicates that the N-terminal portion of the monocosapeptide exists as α -helix and the C-terminal portion contains an irregular or random conformation. Considering that the monocosapeptide exhibits activities quantitatively and qualitatively similar to natural C3a, it is suggested that on the C3a cellular receptor the monocosapeptide adopts a conformation much like that in the intact C3a molecule. The N-terminal helical portion and disulfide-linked "core" of intact C3a may serve to orient or immobilize the C-terminal, active site region and thereby maintain the unique conformation required for function.

M-AM-Pos195 ELECTROSTATIC STRATEGIES FOR DIRECTING DISULFIDE PAIRING IN SYNTHETIC PROTEINS*G.H. Snyder and M.J. Cennerazzo, Div. of Cell and Molecular Biology, SUNY, Buffalo, NY 14260*

The disulfide exchange between acetylcysteine (A) and fragment 85-114 from soybean trypsin inhibitor (B) has been examined as a function of ionic strength. A contains one cysteine with a negative carboxyl neighbor. B contains one cysteine (86) with a single positive neighbor(85) in its immediate local environment but an overall -5 charge for the entire peptide. Equilibrium constants for the protonation of A and B and the four rate constants in the disulfide exchange reaction are determined. Contributions from local electrostatic environments and long range peptide charge are compared. Additional information is provided by the ionic strength dependence of reaction of A and B with neutral or charged sulfhydryl reagents. Decreasing ionic strength from 1 M to 20 mM enhances formation of AB ($-+$) disulfide species while decreasing the population of AA ($--$) or BB ($++$) by 30%.

M-AM-Pos196 MOLECULAR ORBITAL STUDIES OF PROTON TRANSFERS IN PROTEINS

STEVE SCHEINER, DEPT. OF CHEMISTRY & BIOCHEMISTRY, SOUTHERN ILLINOIS UNIVERSITY

Proton transfers between H-bonded protein residues are studied using ab initio molecular orbital methods. Residues which interact through hydroxyl, amine, and sulfhydryl groups are modeled by OH_2 , NH_3 , and SH_2 , respectively. The calculations explicitly consider the wide range of H-bond geometries observed in proteins. It is found that lengthening of the H-bond leads to increases in the height of the energy barrier to proton transfer. Angular deformations of the bond from the linear configuration also produce marked increases in the barrier. With regard to first-row atoms, transfer from N to the less basic O requires a large amount of energy while the reverse process is much more facile. This discrepancy may be used as a "valve" to enable transport of protons in only one direction. The barrier heights for transfer between like atoms are intermediate between the latter two extremes with interoxygen transfer requiring somewhat more energy than the transfer between N atoms. Although H-bonds involving the second-row S atom are somewhat longer, the qualitative features of its proton transfer processes are quite like its first-row analog O. One notable difference is that the increase in proton transfer barrier with H-bond lengthening is not as severe for the second-row atom. The pH dependence of the process was investigated by comparison of transfers between neutral OH_2 and anionic OH^- moieties. For linear H-bonds, the energetics are nearly identical; however, the increase in barrier height with bending of the bond is much less sharp for the anionic system. These facts lead to interesting proposals for a manner in which pH can be used to regulate the proton transport process in proteins. Comparison of HOH with CH_3OH allows analysis of substituent effects and differences between water and protein residues as elements in the transport mechanism.